CHALMERS
UNIVERSITY OF TECHNOLOGY

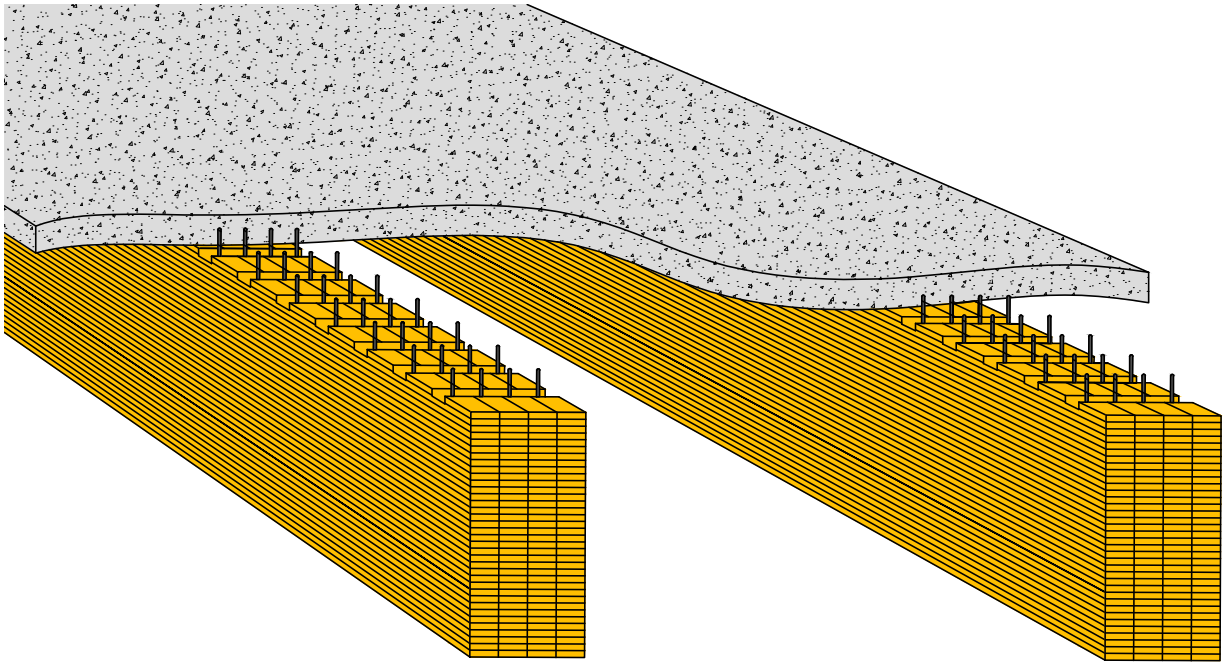

Comparative structural design of a Timber Concrete Composite bridge

LCA and LCC comparison between TCC and concrete integral bridge

Master's thesis in Structural Engineering and Building Technology

ALEXANDER OTTOSSON
IVAR WESTIN

DEPARTMENT OF ARCHITECTURE AND CIVIL ENGINEERING
CHALMERS UNIVERSITY OF TECHNOLOGY
Gothenburg, Sweden 2025
www.chalmers.se

Master's thesis 2025

Comparative structural design of a Timber Concrete Composite bridge

LCA and LCC comparison between concrete and TCC integral bridge

ALEXANDER OTTOSSON
IVAR WESTIN

CHALMERS
UNIVERSITY OF TECHNOLOGY

Department of Architecture and Civil Engineering
Division of Structural Engineering
Lightweight Structures
Chalmers University of Technology
Gothenburg, Sweden 2025

Comparative structural design of a Timber Concrete Composite bridge
LCA and LCC comparison between concrete and TCC integral bridge
ALEXANDER OTTOSSON
IVAR WESTIN

Supervisor: Daniel Josefsson, Inhouse Tech
Supervisor: Samuel Wiik, Inhouse Tech
Supervisor and examiner: Mozhdeh Amani, Department of Architechture and Civil Engineering

Master's Thesis 2025
Department of Architecture and Civil Engineering
Division of Structural Engineering
Lightweight Structures)
Chalmers University of Technology
SE-412 96 Gothenburg
Telephone +46 31 772 1000

Cover: Cross section of a TCC bridge with combined notch and dowel connection, with the dimensions proposed in this report.

Typeset in LaTeX
Printed by Chalmers Reproservice
Gothenburg, Sweden 2025

Comparative structural design of a Timber Concrete Composite bridge
LCA and LCC comparison between concrete and TCC integral bridge
ALEXANDER OTTOSSON
IVAR WESTIN
Department of Architecture and Civil Engineering
Chalmers University of Technology

Abstract

Timber concrete composite (TCC) bridge is a structure system composed of three main structural elements: timber elements, concrete slab and connections to enable composite action. TCC bridges main advantage is the structural efficiency. The materials are used in an efficient manor, with concrete in compression and timber in tension. To be able to profit from the efficiency of the system, a capable connection is essential. This means a connection that can provide enough stiffness to create a good composite action between the materials, strong fasteners to carry the load subjected to the connection and ductility to prevent brittle failure of the structure.

This thesis investigates the possibility of designing a TCC integral bridge based on the prerequisites of an existing concrete integral bridge over a small river. Three connection types are studied: a combination of notches and dowels, dowels alone and a hybrid of adhesive and dowels. These alternatives are evaluated under both short and long term loading to assess their structural performance.

The study resulted in a preliminary design of a TCC bridge. The analysis revealed that the governing stage was the initial service period. Notably, a composite action of approximately 30% led to the lowest material utilization, highlighting a complex relationship between connection stiffness and structural efficiency. Long term effects varied depending on the connection type. For low composite action, utilization decreased over time, while for high composite action, utilization ratio increased.

To compare the bridge alternatives, a life cycle assessment (LCA) and life cycle cost (LCC) analysis are conducted to evaluate whether TCC bridges are environmentally and economically competitive with conventional concrete bridges. The LCA results from the case study indicate that TCC bridges have a lower climate impact than conventional concrete integral slab bridges when comparing CO_2e emissions throughout the construction and maintenance phases. The results from the LCC assessment show that the TCC bridge has a similar expected cost compared to the integral concrete slab bridge from the case study. However, the cost estimates for the TCC bridge shows greater uncertainty, resulting in a wider range between the lower and upper bounds.

Keywords: TCC, timber, bridge, LCA, LCC, notch connection, dowel connection

Acknowledgements

We would like to express our sincere gratitude to everyone who supported us during this master thesis. We sincerely thank our families, who have stood by us every step of the way during our thesis and throughout five years of study.

We are very grateful for our supervisors, Daniel Josefsson and Samuel Wiik at Inhouse Tech. The outcome of this thesis would not have been possible without their support and commitment.

We would also like to acknowledge our supervisor at Chalmers University of Technology, Mozhdeh Amani for her support and guidance.

A big thanks to everyone at Inhouse Tech for making us feel welcome and for letting us work at their offices. The friendly atmosphere has made a big difference and has helped us a lot during the project.

Alexander Ottosson & Ivar Westin

Gothenburg, May 2025

List of Acronyms

Below is the list of acronyms that have been used throughout this thesis listed in alphabetical order:

LCA	Life Cycle Assessment
LCC	Life Cycle Cost
TCC	Timber Concrete Composite
SLS	Serviceability Limit State
ULS	Ultimate Limit State
LM1	Load Model 1
UDL	Uniformly Distributed Load

Contents

List of Figures

List of Tables

1

Introduction

1.1 Background

The construction industry account for 22 percent of the carbon dioxide emissions in Sweden, according to Boverket, 2025, and about a fifth of these emissions is emitted during the production of concrete, in particular the cement. Globally, the production of cement accounts for about 8 percent of the carbon dioxide emissions according to World Economic Forum, 2024. To reduce emissions, new concepts are emerging to supplement portions of concrete in constructions. One of these concepts is Timber Composite Concrete (TCC), which replace parts of concrete with timber.

The concept of TCC is based on the idea of having the right material in the right place. Concrete is strong in resisting compression forces, but weak in tension. To counteract low tensile resistance, reinforcement is traditionally embedded in the concrete to address the tension forces. The concept of TCC is to replace parts of the reinforced concrete structure subjected to tension, and replace it with timber beams. Timber has a high tensile strength in relation to its self weight compared to concrete. A concrete deck is placed on top of the timber beams. This concept has possibilities in optimization of the structure in terms of material efficiency, greenhouse emissions and could also prove to be competitive in terms of economy. However, combining concrete and timber creates complexity in terms of structural response and long term behavior.

1.2 Aim

The aim of this master thesis is to deepen the understanding of TCC bridges and the potential application in modern bridges, particularly in integral bridges. This involves investigating the structural behavior, advantages, disadvantages and limitations of combining timber and concrete. The study aims to evaluate these aspects through life cycle analysis (LCA) and life cycle cost assessment (LCC), comparing the results with conventional concrete integral bridge designs. Ultimately, the project seeks to establish a solid foundation for the implementation of TCC in the construction industry.

1.3 Objectives

- A literature study of different connections to find the most suitable characteristics in terms of structural response.
- Examine how different connections affect TCC structures.
- Design TCC bridge with three different connections.
- Evaluate and compare the TCC bridge to a concrete integral bridge through LCA and LCC.

1.4 Limitations

To concretize and narrow down the project, the following limitations applies:

- The project only considers glulam as the timber material.
- One case of simply supported one span integral bridge with a defined geometry and load will be investigated.
- The project will not investigate the substructure of the bridge.
- The designed TCC cross section will not change for the different connections.
- The only method used in the design is the γ-method.
- Only Load Model 1 will be used for traffic loads.

1.5 Methodology

The impact on structural performance of a TCC bridge will be studied and reviewed for different connection types between timber and concrete. A literature study will be performed to understand the existing research on TCC bridges, structural behavior and production methods. Then, case studies will be conducted with emphasis on reviewing the structural behavior of bridges with three different connections and production methods. This will be done using a version of Eurocode, SIS-CEN/TS 19103:2022, specially made for timber concrete composite.

LCA and LCC analyses will also be performed to address the environmental and economic impact of the bridge concepts. To obtain data for the LCC analysis, a dialogue will be conducted with our supervisors and their corporate partners to gain a clear understanding of costs, including construction methods, material expenses and other relevant factors. Data regarding the environmental impact of building materials will be taken from the Swedish transport administration. In the end, a discussion and conclusion will be performed to review the results of the different case studies.

2

Literature review

To perform case studies off different connections and production methods for TCC bridges, a literature review of relevant subjects is presented below. The literature review will focus on relevant information needed to evaluate the most fitting connection type and production method that will be analyzed in the case studies. The long term effects and structural behavior of the three main elements of a TCC bridge will be covered. In addition, LCA and LCC will be covered as well as calculations methods of TCC structures according to Eurocode.

2.1 TCC bridges

A timber concrete composite (TCC) bridge is comprised of three main elements: timber, concrete and connections allowing for the composite action. Furthermore, the bridge has abutments, foundations, bearings and other components. However, this report will focus on the superstructure of a TCC bridge.

When a structural element is subjected to transversal forces, tension and compression stresses arise in the cross section. The work of a structural engineer is to calculate the stress distribution in members and design the cross section to resist the expected loads. The idea of a TCC bridge is to increase the structural efficiency, either by replacing parts of a reinforced concrete member subjected to tensile forces with timber, or by increasing the stiffness and durability of a timber element by adding concrete in the compression zone.

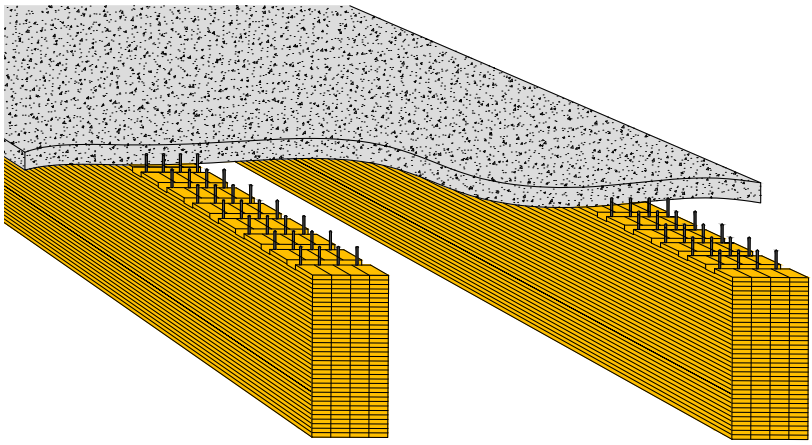

Figure 2.1: Example of a TCC bridge cross section.

The history of TCC bridges dates back to the 1920s and the concept has been a viable option for different reasons throughout its history. According to Wacker et al., 2017, 1644 TCC bridges were still in service in USA, where a majority were built in the 1950s and 1960s. The beginning off TCC bridges began in America in between the two world wars, when steel was a scarce material due to the production of army material. The shortage of steel resulted in new ideas of supplementing steel with another, available material, where timber was an appropriate building material. Another reason for the TCC concept is to rehabilitate or improve existing infrastructure, which is beneficial both in terms of economical and environmental sustainability. In the beginning of the 21st century, the TCC bridge started to rise in popularity, especially in Europe, as it is seen as a sustainable option compared to traditional reinforced concrete constructions.

2.1.1 Timber

Timber is one of the oldest and most important building materials historically. Timber is made from wood and can be modeled as an orthotropic material that has different characteristics in each direction in relation to the fiber orientation. The difference between wood and timber is that wood is "the fibrous substance that makes up a tree", cited from Duffield Timber, 2019, whereas timber is sawn or processed wood. Timber has three main directions: longitudinal, radial and tangential, illustrated in Figure 2.2. The longitudinal direction, parallel to the fibers, has the highest strength of the three directions. The radial and tangential directions are much weaker. (Swedish Wood, 2019) The orthotropic characteristic is crucial in the design phase of timber constructions.

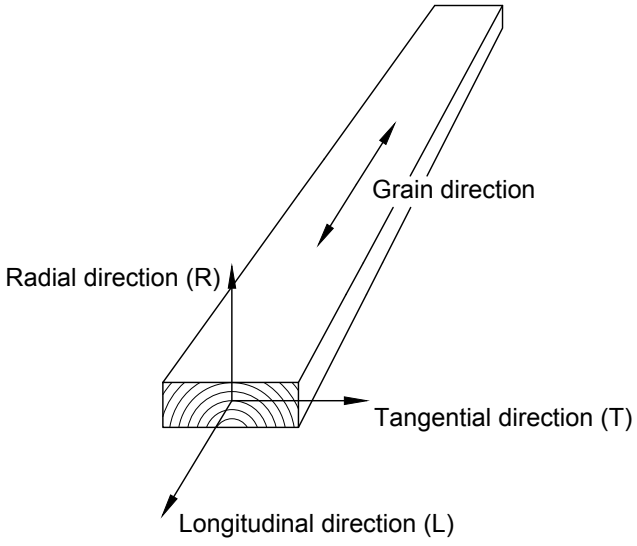

Figure 2.2: Three principal directions in wood; longitudinal, radial and tangential.

Moisture

Wood is a hygroscopic material, meaning that its moisture content influences its properties. Naturally, wood contains moisture since water is essential for photo-

synthesis in trees. Most of this water is stored in the cell walls and hollow cell cavities. During drying, free water in the cell cavities evaporates first, followed by the bonded water. Wood absorbs moisture in humid conditions and releases it in dry environments. While the loss of free water does not affect the wood's volume, the evaporation of bonded water causes shrinkage. (Swedish Wood, n.d.)

Wood is anisotropic, meaning that shrinkage occur differently in the three main directions (Swedish Wood, n.d.). Most shrinkage occur in the tangential direction and least in the longitudinal direction. This causes risk of warping or cracking. Wood also absorbs water at different rates depending on the grain direction. The highest absorption occurs along the grain in the longitudinal direction, where wood can absorb up to 20 times more moisture compared to other directions. This makes the end grain vulnerable to water absorption. The lowest absorption occurs in the radial direction, while the tangential direction absorbs approximately twice as much water as the radial direction (Swedish Wood, n.d.).

To minimize the risk of fungal degradation, Ramage et al., 2017 states that maintaining a moisture content below 20% is effective. Moisture content also affects the mechanical properties of timber. As moisture decreases, strength and stiffness increase. Wood naturally seeks to reach moisture equilibrium with its surroundings, and the rate of moisture change depends on the timber geometry. Thicker beams dry slower than smaller beams due to their larger cross-sections. In a building, the equilibrium moisture content is around 8-12% and for exterior environments, the moisture content is around 16%.

Knots are natural occurring in timber and arise from old tree branches. Knots cause deviations in the fiber direction, creating an area of different orientation of the fibers and thereby a reduction in strength (Swedish Wood, n.d.). Reaction wood is also a phenomenon that arise as a counteraction of wind loads on the tree. Reaction wood causes changes of the timber properties, leading to unpredicted shrinkage and swelling which is unwanted from an engineering perspective. To avoid these effects, engineered timber has been developed. The idea of engineered timber is to reduce the effects of knots and reaction wood and make a more uniform material. Glue laminated timber beams and cross laminated timber slabs are examples of engineered timber.

UV light

Ultraviolet light, a part of the light emitted from the sun, causes damage to the exterior part of the wood. The UV light breaks down the chemical structure of lignin and cellulose, which are essential components of the wood (Teacă et al., 2013). Lignin can be refereed as the glue that bind the cellulose fibers together. When lignin beaks down, the wood strength decreases and gets more susceptible to cracks and color changes. The UV light also causes the timber to lose its moisture, further increasing the risk of cracks.

Glue laminated timber

Glue lambinated timber, or glulam, is the oldest engineered timber product and has been around since the beginning of the 20th century (Swedish Wood, 2019). A comparison of strength to weight ratio between glulam, steel and concrete show that glulam is the strongest, according to Ong, 2015.

The concept of glulam is to glue several small, knot free, laminates together in the same fiber direction which creates a more uniform material. The manufacturing of glulam starts by drying timber in a kiln to desired moisture content. Then, the timber is strength graded according to national standards. Strength grading can be done visually or by machine grading. The latter is considered more accurate and less labour intensive, according to Ong, 2015. To create a material with uniform characteristics, defect areas are removed and the remaining timber are re-joined using finger joints. Then, the timber is laminated and pressed together using adhesives and special equipment. The glulam beam can be optimized by using high strength timber in the top and bottom, where maximal stresses occur. This optimization is denoted with the letter c, as in combined, whereas uniform strength timber laminates are denoted with the letter h, as in homogeneous, as illustrated in Figure 2.3.

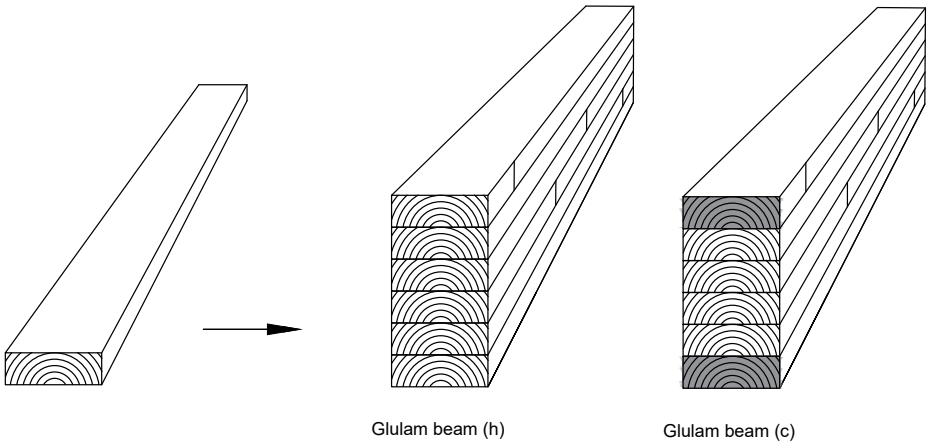

Figure 2.3: Illustration of two glue laminated timber beams, where (h) denotes homogenous and (c) denotes combined.

Since glulam is comprised of many small laminates, the material can be produced in almost any shape and is only prevented by the logistics of transportation. Common widths of glulam beams are between 42-215mm in the Nordic countries ((Swedish Wood, 2019)), but it is possible to achieve wider beams by block gluing glulam beams together.

2.1.2 Concrete

Concrete is made up of cement, aggregates, water and admixtures (Mačiulaitis et al., 2009) and is the second most used material in the world. The material has a

wide range of applications and the concrete mixture can be tweaked to gain desired properties and characteristics. Concrete has a high compressive strength but a low tensile strength. To counteract the low tensile strength of concrete, steel reinforcement are traditionally casted into the concrete to resist the tensile forces.

Concrete experiences long term effects caused by shrinkage and creep. Shrinkage occur partly due to the drying of concrete, called drying shrinkage, and partly due to the hardening of the concrete when the cement hydrates, called autogenous shrinkage (Harapin et al., 2024). Shrinkage can cause tensile stresses if the concrete is subjected to restraint. Since concrete has low tensile strength, cracks can appear in the concrete. Cracks causes reduced durability and non linear behavior.

When concrete is subjected to sustained loads, the stiffness reduces which in term increases deformation. This is a time dependent phenomenon called creep. Creep is influenced by the concrete mix, environmental factors and time(Harapin et al., 2024). Shrinkage and creep are important factors to take into consideration in the design phase, since its consequences, reduced durability and deflection, can be governing.

2.1.3 Connections

The performance of TCC systems is largely dependent on the type of connection between the two materials. According to Dias et al., 2018 the ideal connector should fulfill three mechanical properties: the connection should have enough strength to transfer the shear force between the concrete and steel elements. The connection should be stiff enough to transfer forces without considerable slip. The ideal connection behaves ductile to avoid brittle failure. In addition to these three properties, cost and complexity should be taken into account. However, considering these properties, the ideal connector is not available on the market.

Dowel connector

Dowel type connectors are commonly used in timber structures, and are therefore natural as a option also for TCC structures (Dias et al., 2018). Figure 2.4 illustrates a dowel connection. The performance of dowel type connectors is relatively low in terms of strength and stiffness, but high in ductility. There are different types of dowel connectors; screws, nails, bolts, dowels etc. These dowel alternatives can be attached to the glulam beam by screwing, driving or gluing. According to Dias et al., 2018, the majority of dowel connection in TCC constructions are nails and screws.

There are two types of dowel connections, either perpendicular to the beam or at an angle in relation to the interacting surface at the top of the beam. A perpendicular dowel connection is beneficial in terms of ease of production, but lacks structural efficiency since the connector experience shear and bending (Dias et al., 2018). An inclined connection increase the structural efficiency since higher amount of load is taken axially in the connector, but creates a more complication installation process.

Screwing a dowel 90°into the glulam beam is the fastest way to attach the connector. Since no additional material is required, such as adhesives, this alternative is among the most economical in terms of production. Other connection methods, such as adhesives or inclined connectors, is more complicated but can be beneficial in terms of structural efficiency.

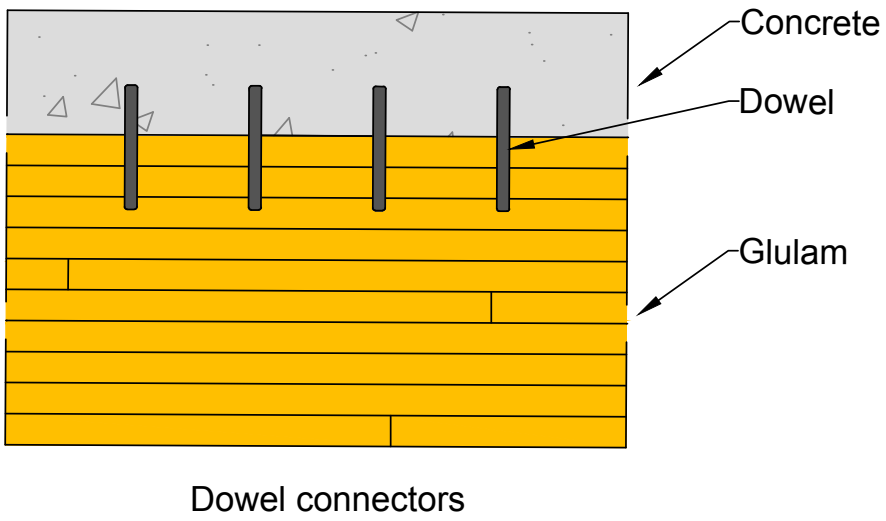

Figure 2.4: Dowel connection

Notch connector

Notch connectors are made by cutting segments in the timber which is filled with concrete during casting. This type of connection is effective due to its simplicity and performance (Dias et al., 2018). An illustration of a notch connector is shown in Figure 2.5. The advantage of notch connections is its high stiffness. However, the shear and axial load capacity is usually not that high and the failure is brittle. The disadvantages can be addressed by combining notch connections with some sort of dowel type fastener to add strength and ductility to the connection. From a production point of view, the notches can be carved before assembly, simplifying the production process and making the connection an economical alternative. Dias et al., 2018 explains that a majority of notched connections are combined with dowel, which combines the stiffness of the notches and the ductility of the dowels.

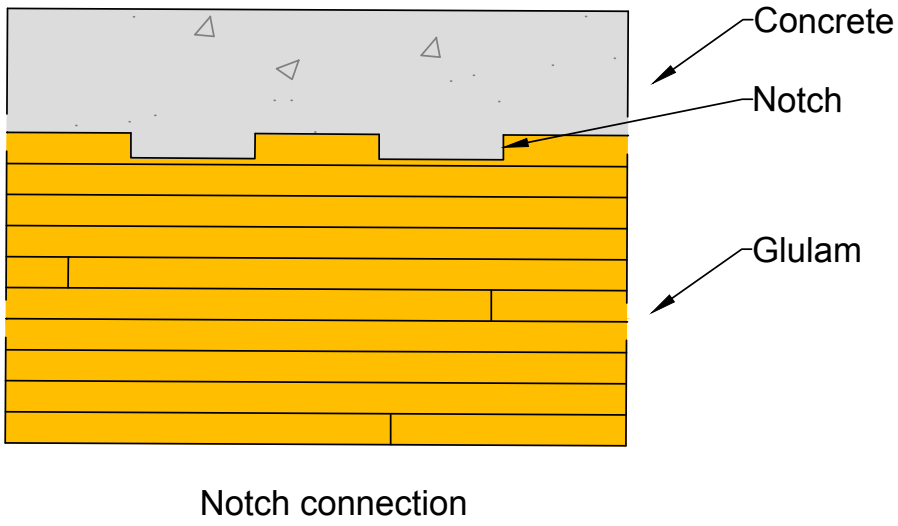

Figure 2.5: Notch connection

Adhesive connector

According to Buka-Vaivade and Serdjuks, 2021, glued connectors are a great alternative due to its high composite actions and good distribution of shear forces throughout the surface. High composite actions creates structural efficiency, and the distribution of shear forces reduces the local stresses. Glue does not corrode as dowel connections can, which is good in terms of durability. However, the downside of glued connections are the problem with quality assurance since inspection is hard to perform. Glued connectors are also hard in terms of construction since the glue requires strict appliance control and curing conditions. Another downside is the brittle failure, which is unwanted (Dias et al., 2018).

Buka-Vaivade and Serdjuks, 2021 did numerical experiments on specimens with defects in the glued connector. The conclusion was that the size of the individual defected areas, that is areas without glue, is more important than the number of defected areas, since large stress concentrations arise. To improve the quality control, an alternative production approached was presented which comprise of adding granite chips to the adhesive layer, and then casting concrete on top. This approach improves the inspection possibilities, since inspection of each glued granite chip can be done before casting, which in terms reduce the defected areas. Figure 2.6 illustrates an adhesive connector.

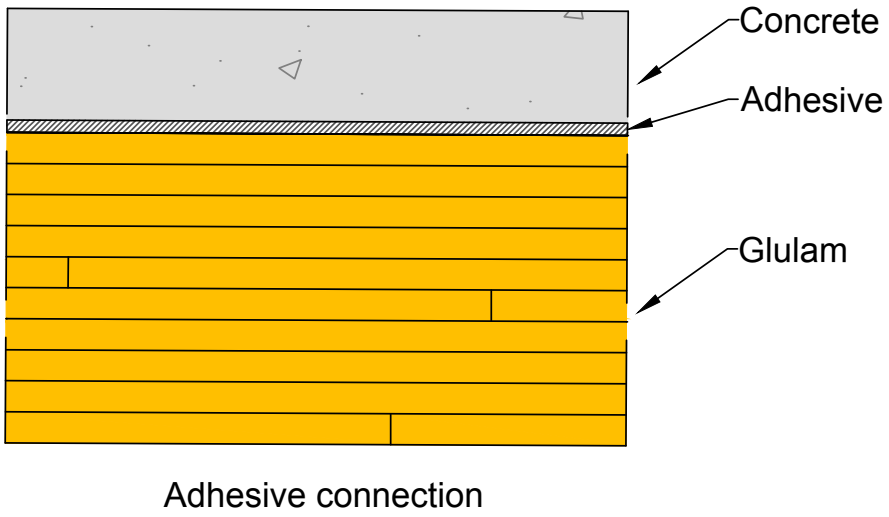

Figure 2.6: Adhesive connection

Combined notches and "X" connector

Jutila et al., 1997 did a field test of a constructed one span, 18 meter long TCC bridge in Finland. The bridge was comprised of glulam beams, concrete slab and connections made from notches and X connectors. The notches were positioned near the support regions where the highest shear forces occur. The X connector was composed of ϕ16 mm rebar connected in a 45° angle into the glulam beam by adhesives, as shown in Figure 2.7. The rebar was positioned at an angle to increase the axial action and thereby the mechanical efficiency, according to Jutila et al., 1997. The X connectors were positioned at an CC-distance of 800 mm and connected to the concrete slab. The reinforced concrete slab was 150 mm thick and its rebar scheme comprised of ϕ12 mm with a spacing of 250 mm at the top and bottom, with additional transversal rebar. There were seven glulam beams with a dimension of 190 mm x 1350 mm. No dimensions of the notches were presented. To perform the field test, two heavy trucks were positioned at the bridge for SLS, according to Finnish codes. The result of the field test indicated that the evaluated connections performed well in terms of composite action. The deflection for short term loading was below 1/1500 of the span.

Marques et al., 2020 performed an experimental comparison of two connection types. Although the experiment focused on rural TCC bridges constructed with timber logs, valuable insights can be gained from the mechanism of the investigated connections. The first was X connectors glued into 45° angle pre-drilled holes in timber logs. The second connector is a dowel hammered into 90° angle pre-drilled timber log without adhesives. The results of the experiment show that the X connections have a higher load carrying capacity and minimal slip, but a more brittle failure and more expensive and complex installation. The dowel connection show a more ductile

behavior and easier installation, but lower strength and more prone to stiffness reduction due to fatigue loads.

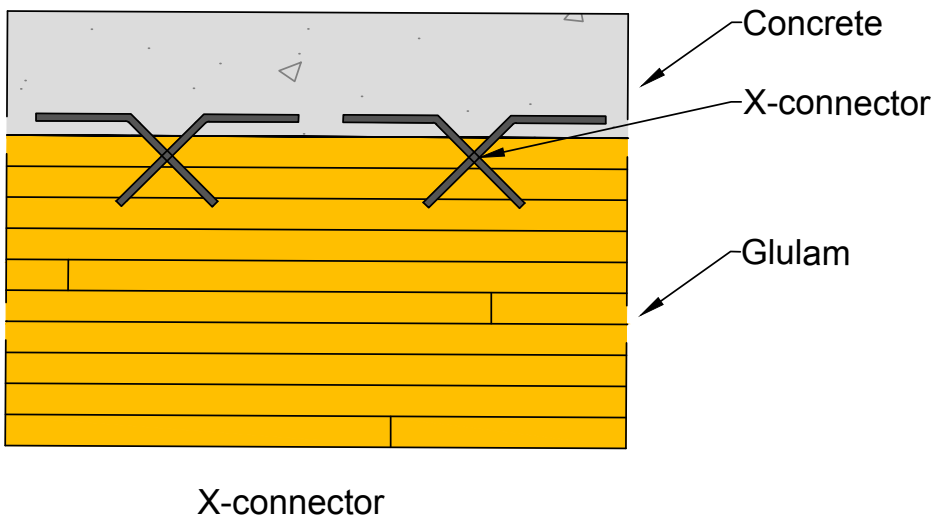

Figure 2.7: X connection

Combined notches, "X" connector and glue connector

Jutila, 2003 explain the evaluation process for determining a suitable connection for a proposed TCC bridge in Finland. The paper evaluated four different connections and fatigue tests were performed. The fatigue test involved a cyclic loading of 160 kN on a million load cycles.

- Specimen 1. X connector and polyurethane adhesive.
- Specimen 2. X connector and epoxy adhesive.
- Specimen 3. Steel bar connector, notched and polyurethane adhesive.
- Specimen 4. X connector, notched and polyurethane adhesive.

The result of the test shows no damage due to fatigue on all four specimen, but softening of the shear connectors were noticed. Further, epoxy generated a higher stiffness than the polyurethane adhesive, and the notched specimen decreased the slip. Jutila further explains that the addition of notches is inexpensive and increase the shear capacity by 35 %. Specimen 4 was the chosen connection for the bridge.

2.1.4 Integral bridges

Bridges are subjected to thermal differences during its lifetime, which causes the material of the bridge to contract or expand in the horizontal direction (Dicleli, 2016). Horizontal forces from braking forces causes movement in the bridge as well.

If these movements are restricted, internal stresses arise which can lead to damages or failure of the bridge. To counteract this, expansion joints are traditionally fitted to bridges which allows the bridge to expand and contract. Expansion joints are normally located at the abutments, or in long bridges over intermediate supports, due to ease of inspection and maintenance. However, expansion joints have their disadvantages; they are often a critical detail in terms of maintenance, and maintenance or replacement of expansion joints can lead to closure of the road which is unwanted.

An integral bridge is an alternative bridge to traditional bridges with expansion joints, where the concept is to transfers the horizontal movements to the soil at the end of the bridge, and thereby eliminating the need for expansion joints (Dicleli, 2016). This reduces maintenance and increases durability of the bridge. Further, it can create a faster and simplified construction. But, integral bridges require careful design where thermal expansion and long term effects are essential to take into consideration. Long term effects include shrinkage and creep of the concrete, soil densification and increased earth pressure due to cyclic loading of the end console and fatigue.

2.2 Loads

When designing a structure, it must be capable of withstanding all loads it will be subjected to throughout its lifetime. Ensuring safety is of high importance, which is why the design process involves analyzing worst case scenarios for various loads and calculating the resulting maximum stresses. Once these stresses are determined, the design of the cross sections begins. The cross sections must be able to resist the acting forces over time, considering the effects of time dependent behaviors and environmental conditions that may influence stress distribution.

To design a structure in accordance with Swedish standards, the loads acting on the bridge must be determined based on SS-EN 1991-2, 2003. This Eurocode specifies the magnitude of various traffic and environmental loads, as well as how these loads should be distributed across the structure using different load models. The load models are the following:

- Load model 1: Relates to vertical distributed loads for trucks and cars. Can be applied in global and local calculations.
- Load model 2: Relates to a single axis load of 400 kN. Can be deciding on short spans.
- Load model 3: Combines several axial loads, representing special vehicles.
- Load model 4: Pedestrian loads.

2.2.1 ULS, SLS and fatigue

Structures needs to be designed for three main types of load combinations: ultimate limit state (ULS), service limit state (SLS) and fatigue. ULS refers to the maximum load a structure can resist before experiencing failure or becoming unsafe (SS-EN 1991-2, 2003). ULS is essential in design to ensure that structures remain stable under extreme conditions. ULS applies amplification factors to account for uncertainties in loading conditions. However, ULS does not take serviceability into consideration, it is only a criteria that ensures no collapse in worst cases.

Partial factors are used in ULS design, which can be found in Annex A in SS-EN 1990, 2002. The Swedish Transport Agency's Code of Statutes (TSFS 2018:57, 2018) explains how load should be combined in order to resist the worst case scenarios. In the code of statutes, Table 4.4 presents two main load cases, "6.10a" and "6.10b", that will be considered in this report. 6.10a is a load combination that gives the worst loading effects for permanent loads. 6.10b, on the other hand, combines variable load that gives the worst loading effects. TSFS 2018:57 further explains that loads can be applied in an unfavourable or favourable way. If a variable load creates a favourable effect, the load can be disregarded, by setting the load factor to zero. For permanent loads, the load factor can be set to 1. G denotes permanent loads and Q denotes variable loads. Equation 2.1 denotes load combination 6.10a and equation 2.2 denotes load combination 6.10b.

$$\sum_{j\geq 1} \gamma_{G,j,\text{sup}} G_{k,j,\text{sup}} + \gamma_{G,j,\text{inf}} G_{k,j,\text{inf}} + \gamma_{Q,1} \Psi_{0,1} Q_{k,1} + \sum_{i\geq 1} \gamma_{Q,i} \Psi_{0,i} Q_{k,i} \tag{2.1}$$

$$\sum_{j\geq 1} \xi \gamma_{G,j,\text{sup}} G_{k,j,\text{sup}} + \gamma_{G,j,\text{inf}} G_{k,j,\text{inf}} + \gamma_{Q,1} Q_{k,1} + \sum_{i\geq 1} \gamma_{Q,i} \Psi_{0,i} Q_{k,i} \tag{2.2}$$

To take service state into consideration, load model SLS is used. The service state criteria refers to, among many things, deflection and crack widths. SLS refers to how a construction is perceived, rather than a maximum load the structure can experience. SLS can often be decisive in the design phase. Equation 2.3 denotes the characteristic combination of SLS, and equation 2.4 refers to frequent combination of SLS.

$$\sum_{j\geq 1} G_{k,j,sup} + G_{k,j,inf} + \text{"}Q_{k,1}\text{"} + \sum_{i\geq 1} \Psi_{0,i} Q_{k,i} \tag{2.3}$$

$$\sum_{j\geq 1} G_{k,j,sup} + G_{k,j,inf} + \text{"}\Psi_{1,1} Q_{k,1}\text{"} + \sum_{i\geq 1} \Psi_{2,i} Q_{k,i} \tag{2.4}$$

Fatigue refers to a local structural damage that increases with cyclic loading (Chang, 2015), and can lead to structural failure. Failure due to fatigue occurs with stresses well below the maximum stress level of a material. Equation 2.5 denotes the quasi permanent combination.

$$\sum_{j\geq 1} G_{k,j,sup} + G_{k,j,inf} + \sum_{i\geq 1} \Psi_{2,i} Q_{k,i} \tag{2.5}$$

2.2.2 Permanent and variable loads

Structural loads are generally classified in two main categories: permanent loads and variable loads. These loads can act in three primary directions: vertical, horizontal, and transversal. The following section presents a detailed list of different load types and their respective directions.

Permanent loads on a bridge include:

- Self weight - Acts in the vertical direction due to the structures weight.
- Earth pressure - Acts in the horizontal and vertical direction. The horizontal direction is of high interest for an integral bridge.
- Differential settlements - Occurs due to a difference in settlement between abutments or supports.
- Shrinkage - Acts in all directions and creates restraint forces.

Variable loads in a bridge include:

- Traffic loads - Acts in the vertical direction and is discussed further below.
- Braking and acceleration forces - Horizontal and transversal forces caused by breaking or acceleration of vehicles on the bridge.

- Wind loads - Acts in all three directions, but is off highest importance in the transversal direction. Wind loads acts on the bridge and on the vehicles, which contributes to a load increase.
- Centrifugal force - Acts in the transversal direction due to vehicles traveling in a radius.
- Thermal effects - Acts in all directions and is a complex effect that causes expansion, contraction and restraints.
- Accidental loads - Acts in the most unfavorable direction, often the transversal direction.

2.2.3 Load model 1

Load model 1 consist of two systems; one system that represents concentrated axle loads symbolizing heavy vehicles, and the other system that represents uniform distributed loads symbolizing vehicle traffic. Load model 1 takes the width of the bridge into account, dividing the width into parallel lanes of 3 meters (SS-EN 1991-2, 2003). The first lane experiences the most amount of loading, followed by the second lane and then the third lane. The remaining areas that is not a part of a lane, experience a distributed load. Table 2.1 summarizes the loads in load model 1.

Table 2.1: Load model 1: Characteristic values

Location	Tandem system TS	UDL system
	Axle loads Q_{ik} (kN)	q_{ik} or q_{rk} (kN/m^2)
Lane number 1	300	9.0
Lane number 2	200	2.5
Lane number 3	100	2.5
Other lanes	0	2.5
Remaining area (q_{rk})	0	2.5

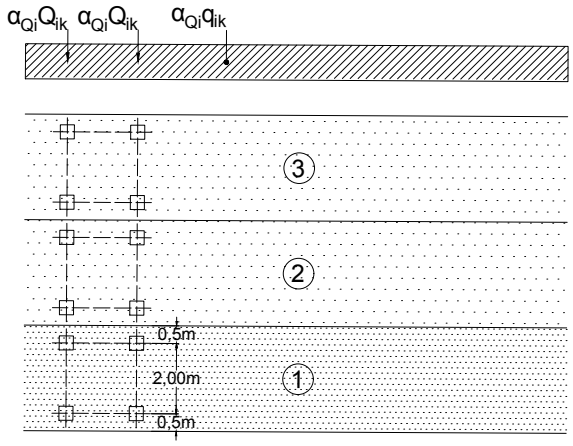

Figure 2.8: Load model 1.

2.3 Mechanical properties

To be able to utilize the benefits of TCC, the connection between timber and concrete must be effective (Dias et al., 2018). For this reason, strength and stiffness are important factors to consider in the design phase. In addition, ductility is important. Ductility can influence how the two materials act together, and enable load redistribution and prevent failure in connection. The stiffness of the cross section is the main factor that determines the deformations of the structure. Connections have a large impact on the bending stiffness of the system and consequently on the forces and stress distribution. Additionally, the size and material of the other parts of the cross section influence the stiffness of the system. Another property that influences the behavior of the system is strength. The strength is mainly referred to in the context of connections. The strength of a connector is the ability to transfer shear forces between timber and concrete. The connection is usually assumed to have a maximum slip of $15mm$ at its maximum load.

In TCC systems, the timber in tension and the concrete in compression behave brittle when failing. Therefore, the ductility in TCC systems is dependent on the connection (Dias et al., 2018). Ductility in TCC connections is usually achieved by steel connectors between the timber and concrete. Other connections, such as notched or glued, usually act brittle. Ductile behavior can be beneficial in terms of load-carrying capacity and deformations. However, if the capacity of the connection is larger than expected, the timber or the concrete can still fail before the connection, resulting in brittle failure mode despite ductile connection (Ceccotti, 2002).

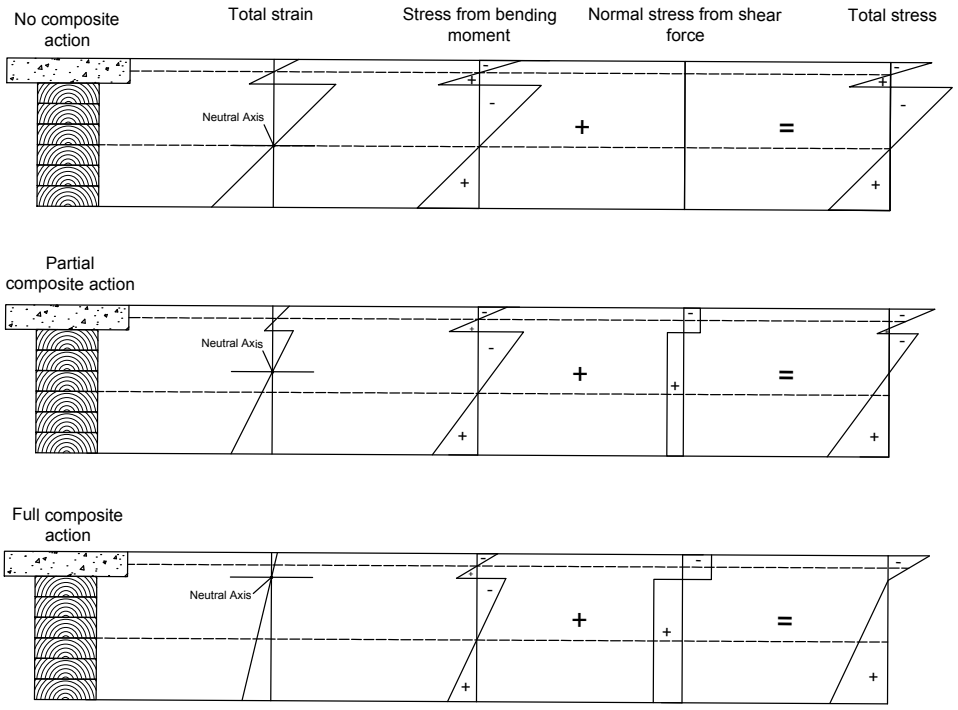

Figure 2.9: Strain- and stress distribution for no-, partial- and full interaction

2.4 Determination of forces

In composite structures, the equilibrium can be described according to Equation 2.6 where N_1 is the compressive force in the concrete and N_2 the tension force in the timber (Ceccotti, 2002). These forces are caused by the bending moment and act as a force couple. The intensity of the forces is related to the stiffness of the connection. The total bending moment in the cross-section can be expressed as the sum of the local moments from the two elements in the structure, see Equation 2.7 where z is the inner lever arm.

$$N_1 = N_2 = N \tag{2.6}$$

$$M_{ext} = M_1 + M_2 + N \cdot z \tag{2.7}$$

In Dias et al., 2018, the process of determining internal forces in TCC structures is described. These forces are influenced by several factors. The bending stiffness of each material in the cross section plays a significant role and depends on both the size of the cross section and the MOE of each material. Additionally, the behavior of the connection between the two materials affects the force distribution. Inelastic strains, as well as long term and non linear effects, also contribute to the development of internal forces.

The stress strain distribution in a TCC cross section is largely influenced by the degree of composite action (see Figure 2.9). The level of interaction, or the rigidity of the connection, affects how normal forces are distributed between the materials. Higher composite action leads to reduced strains in the TCC system, which also impacts the resulting stresses. The normal stress distribution is therefore directly related to the degree of interaction.

When there is no interaction between the materials, the timber and concrete act independently to carry the load. In this case, each material must resist both tension and compression forces. As the composite action increases, the strain distribution decreases and the neutral axis shifts upward toward the concrete. Although both materials are still subjected to tension and compression, the concrete experiences less tension and the timber experiences less compression forces.

In the case of full interaction, the cross section behaves as a single element. The strain distribution becomes linear across the section and is smaller than in cases of partial interaction. As a result, the neutral axis is at the same level as the connection between the concrete and timber. This is because no slip occurs at the connection, making it very stiff (see Figure 2.10). However, full composite action also leads to high shear stresses within the connection.

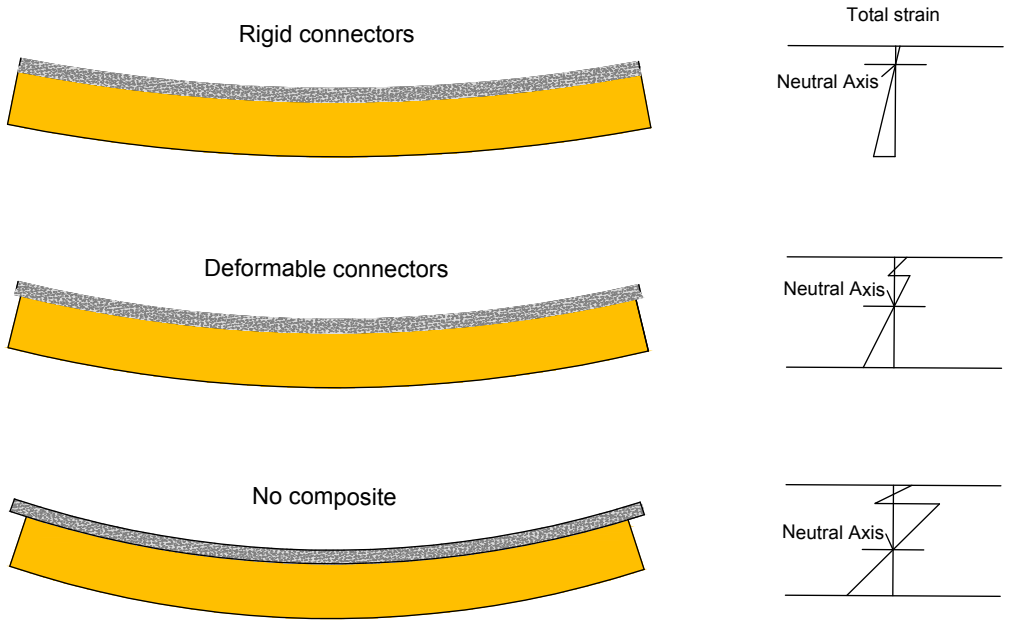

Figure 2.10: Composite action of TCC

2.5 Long term effects

When designing TCC structures, the long term effects of the materials is important to consider. Long term effects often induce larger deformations, which can be critical in SLS calculations (Tannert et al., 2017). All three components in TCC systems have different long term behavior. The timber part of the system is effected by creep, mechano sorptive creep and shrinkage/swelling. Concrete is effected by shrinkage and creep. The connection can also be effected by creep and mechano sorptive creep.

The long term effects in the different materials can cause complications. Due to the materials being constraint to each other, they cannot shrink/swell freely. Therefore, long term effects can induce internal stress. Thus, stiff connections may lead to internal stresses from restraint.

2.5.1 Timber

Timber has various time dependent behaviors. Shrinkage and swelling are long term effects that influence the volume of timber specimens. The volume changes can depend on moisture and temperature variations (Tannert et al., 2017). Timber can reduce its water content through desorption and increase it through adsorption. When the moisture content in the wood increase, the volume increases, and when the moisture decreases, the volume decreases. Swelling occurs when the volume is increased. Shrinkage occurs when the volume decreases. Since timber is modeled as an orthotropic material, these effects are different for different directions in the timber specimen. Similar behavior can be observed when timber is effected by temperature variations. When hot, the volume increases and vice versa.

Timber is also affected by creep. Creep is a stress dependent effect that increases deformation over time. Most of the creep deformations are elastic and will return when unloaded, but a part of the deformations are permanent. Creep in timber is affected by the direction of load, the stiffness of the member, moisture content and temperature. In design, the effect of creep is considered by reducing the MOE of timber with the deformation factor k_{def}.

2.5.2 Concrete

Concrete is affected by several long-term effects, such as shrinkage and creep, which are important to consider in structural design.

Concrete shrinkage

Stress independent strain or shrinkage is a long term effect for concrete. Shrinkage starts when the concrete is casted and develops over time (Engström, 2007). The shrinkage of concrete can be divided into two parts: drying shrinkage and autogenous shrinkage. The drying shrinkage is based on the removal of water from the concrete. Autogenous concrete is based on the chemical process inside the concrete,

and develops under the hardening process.

Moisture exchange between concrete and air can lead to swelling or shrinkage, but shrinkage is more common. Usually, a portion of the water in concrete does not take part in the reaction with cement. This water is stored in the pores, and can be dried out to the surroundings. Consequently, the concrete volume decreases. During concrete hardening, most of the water will react with the cement. The chemical process of water and cement reacting will lead to autogenous shrinkage of concrete.

Concrete Creep

Stress dependent deformation is an effect of concrete. Partially, this deformation is elastic. The other part is called creep deformation, which is a time dependent behavior and increases over time (Engström, 2007). The creep deformation is assumed to reach a specific value after long time, called final creep. Except increased deformation, creep effects concrete by making it less stiff. This is taken into consideration in design by using a reduced modulus of elasticity.

2.6 Design methods

The design of TCC beams has been based on Annex B in SS-EN 1995-1-1, 2004. During recent years, new research knowledge has been collected in a technical specification (SIS-CEN/TS 19103, 2022), which according to Schänzlin and Dias, 2022 can eventually be the foundation for future Eurocodes. In section 2.6.1 the γ-method from Eurocode 5 is described.

2.6.1 The γ-method

In SS-EN 1995-1-1, 2004, Annex B, a method for analyzing TCC elements is suggested, called the γ-method. This method is based on the assumption that the concrete, timber and the connection behave linear elastically. The method follows the following procedure for calculation of TCC elements. Equation 2.8 provides the effective bending stiffness of the cross-section. E_i indicates the modulus of elasticity for the member, I_i is the moment of inertia and A_i the area of the member, a_i is a distance parameter, and γ_c is the shear coefficient. γ_i and a_i is calculated in Equations 2.9, 2.10 and 2.11. In Equation 2.9, s is the spacing, K is the connection stiffness and L is the length of the element. Figure 2.11 illustrates the distance parameter a_i.

$$(EI)_{eff} = E_c I_c + \gamma_c E_c A_c a_c^2 + E_t I_t + E_t I_t a_t^2 \tag{2.8}$$

$$\gamma_c = \frac{1}{1 + \pi^2 \frac{E c A_c s}{K L^2}} \tag{2.9}$$

$$a_c = \frac{h_c + h_t}{2} - a_t \tag{2.10}$$

$$a_t = \frac{\gamma_c E_c A_c (h_c + h_t)}{2(\gamma_c E_c A_c + E_t A_t)} \tag{2.11}$$

The γ-factor describes the composite action of the TCC structure, and its value varies from 0 to 1. For full composite action $\gamma = 1$, which occurs for an infinitely stiff. The closer γ is to 1, the stiffer the connection.

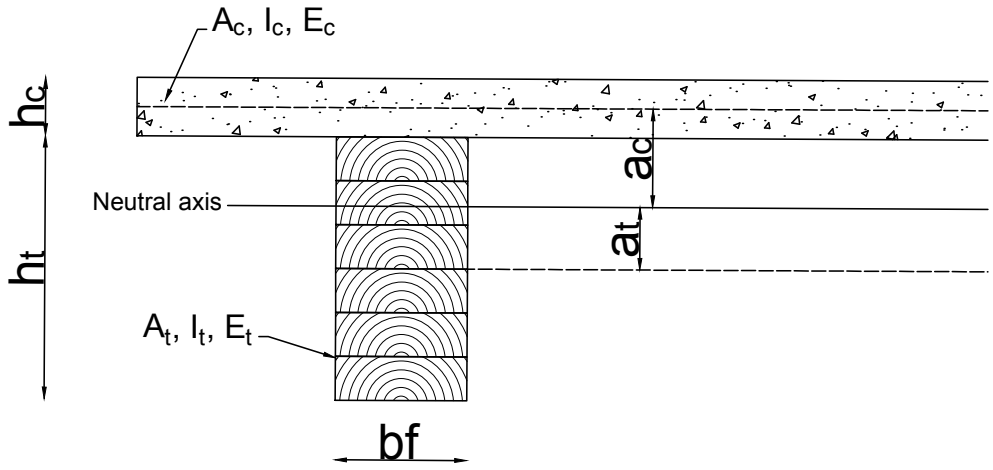

Figure 2.11: Illustration of dimensions used in γ-method.

The stresses in the TCC cross section are defined according to Equations 2.12 and 2.13. σ_i is the stress coming from the composite action of the connection, and $\sigma_{m,i}$ is the flexural stress. The sum of these stresses is the total normal stress in the component.

$$\sigma_i = \frac{\gamma_i E_i a_i M}{(EI)_{eff}} \tag{2.12}$$

$$\sigma_{m,i} = \frac{0,5 * E_i a_i M}{(EI)_{eff}} \tag{2.13}$$

The shear stress in TCC systems is assumed to be worst in the timber part of the system. The shear stress in timber is calculated according to Equation 2.14, where t_v is the distance from the bottom of the timber beam to the centroid of composite action. The shear force in the fastener is calculated according to Equation 2.15.

$$\tau_{t.max} = \frac{0,5 E_t h_v}{(EI)_{eff}} V_{Ed} \tag{2.14}$$

$$F_i = \frac{\gamma_i E_i A_i a_i s_i}{(EI)_{eff}} V \tag{2.15}$$

2.6.2 Slip modulus

K is the slip modulus, or the stiffness of the connection. To determined the slip modulus, there are different formulas depending on type of connection. When SLS design is considered, the slip modulus is noted as K_{ser}. In ULS design, the slip modulus is noted as K_u, where the slip modulus is a reduced value of K_{ser}, see Equation 2.16.

$$K_u = \frac{2}{3} K_{ser} \tag{2.16}$$

In SIS-CEN/TS 19103, 2022, the slip modulus of different types of connections is described. For dowel type fasteners Equation 2.17 and 2.18 is used. Equation 2.17 is used for dowels, bolts screws and nails (with predrilling). Equation 2.18 is used for nails (without predrilling). ρ_m is the mean value of timber density and d is the fastener diameter.

$$K_{ser} = 2\frac{\rho_m^{1.5} d}{23} \tag{2.17}$$

$$K_{ser} = 2\frac{\rho_m^{1.5} d^{0.8}}{30} \tag{2.18}$$

For fasteners with steel rebar glued into timber perpendicular to the shear plane, Equation 2.19 is used to calculate the slip modulus.

$$K_{ser} = 0,10 * E_t * d \tag{2.19}$$

The slip modulus of notched connections can be calculated according to Equation 2.20, where h_n is the depth of the notch. The slip modulus for ULS can be assumed as the same as in SLS. Linear interpolation can be used for notches with a height between $20mm$ and $30mm$.

$$K_{ser} = K_u = \begin{cases} 1000 \dfrac{N/mm}{mm} & \text{for } h_n = 20mm, \\ 1500 \dfrac{N/mm}{mm} & \text{for } h_n \geq 30mm. \end{cases} \tag{2.20}$$

2.6.3 Load-carrying capacity of connections

To ensure that the connections in TCC systems have enough strength to carry the load between the concrete slab and the timber beams, the load carrying capacity of the connection has to be verified. The method for determining the load carrying capacity is dependent on the type of fastener.

According to SIS-CEN/TS 19103, 2022, for dowel type fasteners, the load carrying capacity should be determined by using Johansen models for timber to timber connections in single shear. This method is given in Chapter 8 of SS-EN 1995-1-1, 2004. The characteristic embedded strength of the concrete member can be taken as 3 times the characteristic compression strength of concrete. This can be done if the embedded length of the fastener in the concrete member is at least three times the diameter of the fastener. For notched connections, load carrying capacity is taken as the minimum value of 4 failure modes. The formulas for these failure modes are given in Chapter 10 of SIS-CEN/TS 19103, 2022.

2.6.4 Long term effects

Several long term effects occur in the different components of a TCC system. To account for these effects, the stiffness of each part is reduced by a specific factor. The adjustment for long term effects is made individually for each component in the system. In TCC systems, the period between three to seven years can be particularly critical. This is because the rate of creep in concrete is relatively high during this time, when compared to that of timber (Dias et al., 2018). After this period, the creep in concrete becomes minimal, whereas the creep deformation in timber is more gradual and continues over a longer period.

SLS

In SLS, each stiffness of the members is reduced according to Equation 2.21-2.23.

$$E_{c.fin} = \frac{E_c}{1 + \varphi(t, t_0)} \tag{2.21}$$

$$E_{t.fin} = \frac{E_t}{1 + k_{def}} \tag{2.22}$$

$$K_{fin} = \frac{K_u}{1 + 2k_{def}} \tag{2.23}$$

For concrete, the MOE is reduced with the creep factor φ. The creep of concrete is analyzed according to Eurocode 2. For timber, the MOE is reduced with the long term factor k_{def}. This factor depends on the service class of the timber. For higher service classes, the timber is exposed to more humidity and outside air, which leads to more creep in the timber member. Therefore, service class 3 gives a higher value of creep, and the lower service classes provides lower values for k_{def}.
For the connection, the slip modulus is reduced with the creep factor of timber k_{def}. However, the reduction factor is twice as high for the connection.

ULS

In ULS, each stiffness of the members is reduced according to Equation 2.24-2.26.

$$E_{c.fin} = \frac{E_c}{1 + \psi_{conc}\varphi(t, t_0)} \tag{2.24}$$

$$E_{t.fin} = \frac{E_t}{1 + \psi_{tim}k_{def}} \tag{2.25}$$

$$K_{fin} = \frac{K_u}{1 + \psi_{conn}2k_{def}} \tag{2.26}$$

During design of TCC elements in ULS in long term loading, the stiffness of each element is reduced by the creep factor of each material as in the SLS design procedure. Additionally, a ψ-factor is multiplied with the creep factor, see Table 2.2. This factor is included to consider the composite action of TCC systems during long term loading.

Table 2.2: Modification of creep coefficients for composite action in slab systems (where $b_{tim} = b_{conc}$ and $\frac{1}{5} < \frac{A_{conc,ef}}{A_{tim}} \leq 1$) and in beam systems (where $\frac{b_{conc,ef}}{b_{tim}} > 5$ and $1 < \frac{A_{conc,ef}}{A_{tim}} \leq 5$)[a].

	for $t = \infty$	**for $t = 3$ to 7 years**
Concrete, $\varphi = 3.5$:		
$k_{def} = 0.6$	$\psi_{conc} = 2.6 - 0.8\gamma_1^2$	$\psi_{conc} = 2.5 - \gamma_1^{1.1}$
$k_{def} = 0.8$	$\psi_{conc} = 2.3 - 0.5\gamma_1^{2.6}$	$\psi_{conc} = 2.2 - 0.8\gamma_1^{1.2}$
Concrete, $\varphi = 2.5$:		
$k_{def} = 0.6$	$\psi_{conc} = 2.0 - 0.5\gamma_1^{1.9}$	$\psi_{conc} = 1.9 - 0.6\gamma_1^{1.1}$
$k_{def} = 0.8$	$\psi_{conc} = 1.8 - 0.3\gamma_1^{2.5}$	$\psi_{conc} = 1.7 - 0.5\gamma_1^{1.1}$
Timber:		
All cases	$\psi_{tim} = 1.0$	$\psi_{tim} = 0.5$
Connection:		
All cases	$\psi_{conn} = 1.0$	$\psi_{conn} = 0.65$
NOTE: For $t = 0$, the values of ψ_{conc}, ψ_{tim}, and ψ_{conn} are 0.		
[a] Linear interpolation may be used for different creep coefficients of timber and concrete.		

2.7 Production

According to Fragiacomo et al., 2018, TCC bridges have benefits in the production stage compared to reinforced concrete systems. There are two main production methods used for TCC bridges, cast in-situ and prefabrication.

2.7.1 Prefabrication

Prefabricated TCC systems can be done in several ways. There are two main types of prefabricated TCC bridges. The first way of production is to manufacture the timber parts and the concrete parts separately and assembling the parts on the construction site. To create a good composite action, glued connections is a viable option for prefabricated elements. For connections with mechanical fasteners, these are preferably cast into concrete. In these cases, the space for the fasteners and a space around them is left free. When assembled, these spaces are filled with epoxy concrete.

The other method is to cast the concrete on top of the timber beams in the factory and transport the whole system to the construction site. This production method is beneficial for bridges with a short span or widths, but gets more complicated in terms of transportation for bridges with large spans or widths.

2.7.2 Cast in situ

One of the two main ways to manufacture a TCC system is to use cast in situ. This means that the concrete is casted on top of the timber beams. The issue with this method is that the timber beams must carry the self weight of the concrete during the curing process, when the fresh concrete has no or low strength. However, this could be positive compared to standard concrete bridges, where the casting frame and the fresh concrete need to be held by temporary structures. This might also be necessary with TCC systems, but the timber beams can carry parts of the load coming from the self weight of the fresh concrete.

If the weight of the fresh concrete cannot be carried by the timber beams alone, the casting of the concrete can be divided into parts. Therefore, the concrete can achieve composite action at certain strategic locations along the bridge and add strength to the structure. With this method, temporary structures or supports may be avoidable.

For longer spans, temporary structures may be unavoidable. Temporary supports can be placed in one or a few places along the bridge to support the timber beams. Moreover, the casting form can be built on top of the timber beams and the concrete can be casted. As described in the previous method, it can be beneficial to divide the castings in steps, to give strength in some parts of the structure before adding all of the self weight of the concrete.

2.8 Life cycle assessment (LCA)

In Swedish Standard SS-EN ISO 14040, 2006, Life Cycle Assessment (LCA) is described. LCA covers the whole life cycle of a product in order to review the environmental impact of the product. When analyzing the environmental impact of a product, the contributions from each part of the life cycle can be acknowledged. When the source of environmental impacts are known, these can be assessed and possibly improved on. There are four phases needed to conduct an LCA:

1. Defining goal and scope
2. Analyze inventory
3. Impact assessment
4. Interpretation

2.8.1 Goal and scope definition phase

The first step in a LCA is to define its goal and scope. The goal should specify the purpose of the assessment, the intended audience, the reason for conducting the study, and how the results will be used. For example, whether the LCA is comparative or intended for public disclosure. The scope should clearly describe the product being studied, its function, and the functional unit. It must also define the system boundaries, allocation procedures, impact categories, assumptions, limitations, data requirements, the type of critical review, and how the results will be presented.

2.8.2 Life cycle inventory analysis phase (LCI)

The second phase of an LCA is the life cycle inventory analysis phase, where the data is collected and the calculations are made. This phase is an iterative process, as more information about the system is acquired during the process. The LCI begins with collecting data for each of the processes in the life cycle of the product. This includes the energy usage, raw materials, and other inputs. Also, the outputs need to be accounted for. All products at the end of life, waste, emissions and other environmental aspects. After collecting the data, procedures for calculation are needed. The data needs to be validated and related to the correct process and the reference flow of the functional unit.

2.8.3 Life cycle impact assessment phase (LCIA)

The next phase of an LCA is the impact assessment. This phase determines the potential environmental impact with the result of the previous phase. This process is based on inventory data sorted into environmental impact categories. LCIA can be iterative and correlate with the scope and goal of the study to see if they are fulfilled. Consequently, the goal and scope might need to be revised. Factors in this phase can introduce subjectivity in the LCIA. Therefore, transparency in the reporting of this phase is required to guarantee the quality of the LCA. The LCIA

phase can be divided into elements:

- the elements in LCIA is clearly defined
- the scope and goal reflects every element in LCIA
- quality evaluation of the methods and assumptions for each element
- transparency of methods, assumptions and other actions within every element
- transparency of values and subjectivity of every element

There are also limitations of LCIA; it only addresses the aspects given in the goal and scope. Therefore, LCIA is not a complete valuation of the environmental impact of the system studied.

2.8.4 Life cycle interpretation phase

In the interpretation phase, the results from the LCI and the LCIA are considered. The interpretation phase should produce results that reflects the goal and scope of the LCA and should include conclusions and recommendations.

2.8.5 Klimatkalkyl

The Swedish Transport Administration, Trafikverket, has developed a tool called Klimatkalkyl, or Climate Calculation, that quantifies energy use and climate impact of infrastructure projects. The tool is useful in LCA, as it provides standardized methods for estimating emissions associated with construction, operation, and maintenance. Klimatkalkyl takes material usage into account, as well as emissions from the construction phase such as transportation of materials and maintenance throughout its lifetime. However, it is important to note that Klimatkalkyl does not account for end of life recycling or material reuse.

2.9 Life cycle cost assessment (LCC)

Life cycle cost (LCC) is the process of quantifying a products cost throughout its lifetime, serving as a good evaluation for decision making (SS-ISO 15686-5, 2022). LCC should, however, be combined with other evaluations, such as LCA, safety assessment and functionality assessment, to provide a solid foundation for decision making. Furthermore, it is of high importance to clarify what costs are included and what cost are excluded, which results in a clarity for the decision making.
LCC is a part of the whole life cost, where externalities, non construction costs and income are accounted for. According to SS-ISO 15686-5, 2022, LCC is comprised of four categories;

- Construction - Cost related to project design, material cost, formwork and work site.
- Operation - Cost related to insurance, utility and taxes.
- Maintenance - Cost related to repairs, replacement, cleaning and redecoration.
- End of life - Cost related to demolition and disposal.

To perform a sufficient LCC analysis, the scope of the analysis should be clear and defined, as well as the intention of the project and the expected outcomes. When the scope is clear, it is easier to understand what types of cost should be included. This report will focus on TCC bridges and will be evaluated against a conventional concrete integral bridge. The scope of the LCC analysis is to compare the bridge types in terms of cost related to construction, materials and maintenance. Cost related to insurance and taxes are off less importance for the specific scope.

SS-ISO 15686-5, 2022 also addresses the importance of the impact of early decision making. The earlier an improvement is presented in the life cycle, the higher potential for improvement and lower cost, and vice versa.

2.10 Reference bridge

For reference in the following case study, a concrete integral bridge in one span is used. The bridge has been designed by Inhouse Tech AB. The bridge is part of road 315 in Ånge kommun, Västernorrlands län, Sweden. The bridge spans over the river Länsterån, 3 kilometers east of Överturningen.

The prerequisites from the reference bridge is used in design for the TCC bridge. This includes loads, span length and site conditions. The theoretical span length of the reference bridge is $16,4m$. The width is $7,5m$, which allows for two traffic lanes. The bridge abutments are supported by drilled steel piles. The concrete bridge is designed for life length L100 (120 years).

3
Methods

This chapter describes the methodology used in the thesis. It includes the design process of a TCC bridge with three different connection types, as well as the methods used for the LCA and LCC assessments.

3.1 Design procedure

The design procedure for the TCC bridge was performed in Mathcad Prime 10.0.0.0. The design was made in nine separate files, one for each time stamp and for the three connections. The first file was for short term analysis, the second for the time period 3-7 years, and the third for end of life analysis of 80 years. The end of life time stamp was in accordance with the theoretical length of the service life of the bridge. Each Mathcad file included both ULS and SLS analysis.

3.1.1 Input data

The design process started with defining the material properties. Concrete class C35/45 was chosen due to the exposure class of the edge beam, and glulam beams with strength class GL30c was chosen as well. Furthermore, the geotechnical prerequisites was defined as well as the properties of the different types of connections. Moreover, the preliminary dimensions of the cross section was stated, as well as an effective width of the slab. As the design procedure is an iterative process, the dimensions were redefined during the design to optimize the system. However, some geometries were fixed from the start, such as the length and width of the bridge as stated in Chapter 2.10. These geometries are fixed in order to perform a good case study comparison.

3.1.2 Loads

When the input data was determined, the next step was to determine the loads. As explained in Chapter 2.2, there are different types of loads subjected to the bridge, and each load has its unique time duration and applied direction. First, the self weight was calculated. Since the production method was not determined, the possibility of cast in situ had to be taken into account. During the in situ casting of a concrete slab on top of glulam beams, the concrete has no strength but all of its weight. No composite action is obtained, and thus the glulam beams have to be

verified against lateral torsional buckling of the beams.

Also, this phenomenon creates a difference in creep duration for the timber and concrete. The combined self weight will create an initial deflection of the system with only the timber beams stiffness. The initial deflected position is where the concrete will harden and create the composite effect. As a result, there will be a higher permanent load acting on the timber, which creates an increase of creep for the timber. However, this is beneficial for the concrete since less permanent loads and thus less creep will arise. The concrete is only subjected to permanent loads from the pavement. This difference in permanent loads has to be taken into account for the two materials for the time dependent stress calculations.

After the self weight was calculated, the traffic loads had to be determined. This was done, as explained in Section 2.2.3, by using Load Model 1 (LM1) from SS-EN 1991-2, 2003. In LM1, traffic lanes are positioned on the bridge which represents distributed loads and axle loads from traffic. To take the worst load position into consideration, the traffic lanes was positioned as far to one side as geometrically possible. This approach is called "Lane factor", which calculates the worst amount of load acting on one beam in the system. This gives a factor to increase the load acting on one beam, and one lane factor is calculated for boogie loads and UDL each. Figure 3.1 illustrates the worst traffic load positioning for a beam, which is then used to calculate the lane factor. The traffic loads and self weight causes bending moment in the longitudinal and transversal direction.

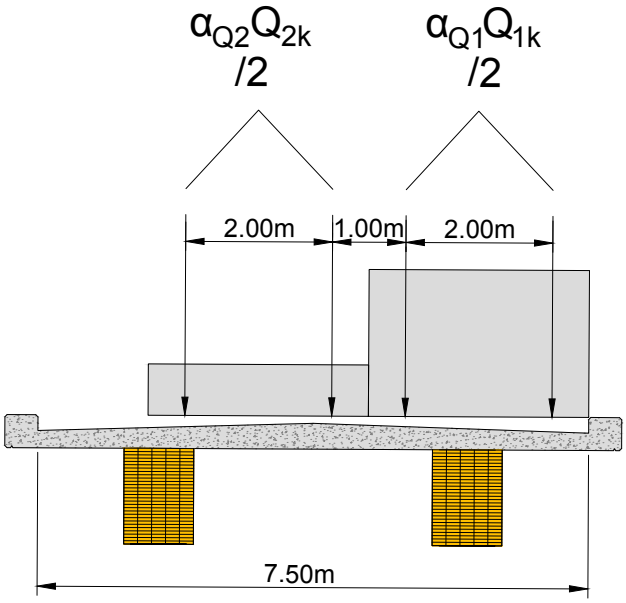

Figure 3.1: Traffic load placement for calculating the lane factors

With the calculated lane factor, traffic loads were determined. The traffic loads act both vertically and horizontally. The horizontal component arises from braking forces and surcharge. In addition, earth pressure was calculated for at rest, passive,

and active conditions, along with the additional pressure caused by thermal expansion of the bridge. Earth pressure, surcharge, braking force, and thermal expansion each generate moments in the end cantilever and over the support. These moments depend on both the magnitude of the forces and their points of application. The lever arms of the horizontal forces are influenced by the load distribution. For the surcharge, the lever arm is calculated as the distance between the centroid of the rectangular distributed load and the neutral axis. For the remaining horizontal loads, the lever arm is based on the distance from the centroid of a triangular load distribution to the neutral axis.

3.1.3 Long-term effects

Several long term effects were considered in the case study to produce a good comparison. Each effect are influenced by factors such as load duration, material properties, environmental conditions, and whether the analysis is performed for ULS or SLS. These long term effects need to be identified and categorized accordingly.

To evaluate creep for each component of the composite system, the final concrete creep was first calculated in accordance with SS-EN 1992-1-1, 2005. Based on the final concrete creep as well as an initial gamma value, Table 2.2 was then used to determine the creep coefficients for the three defined time steps, as well as for each material. The calculations were carried out for both ULS and SLS conditions. When creep was calculated, the MOE could be determined for each load and timestamp. Figure 3.2 provides an overview of the creep calculation process. Self weight and earth pressure are permanent loads, which causes creep to reduces the MOE and thus the stiffness. In contrast, traffic load is considered an instant load and is therefore not affected by creep. For temperature loads, a creep coefficient of 0.3 was used to reflect long term effects for concrete.

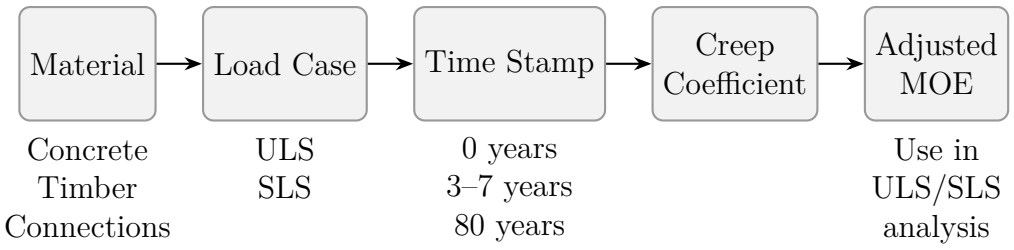

Figure 3.2: Flowchart of creep calculations.

The long terms effect of the TCC structure is analyzed 3-7 years and 80 years. The bridge is assumed to have a theoretical life span of 80 years. Therefore, this time stamp was analyzed. Specific for TCC structure is that concrete and timber have different rates of the creep in the two materials (Dias et al., 2018). Therefore, the technical specification (SIS-CEN/TS 19103, 2022) suggest to check the long terms effect in the time stamp 3-7 years into the service life of the bridge.

3.1.4 Effect of inelastic strains

In SIS-CEN/TS 19103, 2022 the effects of inelastic strain is described. Inelastic strain is strains that are not caused by stress, but by shrinkage, swelling and and thermal expansion. To consider the effect of inelastic strains in TCC systems, the method in SIS-CEN/TS 19103, 2022, Appendix B is used. The total strains from shrinkage, swelling and thermal expansion is added together by using a factor from Appendix B. The strains can be converted into a fictitious load acting on the structure. This fictitious load is based on the different parameters of the materials in the TCC system, and it creates an additional moment. The inelastic strains influence the effective bending stiffness,by a factor that reduces the effective bending stiffness from the γ-method. The effect of inelastic strain is done separately for the 3 time stamps.

3.1.5 Determination of stresses

The bending stiffness was calculated according to the γ-method, see Section 2.6.1 for more details. This was done separately for each unique combination of time stamp and load. With the bending stiffness known, as well as the calculated moment from Section 3.1.2, the internal stresses in the cross section could be determined. According to the γ-method, the moment in the cross section causes two separately calculated stresses: one stress from bending, and a normal stress caused by the composite action. The separation of bending and normal stresses were performed to take the different strength properties of timber into consideration. The stress calculations were done separately for concrete and timber, and at the top and bottom of the two members. The analysis checked the capacities at two sections. The first check was in the middle of the span where the highest bending moment occurs. The second check was over the support, where the maximum negative moment and largest shear force occur. Moreover, the maximum shear stress and the fasteners load was calculated. This was checked over the support, where the largest shear force occur, due to both being dependent on the shear force.

3.1.6 Load combinations

The load combinations in ULS were done according to load combination model 6.10a and 6.10b in SS-EN 1990, 2002, explained in detail in Section 2.2. In SLS, the loads were combined in; a characteristic combination, a frequent combination and a quasi-permanent combination. All combinations were done at the two sections and at the top and bottom of each material, as well as for the connections. The load combination of stresses were calculated twice to determine both the maximum and the minimum stresses, which both can be governing for each material. When load combining stresses, a differentiation between favorable and unfavorable stresses for permanent and variable loads had to be done. If a variable load was favorable, it could set to zero in order to get the worst stresses. However, a permanent load that is favorable can not be neglected and has to be taken into account.

3.1.7 Capacity checks

When the load combinations were completed, capacity checks were performed. This was done in order to determine the total utilization of each component and to optimize the TCC bridge.

Capacity of the TCC superstructure

The capacity was checked for each load combination in ULS. The stresses were compared against the corresponding material strengths. For concrete, the bending and shear stress components were summed, as concrete has the same strength in all directions. The stresses was checked if it was in tension or compression, and the appropriate material strength was selected accordingly to ensure a correct comparison. For timber, all stress components were treated separately and checked against the corresponding strength. Bending stresses were compared to the bending capacity, tensile forces to the "tension parallel to grain" strength, and compressive forces to the "compression parallel to grain" strength. The utilization ratios of the individual components were then summed to determine the total utilization.

Deflection

To calculate deflection, the frequent load combination for SLS was used. In normal deflection calculations, only the frequent traffic loads should be used. Thus, the calculated deflection in this report is conservative. Deflection was calculated at mid span and checked to be less than 1/400 of the span length. Further, the end console was checked for both downward and upwards deflection, which had to be less than 5 millimeters.

Connections

To verify the load carrying capacity for the fasteners, the methods provided in Section 2.6.3 was used to determine the capacity for each failure mode. The failure mode with the lowest capacity was used to determine whether the capacity was enough to carry the load. The procedure was iterative, and the dimensions of the fasteners was changed to resist the load acting on the fastener.

Other capacity checks

Furthermore, the lateral torsional buckling capacity was calculated. This was done by comparing the moment the glulam beams were subjected to during casting of the concrete slab with the elastic critical moment for lateral torsion. Concrete cracking over the support was evaluated by comparing the concrete tensile capacity to the tensile stresses resulting from the loading. Crack width was calculated according to Chapter 7.4.2 in SS-EN 1994-1-1, 2005, and compared to the maximum crack width of 0.20 millimeters. Bearing stress perpendicular to grain was verified according to Chapter 6.1.5 in SS-EN 1995-1-1, 2004.

3.2 LCA

To conduct the LCA comparison in the case study, the tool Klimatkalkyl was used. Klimatkalkyl is divided into several modules, each corresponding to different phases of an infrastructure project. Figure 3.3 illustrates a flowchart off the different modules from Klimatkalkyl. The first step involves defining the type of construction, referred to as "Predefined Measures - Construction and Reinvestment". As earlier explained, the case study will compare two bridge types, a concrete integral bridge and a TCC bridge, and the appropriate bridge type will be specified accordingly. The predefined measure approach ensures accurate representation of emissions from all construction phases, including maintenance, geological work and on site activities.

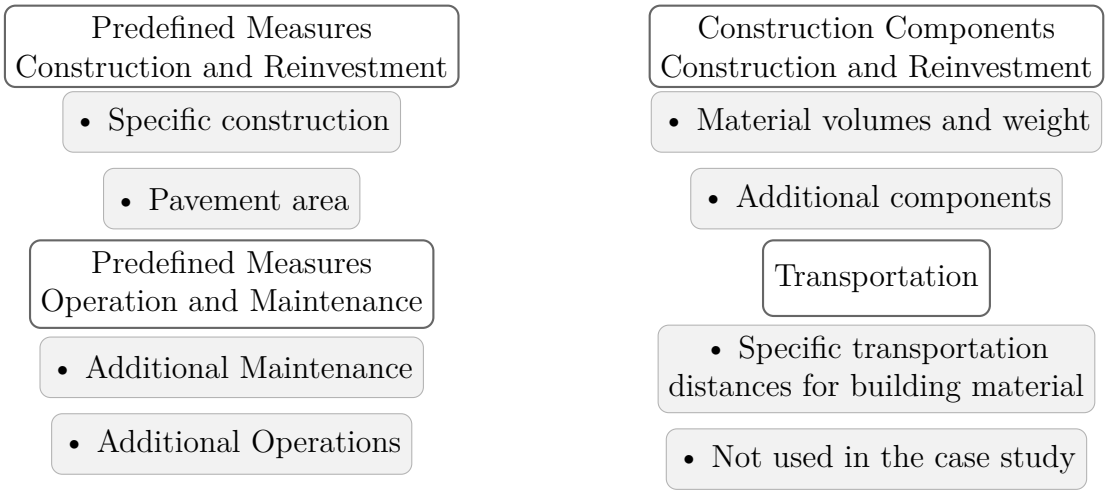

Figure 3.3: Structure of the tool Klimatkalkyl.

Predefined measures are based on emission factors derived from reports and previous studies on similar constructions. There are no predefined measures for the TCC bridges in the case study. However, further investigation of alternative predefined measures resulted in two alternatives. The first alternative was a timber road bridge, where a report by Pousette et al., 2014 was the foundation in the tool Klimatkalkyl from which predefined measures are retrieved. Pousette et al., 2014 conducted an LCA comparison of a built reinforced concrete superstructure to that of an alternative timber superstructure. The predefined geometry of the bridge from the report was similar to the predefined geometry in this case study, with a difference in span length of one meter and the same bridge width. The maintenance procedures taken into account for the timber bridge included repainting of the timber, as well as replacement of the side panel and the pavement.

The second alternative regarding predefined measures was a concrete slab bridge in which emission values were taken from an average of 96 similar bridge types. The maintenance procedures taken into account for the concrete slab bridge included replacement of the pavement and the edge beam. When investigating and comparing what was included in the two different predefined measures, the concrete slab

bridge was the most similar to the TCC bridge in the case study. This was because the concrete slab bridge maintenance included replacement of the edge beam, which was similar to the maintenance required of the concrete slab on the TCC bridge. As a result, the concrete slab predefined measures were chosen in the tool Klimatkalkyl.

Following the predefined measures phase, the next phase was "Construction Components – Construction and Reinvestment". Materials such as glulam, concrete, and reinforcement were specified in terms of volume and weight. These values were manually calculated for each bridge type and then inserted into the program. The calculated material data is presented in Appendix A. The next phase allowed for the addition of maintenance related emissions. However, in most cases, operation and maintenance emissions were already included in the initial phase. The final step of the process relates to transportation emissions. Klimatkalkyl includes standard values for the transport of construction materials and equipment, but users can enter specific values if location and data are available.

Once all input data had been provided, Klimatkalkyl calculated the total climate impact and energy use. The results were presented as a detailed Excel output, presented in Appendix B, categorized by material type and predefined measures, as well as summarized by the total emissions for the entire construction process.

3.3 LCC

The life cycle cost assessment was carried out with the guidance and support of two supervisors, Daniel Josefsson and Samuel Wiik, who referred to previous budgets from construction projects undertaken by Inhouse Tech. In addition, industry partners working closely with Inhouse Tech provided valuable input regarding costs related to construction, maintenance, materials and demolition. The quantities of required materials for both the TCC bridge and the concrete bridge were calculated in the case study and used in the LCC assessment.

The LCC was structured into four main categories: *design*, *construction*, *maintenance* and *end of life*. Costs associated with the design phase primarily covered structural engineering services, such as calculations and technical drawings. Construction costs included materials such as concrete, reinforcement steel and glulam beams. Other items included in this phase were bearings, pavement, railings, formwork, crane rental, and site establishment and management.

For maintenance, the assessment considered costs for edge beam and pavement replacement, which were assumed to be the same for both bridge types. In addition, the TCC bridge required further maintenance in the form of repainting and bearing replacement. The demolition category was represented by a predicted fixed cost. Some costs were presented as fixed amounts, for example crane rental, while others were volume or area dependent, such as concrete volume or formwork area. Construction pricing can be difficult to predict, and an alternative approach is to estimate both minimum and maximum costs for each activity. The actual cost of a bridge is expected to fall somewhere within this range.

4
Results

This chapter presents the results from calculations of three different connection types. Each connection has its own section, where results are presented in tables that include the utilization ratio for each main structural element. Further, the maximum shear stress and fastener load are presented, as well as calculated deflections for mid span and end console. These calculations are presented for each of the three time stamps. Capacity checks that are not influenced by a specific connection are presented in a separate section. The outcome of the LCA and LCC case studies are also presented in separate sections. A brief interpretation of each result is included to explain the results more easily. The full discussion are presented in the following chapter.

4.1 TCC bridge with notched and dowel connections

In this section, the results from the calculations of a TCC bridge with notched and dowel connections are presented. Detailed calculations can be found in Appendix A. Figure 4.1 illustrates the preliminary design of the evaluated connection, consisting of notches measuring 150×50mm spanning the full width of the glulam beam. Dowels with a diameter of 20mm and a length of 400mm are distributed along the center to center spacing of 775mm between notches, at a rate of 16 dowels per interval. The exact dowel arrangement is not fixed in this stage, as the design is evaluated based on an average dowel density per meter rather than precise positioning. The dowels are embedded halfway in the glulam and halfway in the concrete to balance the failure modes between dowel yielding, concrete breakout, and glulam crushing.

Table 4.1 shows the critical stresses at midspan at the initial time stamp. Table 4.2 depicts the critical stresses over support at 0 year. The critical stresses are defined as the highest utilization ratio among the calculated maximum and minimum stress values. In Table 4.1-4.6, the normal and bending stresses have been separated, as explained in Section 3.1.7. The risk of cracking was calculated over the support, and since the tensile forces exceed the concrete tensile strength, cracks are expected to appear. Thus, the utilization ratio for the concrete over the support is governed by the reinforcement. The results for the critical stresses at midspan show that the highest utilization occurs at the bottom of the glulam beam, decreasing slightly when long term effects are considered. Similarly, the concrete slab experiences its highest stresses in the top region. The long term effects lead to a slight decrease in

utilization ratio of the concrete slab.

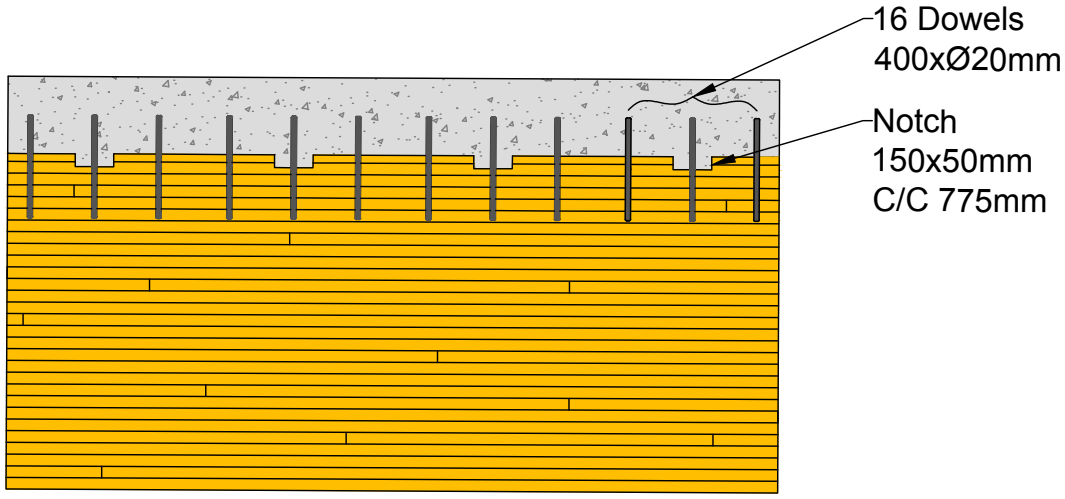

Figure 4.1: Design of the notched and dowel connection.

Table 4.1: Critical stresses in midspan at the initial time stamp for notch and dowel connection.

Notch and dowel, midspan, 0y		Critical stress [MPa]	Utilization ratio
Top of concrete	Normal	-5,79	42%
	Bending	-4,11	
Bottom of concrete	Normal	-5,79	7%
	Bending	4,11	
Top of timber	Normal	4,92	10%
	Bending	-9,69	
Bottom of timber	Normal	4,92	80%
	Bending	9,69	

Table 4.2: Critical stresses over support at the initial time stamp for notch and dowel connection.

Notch and dowel, support, 0y		Critical stress [MPa]	Utilization ratio
Reinforcement at top of concrete	Normal	41,03	13%
	Bending	17,10	
Reinforcement at bottom of concrete	Normal	41,03	6%
	Bending	-17,10	
Top of timber	Normal	-0,64	22%
	Bending	5,64	
Bottom of timber	Normal	-0,64	30%
	Bending	-5,64	

Table 4.3 shows the critical stresses at midspan at 3-7 years. Table 4.4 depicts the critical stresses over support at 3-7 years. The reason for checking time stamp 3-7 years is because the difference in creep between timber and concrete can be governing. The utilization ratios for the midspan is similar to the utilization ratios for the initial time stamp. However, a difference in critical stresses can be seen in terms of a larger proportion of bending stresses and lower for normal stresses. The critical stresses over support follow the same trend as the midspan results.

Table 4.3: Critical stresses in midspan at 3-7 years for notch and dowel connection.

Notch and dowel, midspan, 3-7y		Critical stress [MPa]	Utilization ratio
Top of concrete	Normal	-5,45	38%
	Bending	-3,53	
Bottom of concrete	Normal	-5,45	8%
	Bending	3,53	
Top of timber	Normal	4,61	13%
	Bending	-9,90	
Bottom of timber	Normal	4,61	79%
	Bending	9,90	

Table 4.4: Critical stresses over support at 3-7 years for notch and dowel connection.

Notch and dowel, support, 3-7y		Critical stress [MPa]	Utilization ratio
Reinforcement at top of concrete	Normal	41,86	14%
	Bending	17,82	
Reinforcement at bottom of concrete	Normal	41,86	6%
	Bending	-17,82	
Top of timber	Normal	-0,65	22%
	Bending	5,53	
Bottom of timber	Normal	-0,65	29%
	Bending	-5,53	

Table 4.5 shows the critical stresses at midspan at the end of life. Table 4.6 depicts the critical stresses over support at the end of life. In this timestamp, the final long term effects are obtained, and the lowest utilization ratios are generated. The critical stresses and the utilization ratios for the midspan and over support are similar to the results for 3-7 years.

Table 4.5: Critical stresses in midspan at 80 years for notch and dowel connection.

Notch and dowel, midspan, 80y		Critical stress [MPa]	Utilization ratio
Top of concrete	Normal	-5,48	39%
	Bending	-3,57	
Bottom of concrete	Normal	-5,48	8%
	Bending	3,57	
Top of timber	Normal	4,64	13%
	Bending	-9,87	
Bottom of timber	Normal	4,64	79%
	Bending	9,87	

Table 4.6: Critical stresses over support at 80 years for notch and dowel connection.

Notch and dowel, support, 80y		Critical stress [MPa]	Utilization ratio
Reinforcement at top of concrete	Normal	43,4	14%
	Bending	18,9	
Reinforcement at bottom of concrete	Normal	43,4	6%
	Bending	-18,9	
Top of timber	Normal	-0,66	22%
	Bending	5,51	
Bottom of timber	Normal	-0,66	29%
	Bending	-5,51	

Table 4.7 presents the highest calculated shear stresses and utilization ratios over support for three time stamps. The difference in shear stresses for each time stamp is very low. Table 4.8 presents the maximum fastener load for notch and dowel connection at three time stamps. The utilization ratio increases with time, resulting in an almost full utilization ratio in the end of life time stamp.

Table 4.7: Maximum shear stresses at 3 time stamps for notch and dowel connection.

Time stamp	τ_{max} [MPa]	Utilization
0 years	1,98	78%
3-7 years	1,98	78%
80 years	1,99	79%

Table 4.8: Maximum fastener load at 3 time stamps for notch and dowel connection.

Time stamp	F_{Ed} [kN]	F_{Rd} [kN]	Utilization
0 years	2016	2116	95%
3-7 years	2044	2116	97%
80 years	2072	2116	98%

Table 4.9 presents the calculated deflections for critical sections and different time stamps. Midspan deflection calculations are presented in Appendix A. To get the utilization ratio, the calculated deflection are compared with the deflection requirement limit of 1/400 of the span. The highest deflections in midspan occur in the end of life time stamp. Two deflection checks for the end console are presented, one for downward deflection and one for uplift deflection. The calculated deflections are compared to the deflection requirement limit of 5 mm to get the utilization ratio. The downward deflection have a low utilization ratio, but the uplift deflection is close to full utilization. The highest utilization ratio occur in the end of life time stamp.

Table 4.9: Deflections for notch and dowel connection.

Deflection notch+dowel	**0 years**		**3-7 years**		**80 years**	
	w [mm]	**Util.**	**w [mm]**	**Util.**	**w [mm]**	**Util.**
Midspan	21,4	52%	34,0	83%	34,1	83%
Deflection end console	0,17	3%	0,3	6%	0,3	6%
Uplift end console	3,95	79%	4,42	88%	4,42	88%

Interpretation of the results from notch and dowel connection

The results indicate that the notch and dowel connection achieves high utilization ratios at midspan, particularly in the bottom of the timber beam, while the concrete remains low utilized. The utilization ratios are relatively constant across all time stages, which reflects the balance between increasing bending stresses and decreasing normal stresses due to long term effects. Shear and fastener utilization increase slightly over time, which is as expected because of the reduction in stiffness over time. Deflections at midspan increases with time, confirming the effect of influence of creep which lowers the stiffness. Overall, the connection offers good composite action and ductility but leads to increased normal stresses in the timber, which slightly reduces the structural efficiency.

4.2 TCC bridge with dowel connections

In this section, the results from the calculations of a TCC bridge with dowel connections are presented. Detailed calculations can be found in Appendix A. The preliminary design are presented in Figure 4.2, where six dowels are placed in a row at the width of each glulam beam. The distance between each row are 100mm, and the dowels have a diameter of 16 mm and a length of 200 mm, embedded halfway in the glulam and halfway in the concrete slab.

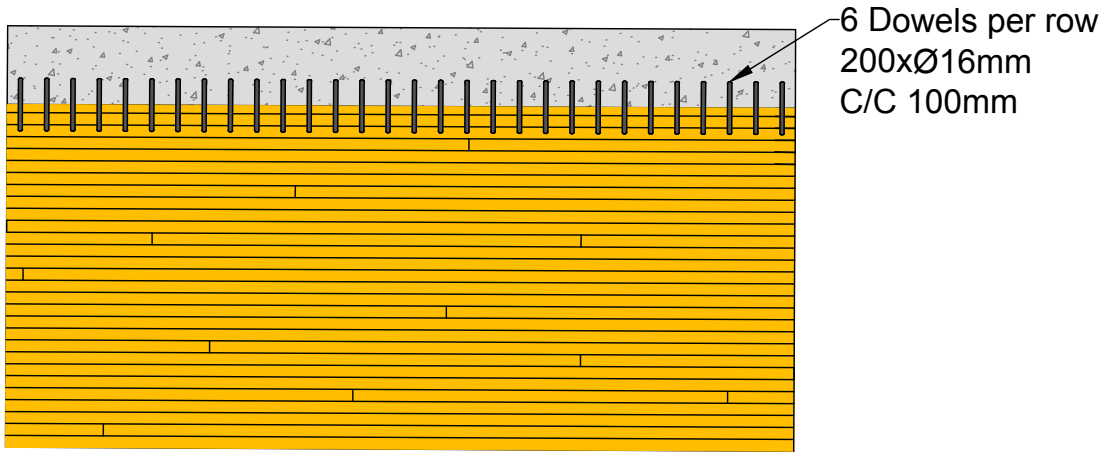

Figure 4.2: Design of the dowel connection.

To create continuity, all three section of connections will present results in a similar way. Table 4.10 presents the critical stresses at midspan at the initial time stamp. Table 4.11 depicts the critical stresses over support at the initial time stamp. The highest utilization ratio in midspan occur in the bottom of the timber.

Table 4.10: Critical stresses in midspan at the initial time stamp for dowel connection.

Dowel, midspan, 0y		Critical stress [MPa]	Utilization ratio
Top of concrete	Normal	-4,82	41%
	Bending	-4,73	
Bottom of concrete	Normal	-4,82	0%
	Bending	4,73	
Top of timber	Normal	4,05	20%
	Bending	-10,60	
Bottom of timber	Normal	4,05	78%
	Bending	10,60	

Table 4.11: Critical stresses over support at the initial time stamp for dowel connection.

Dowel, support, 0y		Critical stress [MPa]	Utilization ratio
Reinforcement at top of concrete	Normal	37,78	13%
	Bending	17,21	
Reinforcement at bottom of concrete	Normal	37,78	5%
	Bending	-17,21	
Top of timber	Normal	-0,60	23%
	Bending	5,66	
Bottom of timber	Normal	-0,60	30%
	Bending	-5,66	

Table 4.12 shows the critical stresses at midspan at 3-7 years. Table 4.13 depicts the critical stresses over support at 3-7 years. The utilization ratio for the bottom of timber and top of concrete at midspan decreases slightly, when compared to the the initial time stamp results. The utilization over support is nearly unchanged.

Table 4.12: Critical stresses in midspan at 3-7 years for dowel connection.

Dowel, midspan, 3-7y		Critical stress [MPa]	Utilization ratio
Top of concrete	Normal	-4,44	37%
	Bending	-4,13	
Bottom of concrete	Normal	-4,44	1%
	Bending	4,13	
Top of timber	Normal	3,72	22%
	Bending	-10,38	
Bottom of timber	Normal	3,72	75%
	Bending	10,38	

Table 4.13: Critical stresses over support at 3-7 years for dowel connection.

Dowel, support, 3-7y		Critical stress [MPa]	Utilization ratio
Reinforcement at top of concrete	Normal	38,22	13%
	Bending	17,99	
Reinforcement at bottom of concrete	Normal	38,22	5%
	Bending	-17,99	
Top of timber	Normal	-0,60	22%
	Bending	5,56	
Bottom of timber	Normal	-0,60	29%
	Bending	-5,56	

Table 4.14 shows the critical stresses at midspan at the end of life. Table 4.15 depicts the critical stresses over support at the end of life. In this timestamp, the final long term effects are obtained, and the lowest utilization ratios are generated.

Table 4.14: Critical stresses in midspan at 80 years for dowel connection.

Dowel, midspan, 80y		Critical stress [MPa]	Utilization ratio
Top of concrete	Normal	-4,46	37%
	Bending	-4,16	
Bottom of concrete	Normal	-4,46	1%
	Bending	4,16	
Top of timber	Normal	3,73	21%
	Bending	-10,35	
Bottom of timber	Normal	3,73	74%
	Bending	10,35	

Table 4.15: Critical stresses over support at 80 years for dowel connection.

Dowel, support, 80y		Critical stress [MPa]	Utilization ratio
Reinforcement at top of concrete	Normal	39,33	13%
	Bending	19,11	
Reinforcement at bottom of concrete	Normal	39,33	5%
	Bending	-19,11	
Top of timber	Normal	-0,62	22%
	Bending	5,54	
Bottom of timber	Normal	-0,62	29%
	Bending	-5,54	

Table 4.16 presents the highest calculated shear stresses and utilization ratios over support for three time stamps. The shear stress results are identical for the three time stamps. Table 4.17 presents the maximum fastener load for notch and dowel connection at three time stamps.

Table 4.16: Maximum shear stresses at 3 time stamps for dowel connection.

Time stamp	τ_{max} [MPa]	Utilization
0 years	1,99	79%
3-7 years	1,99	79%
80 years	1,99	79%

Table 4.17: Maximum fastener load at 3 time stamps for dowel connection.

Time stamp	F_{Ed} [kN]	F_{Rd} [kN]	Utilization
0 years	193	244	79%
3-7 years	196	244	80%
80 years	199	244	82%

Table 4.18 presents the calculated deflections for critical sections and different time stamps. The highest deflections in midspan occur in the end of life time stamp. Two

deflection checks for the end console are presented, one for downward deflection and one for uplift deflection. The downward deflection have a low utilization ratio, but the uplift deflection is close to full utilization. The highest utilization ratio occur in the end of life time stamp.

Table 4.18: Deflections for dowel connection.

Deflection dowel only	**0 years**		**3-7 years**		**80 years**	
	w [mm]	**Util.**	**w [mm]**	**Util.**	**w [mm]**	**Util.**
Midspan	23,2	57%	35,1	86%	35,4	86%
Deflection end console	0,18	4%	0,3	6%	0,31	6%
Uplift end console	4,01	80%	4,41	88%	4,41	88%

Interpretation of the results from dowel only connection

The dowel only connection shows the lowest utilization ratios among the three connections, particularly at midspan, indicating an improved structural efficiency when compared to the notch and dowel connection. This outcome is linked to the lower degree of composite action, which results in increased bending stresses and reduced normal stresses. As explained in the previous chapter, this effect is favorable for timber, which performs better in bending. While shear and fastener utilization remain similar to the notch and dowel case, the lower γ-factor leads to reduced connection forces. However, this connection type also results in higher deflections, which may become critical in certain design scenarios.

4.3 TCC bridge with adhesive and dowel connection

In this section, the results from the calculations of a TCC bridge with adhesive and dowel connections are presented. Figure 4.3 illustrates the preliminary design of the adhesive and dowel connection. The thickness of the adhesive layer has not been specified. Table 4.19 shows the critical stresses at midspan at the initial time stamp. Table 4.20 depicts the critical stresses over support at the initial time stamp.

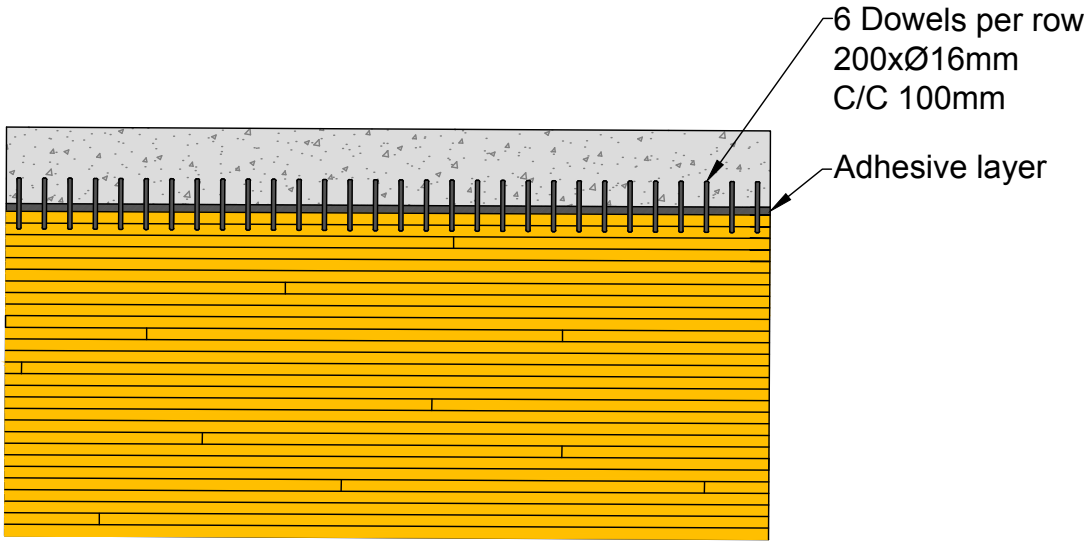

Figure 4.3: Design of the adhesive and dowel connection.

Table 4.19: Critical stresses in midspan at the initial time stamp for adhesive and dowel connection.

Adhesive, midspan, 0y		Critical stress [MPa]	Utilization ratio
Top of concrete	Normal	-6,37	44%
	Bending	-3,88	
Bottom of concrete	Normal	-6,37	11%
	Bending	3,88	
Top of timber	Normal	5,43	5%
	Bending	-9,35	
Bottom of timber	Normal	5,43	82%
	Bending	9,35	

Table 4.20: Critical stresses over support at the initial time stamp for adhesive and dowel connection.

Adhesive, support, 0y		Critical stress [MPa]	Utilization ratio
Reinforcement at top of concrete	Normal	42,93	14%
	Bending	17,29	
Reinforcement at bottom of concrete	Normal	42,93	6%
	Bending	-17,29	
Top of timber	Normal	-0,66	23%
	Bending	5,67	
Bottom of timber	Normal	-0,66	30%
	Bending	-5,67	

Table 4.21 shows the critical stresses at midspan at 3-7 years. Table 4.22 depicts the critical stresses over support at 3-7 years. The utilization ratio in the bottom of timber at midspan increases, when comparing to the utilization ratio at the initial time stamp, but is unchanged over support.

Table 4.21: Critical stresses in midspan at 3-7 years for adhesive and dowel connection.

Adhesive, midspan, 3-7y		Critical stress [MPa]	Utilization ratio
Top of concrete	Normal	-6,28	41%
	Bending	-3,4	
Bottom of concrete	Normal	-6,28	12%
	Bending	3,4	
Top of timber	Normal	5,35	8%
	Bending	-10,01	
Bottom of timber	Normal	5,35	84%
	Bending	10,01	

Table 4.22: Critical stresses over support at 3-7 years for adhesive and dowel connection.

Adhesive, support, 3-7y		Critical stress [MPa]	Utilization ratio
Reinforcement at top of concrete	Normal	44,01	14%
	Bending	17,99	
Reinforcement at bottom of concrete	Normal	44,01	6%
	Bending	-17,99	
Top of timber	Normal	-0,67	22%
	Bending	5,56	
Bottom of timber	Normal	-0,67	30%
	Bending	-5,56	

Table 4.23 shows the critical stresses at midspan at the end of life. Table 4.24 presents the critical stresses over the support at the same time. The maximum

utilization ratio occurs at midspan in the bottom of the timber at the end of life stage. At the support, the differences compared to the other two time stamps are marginal.

Table 4.23: Critical stresses in midspan at 80 years for adhesive and dowel connection.

Adhesive, midspan, 80y		Critical stress [MPa]	Utilization ratio
Top of concrete	Normal	-6,33	42%
	Bending	-3,44	
Bottom of concrete	Normal	-6,33	12%
	Bending	3,44	
Top of timber	Normal	5,39	8%
	Bending	-9,98	
Bottom of timber	Normal	5,39	85%
	Bending	9,98	

Table 4.24: Critical stresses over support at 80 years for adhesive and dowel connection.

Adhesive, support, 80y		Critical stress [MPa]	Utilization ratio
Reinforcement at top of concrete	Normal	45,81	15%
	Bending	19,07	
Reinforcement at bottom of concrete	Normal	45,81	6%
	Bending	-19,07	
Top of timber	Normal	-0,69	22%
	Bending	5,533	
Bottom of timber	Normal	-0,69	30%
	Bending	-5,53	

Table 4.25 presents the highest calculated shear stresses and utilization ratios over support for three time stamps.

Table 4.25: Maximum shear stresses at 3 time stamps for adhesive and dowel connection.

Time stamp	τ_{max} [MPa]	Utilization
0 years	1,97	78%
3-7 years	1,97	78%
80 years	1,97	78%

Table 4.26 presents the calculated deflections for critical sections and different time stamps. The downward deflection have a low utilization ratio, but the uplift deflection is close to full utilization. The highest utilization ratio occur in the end of life time stamp for all deflection checks.

Table 4.26: Deflections for adhesive and dowel connection.

Deflection adhesive+dowel	**0 years**		**3-7 years**		**80 years**	
	w [mm]	**Util.**	**w [mm]**	**Util.**	**w [mm]**	**Util.**
Midspan	19,7	48%	33,2	81%	33,2	81%
Deflection end console	0,15	3%	0,3	6%	0,3	6%
Uplift end console	3,88	78%	4,45	89%	4,45	89%

Interpretation of the results from adhesive and dowel connection

The adhesive and dowel connection has the highest degree of composite action, resulting in full interaction and the lowest deflections among the three connections. Unlike the other cases, the utilization ratio does not decrease over time, as long term effects do not change the internal force distribution when full interaction is assumed. However, despite favorable results from the deflections, the connection has the highest utilization ratios when looking at the bottom of timber at midspan. Further, the connection introduces significant uncertainties related to construction feasibility and quality assurance. While the concept shows potential from a theoretical standpoint, its practical implementation remains limited due to lack of familiarity and proven methods in real bridge projects.

4.4 Capacity checks for various structural components

In this section, other capacity checks are presented. Detailed calculations of the capacity checks are presented in Appendix A, and the results are presented in Table 4.27. The different capacity checks have different units, which are also presented in combination with the utilization ratio. The results from the calculations of bearing stress perpendicular to the grain and concrete cracking over the support indicate that full utilization has been reached.

Table 4.27: Summary of capacity checks for various structural components.

Check	**Calculated**	**Limit**	**Utilization Ratio**
Lateral torsional buckling	1.7 MNm	63.5 MNm	2.7%
Concrete cracking over support	3.4 MPa	1.5 MPa	179%
Reinforcement area to prevent critical crack width 0.20mm	235 cm^2	118 cm^2	50%
Bearing stress perpendicular to grain	3.7 MPa	1.8 MPa	206%

Interpretation of the results from various structural components

The additional capacity checks confirm that lateral torsional buckling is not a concern due to the compact cross section of the glulam beams. Cracking in the concrete above the supports is expected but effectively controlled by the large amount of reinforcement from the end console provided, ensuring that crack widths remain within acceptable limits. Lastly, bearing stress perpendicular to the grain is identified as a critical design point in the timber detailing, suggesting the need for further investigation in future work.

4.5 Results from gamma factor variations

In this section, a modification of the results is presented. To understand the influence of the γ-factor, or composite action, on the structural behavior, different γ-factors is plotted against maximum utilization in bottom of timber at midspan. The graph is shown in Figure 4.4 where the distribution is plotted for the time stamps: 0, 3-7 and 80 years.

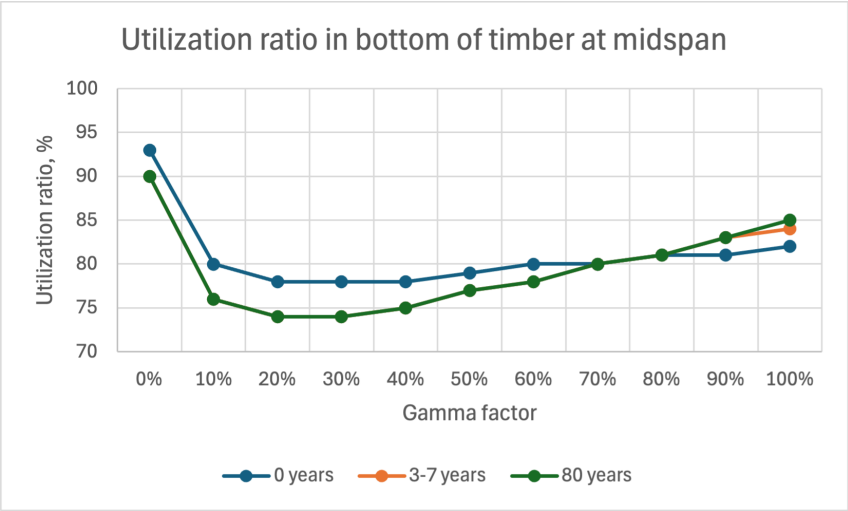

Figure 4.4: Utilization variations for bottom of timber at midspan for different gamma factors.

In Figure 4.5 the influence γ-factors has on deflection at midspan is presented. The distribution is plotted for the time stamps: 0, 3-7 and 80 years.

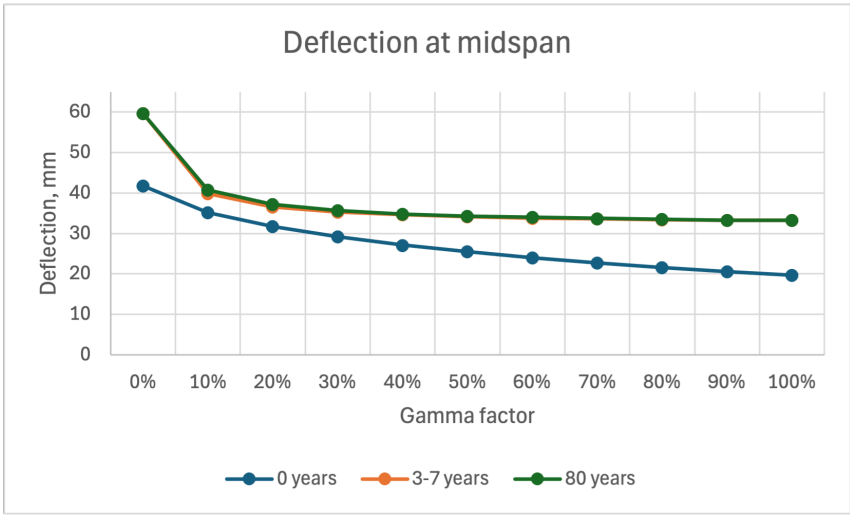

Figure 4.5: Deflection variations for different gamma factors.

Interpretation of the results for gamma factor variations

The results indicate that structural efficiency does not improve linearly with increased composite action. Instead, the lowest utilization ratio in the bottom of the timber at midspan occurs around a γ-factor of 30%, suggesting an optimal balance between bending and normal stresses. Both very low and very high interaction levels lead to higher utilization, which highlights the importance of evaluating a range of γ-factors during design. The findings also show that long term effects stabilize within the first few years of service life. Additionally, the influence of unaccounted friction between materials may affect the effective γ-factor and should be considered in future design evaluations.

4.6 Results from the LCA

In this section, the results from the LCA of the TCC bridge and the concrete integral bridge will be presented. The LCA has been conducted using the tool Klimatkalkyl, which is explained more in detail in Section 3.2. The comprehensive results from the tool Klimatkalkyl is presented in Appendix B.

Table 4.28 present the results from the LCA of the TCC bridge. The emission and energy usage are presented for the predefined measure as well as the construction materials. The total emission and energy usage are summarized at the bottom of the graph. Table 4.29 present the results from the LCA of the concrete integral bridge.

Table 4.28: Climate impact and energy use for the TCC bridge.

Phase	Unit	CO_2e (ton)	Energy (GJ)
Predefined measure			
Concrete slab bridge (reference)	215.25 m^2	139.12	1,374.42
Construction material			
Reinforcement	10.2 ton	7.47	119.51
Concrete	91.49 m^3	36.75	222.18
Glulam	44.14 m^3	2.70	501.97
Total		**186**	**2218**

Table 4.29: Climate impact and energy use for the concrete integral bridge.

Phase	Unit	CO_2e (ton)	Energy (GJ)
Predefined measure			
Concrete slab bridge (reference)	215.25 m^2	139.12	1,374.42
Construction material			
Reinforcement	19.1 ton	13.99	223.79
Concrete	165.61 m^3	66.53	402.18
Total		**220**	**2000**

Interpretation of the results from LCA

The LCA results show that the TCC bridge emits less CO_2e than the concrete bridge, primarily due to lower emissions from construction materials. However, the TCC alternative has slightly higher energy use, which is harder to interpret since the energy source could be either fossil based or renewable. The comparison is also affected by differing design life assumptions, although the LCA tool uses a service life of 80 years for both bridges. Overall, the results suggest that TCC bridges can offer environmental advantages, especially in regions with access to renewable energy and timber, though lifespan differences and maintenance needs are important factors to consider.

4.7 Results from the LCC

In this section, the results from the LCC analysis are presented. Table 4.30 shows the life cycle cost of the TCC bridge, while Table 4.31 presents the life cycle costs for the concrete integral bridge. The costs are divided into the different phases of the service life. For each bridge, both a lower and an upper cost estimate are provided. Figure 4.6 illustrates the lower and upper cost for each phase and bridge. A detailed version of the LCC assessment are presented in Appendix C. The maximum and minimum cost assessments from the LCC are obtained for the TCC bridge.

Table 4.30: LCC results for TCC bridge.

TCC bridge	**Low**	**High**
Design	350 000 kr	450 000 kr
Production	1 791 864 kr	2 427 189 kr
Maintenance	743 500 kr	893 000 kr
End of life	4 028 kr	4 834 kr
Total	2 889 392 kr	3 775 023 kr

Table 4.31: LCC results for concrete integral bridge.

Concrete bridge	**Low**	**High**
Design	200 000 kr	250 000 kr
Production	2 032 600 kr	2 496 900 kr
Maintenance	723 500 kr	868 000 kr
End of life	3 222 kr	4 028 kr
Total	2 959 322 kr	3 618 928 kr

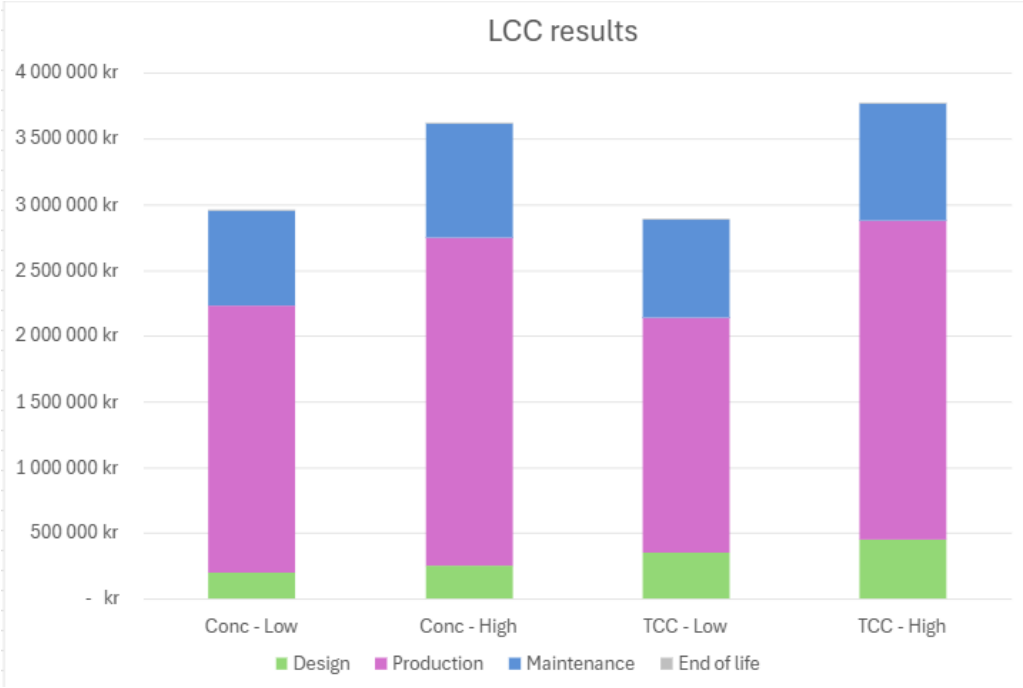

Figure 4.6: Maximum and minimum cost estimates from the LCC of concrete integral bridge and TCC bridge, only for the superstructure.

Interpretation of the results from LCC

The LCC results suggest that the TCC bridge has the potential to be either more economical or more expensive than the concrete bridge, depending on project specific factors. While construction costs may be slightly lower for the TCC bridge, design costs are higher due to the concept being new. Maintenance costs are similar, with only minor differences. Overall, the TCC option presents greater cost uncertainty, especially in early stage projects. However, if the concept becomes more established, cost efficiency could improve over time. This highlights the importance of continued development and industry experience.

5
Discussion

This chapter discusses the method and the results of the case study, including structural performance for each TCC bridge with its unique connections, as well as the outcomes of the LCA and LCC analyses. In addition, limitations associated with each part are addressed. The chapter is organized into sections in a similar structure as the results chapter.

5.1 Evaluation of the method

The γ-method was applied in the design process of the TCC bridge. It was used to evaluate the degree of composite action and, based on that, determine the effective bending stiffness and the stress distribution across the cross section. This method, as defined in Eurocode 5, is a widely accepted and validated analytical approach for timber concrete composite systems. Its main advantages lie in its simplicity and compatibility with standard cross sections and design procedures. Moreover, it provides a clear and traceable framework for structural calculations.

However, the method has several limitations. It relies on simplifying assumptions to be applicable, the most significant being the assumption of fully linear elastic material behavior. In practice, materials such as concrete and timber may exhibit non linear behavior, particularly in cases involving concrete cracking or long term effects such as creep and shrinkage. Nevertheless, the design approach in this thesis was adjusted to partially account for these effects. For instance, the non linearity of cracked concrete was considered in the support region, where compression governs the behavior. In this case, reinforcement steel was incorporated into the γ-method model instead of the concrete, better reflecting the actual structural behavior.

Long term effects were also addressed by separating the analysis into different load types and evaluating the structure at three distinct time steps. While this approach does not provide an exact representation of long term behavior, it captures the general trends and is considered acceptable for the scope of this analysis. It is worth noting that this limitation is not unique to the γ-method; analytical methods in general are unable to fully capture complex time dependent behaviors. For more detailed and accurate predictions, numerical methods such as finite element analysis are typically more suitable.

The γ-method is well established for the design of TCC buildings, but it was not orig-

inally developed for bridge applications. The method relies on assumptions suited to buildings: such as simplified support conditions, load models, and shorter span lengths. These assumptions do not always align with the characteristics of bridge structures. In bridge design, where spans are typically longer and load models more complex, the γ-method may not fully capture the structural behavior. In this thesis, several modifications were made to adapt the method to bridge specific conditions, which proved to be effective. While the calculations became more advanced due to considerations of loading types and boundary conditions at the supports, the method still offered an adequate level of detail for the scope of this project and successfully captured the key aspects of the bridge behavior.

5.2 Influence of Connections on Structural Performance

This section is divided into subsections, each addressing a different connection used in the case study. It includes a discussion of the results from the capacity checks not influenced by connections, as well as a general discussion and comparison of the case study.

5.2.1 Notch and Dowel Connection

The results from the case study show that the bottom of the timber experiences the highest utilization ratios at midspan for the combined notch and dowel connection, reaching 80% at the initial time stamp. The top of the timber is subjected to the same magnitudes of normal and bending stresses. However, negative bending stresses and positive normal stresses gives a combined effect which result in a low utilization ratio. At the support, the bottom of the timber is primarily subjected to compressive forces, which also yield a lower utilization ratio.

The concrete slab has a low utilization ratio at midspan, primarily because it is under compression in the global analysis. When comparing the compressive stress to the compressive strength of the concrete, the resulting utilization remains low. Cracking occurs at the top of concrete over support, and the resulting tensile forces are resisted by the reinforcement. Given that reinforcement has a high tensile strength, the utilization ratio remains low. The low utilization of the reinforcement is due to the fact that a lot of reinforcement comes from the end console, further discussed in Section 5.2.4.

The stress distribution within the cross section aligns well with expectations. Normal stresses act uniformly within each material and are equal in magnitude but opposite in direction between the timber and concrete. Bending stresses also act in opposite directions in the top and bottom parts of each material. When these stresses are combined and compared to the respective material strengths, the resulting utilization ratios align with expectations, higher near the outer edges of the cross section and decreasing toward the center.

When comparing the results for the three time stages, the utilization ratios are similar. At year 0, the maximum utilization ratio in midspan is 80%, while at both 3–7 years and 80 years, the ratio is 79%. These results may initially seem counterintuitive, as the stresses are generally expected to be most unfavorable at the end of the lifespan of the structure. However, a closer evaluation shows that while bending stresses increase over time, normal stresses decrease, and thus the total stress remain largely unaffected. The underlying reason for the similar utilization ratios over time is that both materials, timber and concrete, are affected by creep which applies to the permanent loads such as self weight and earth pressure. This time dependent behavior is accounted for in design by reducing the modulus of elasticity of the materials. In this case, the self weight of the structure, excluding the pave-

ment, is assumed to be carried solely by the timber beams without any composite action. Consequently, the stresses resulting from the self weight are not evaluated using the γ-method, meaning the reduced MOE is not applied. As a result, these stresses remain unaffected by long term effects and stay constant throughout the service life of the bridge.

In contrast, the pavement is cast after the concrete has hardened. Thus, its self weight is carried by the full cross section, considering composite action between the materials. The same principle applies to fictitious loads resulting from inelastic strains due to shrinkage, moisture variations, and temperature effects. For these loads, the increased γ-factor and the reduced effective stiffness lead to higher bending stresses and lower normal stresses over time, an effect clearly reflected in the results. The reason for the small difference in utilization ratios despite total stress levels being nearly constant is due to the direction dependent capacity of the timber.

The results from the calculated maximum shear stress show a high utilization ratio. This ratio increases slightly at the 80 year time stamp. This outcome is expected, as shear stress is largely unaffected by the long term effects in most load cases. The effective stiffness in ULS remains unchanged by time dependent factors. The slight increase in shear stress at the end of life stage is primarily due to the change in effective stiffness from the permanent load of the pavement. However, since the pavement contributes only marginally to the total load, the resulting variation in shear stress is minimal.

Table 4.8 shows that the fasteners are nearly fully utilized. A notable difference between the trends of the connection calculations and those of the beams and slab is that the utilization ratio for the connections increases slightly over time. This variation arises from the way long term effects are considered. In the connection calculations, only the stiffness changes over time, whereas in the superstructure, both the modulus of elasticity and stiffness decrease.

Unlike the progression of stresses, the deflection results show a clear increase over time. The utilization ratios for both the midspan deflections and the uplift at the end console are high, yet remain below full utilization. An increase is observed in all three analyses, with the most significant change occurring at midspan, where the deflection rises from 21.4 mm to 34 mm between the two time stages. This increase is primarily linked to creep effects in the materials, which lead to a reduction in stiffness over time. The decreased stiffness significantly influences deformation behavior, resulting in the observed increase in deflection.

To summarize the notch and dowel connection, the advantages are reduced deflections due to the higher degree of composite action and a ductile failure mode provided by the dowels. However, there are also disadvantages. The high composite action increases normal stresses, which timber has a lower capacity to resist, making the concept less structurally efficient.

5.2.2 Dowel Connection

The results from the dowel only connection show strong similarities to those of the notch and dowel connection, with the highest utilization in the bottom of the timber at midspan. At the supports, the utilization ratios for bending and normal stresses remain low. Notably, the dowel only connection results in the lowest overall utilization ratios among the connections.

The observation that the dowel only connection performs better in terms of utilization than the combined notch and dowel connection raises questions regarding the optimal choice of the γ-factor. In this case, the TCC bridge with dowel connection has a lower γ-factor and lower utilization ratios compared to the notch and dowel connection. One explanation is that a lower degree of composite action leads to increased bending stresses, while the tension stresses decrease. Since timber has a higher strength in bending than in tension or compression, the stresses result in a more favorable utilization profile. This trend is evident in the case study, where the notch and dowel connection shows higher normal stresses and lower bending stresses than the dowel only connection. Additionally, long term effects lead to a decrease in utilization ratio for the bottom of the timber at midspan. This outcome is in line with the explanation provided in Section 5.2.1.

The results for the utilization of the shear stresses are similar to those presented in Section 5.2.1, showing a utilization of 79%. The dowels have a utilization of approximately 80%, with a slight increase when long term effects are considered. It is worth noting that the maximum fastener load is lower for the dowel only connection compared to the notch and dowel connection. This can be explained by the fact that a lower γ-factor leads to reduced normal forces, which are the primary forces resisted by the connections. The connection design is based on the worst case scenario forces, meaning that the case study presents results for the maximum shear stresses over the support. However, there is great potential for optimization, as the shear stresses decrease near midspan. This suggests that the quantity and spacing of the connections could be modified and optimized along the length of the bridge.

One notable difference between the notch and dowel connection and the dowel only connection is the increase in deflections observed for the dowel only case. This is expected, as a lower γ-factor leads to greater deflection, as explained in Section 2.4. Although the deflections are higher, they remain within acceptable limits. However, this aspect should be carefully considered, as deflection may become a governing factor in certain cases.

To summarize, the advantages of the dowel only connection are the improved structural efficiency due to the lower composite action. This results in a higher proportion of bending stresses, which timber can resist more effectively than normal stresses. Another benefit is the ductile failure behavior provided by the dowels. The main disadvantage is the increased deflection caused by the low level of composite action.

5.2.3 Adhesive and Dowel Connection

The results from the adhesive and dowel connection align with a more traditional approach to structural analysis, where long term effects result in higher utilization ratios. The adhesive layer is modeled as an infinitely strong connection, yielding a γ-factor of 1 which creates full interaction between the timber and concrete. With a γ-factor of 1, long term effects do not influence the composite action, which means that the ratio of bending and normal stresses remains largely unchanged, and consequently, the utilization ratio does not decrease. The utilization ratio for the shear stress is high but remains below full capacity. Regarding deformations, the adhesive and dowel connection exhibits the lowest deflection among all three case studies. This outcome is expected, as full interaction typically results in reduced deflections.

Adhesive connections present several limitations, primarily due to uncertainties in the construction processes and for quality assurance. Even if adhesive connections demonstrate good characteristics during the design phase, practical challenges emerge during construction. Industry experience and familiarity with adhesive connections are low compared to more conventional alternatives. This decreases the likelihood of implementation. Extensive on site testing would be necessary to confirm the concrete surface bond strength, and maintaining adequate quality assurance throughout the process would be demanding.

An alternative method involving granite chips to create an initial bond between the adhesive layer and the concrete, discussed in Section 2.1.3, offers a partial solution to these concerns. However, this production technique is also relatively unknown in the construction industry. Given that TCC bridges are already a new concept, introducing an additional unfamiliar element such as adhesive connections may further reduce its acceptance as a viable bridge concept. The combination of a new structural system and an unproven connection method could increase skepticism and risk of rejection within the industry. The adhesive connection was included in the case study to explore the potential of a TCC bridge with full composite action. However, the literature review revealed that adhesive connections are the least researched among the options, with the highest level of uncertainty regarding production practices and product performance.

5.2.4 Discussion on other capacity checks

The results from the other capacity checks show that there is no risk of lateral torsional buckling of the glulam beams during the production stage. This outcome is expected, as the glulam beams have a bulky, almost square cross section. Lateral torsional buckling typically occurs in slender cross sections, such as steel beams with thin webs.

The results from Section 3.1.7 also indicate that the concrete will crack above the supports. This is as expected, since the end console introduces significant bending moments which, when combined with traffic loads, generate high tensile stresses

in the concrete above the supports that exceed its tensile strength. However, this cracking is not problematic due to the large amount of reinforcement extending from the end console. This reinforcement effectively limits crack widths. As shown in Table 4.27, the amount of reinforcement is twice what is needed to restrict the crack width to 0.20 mm. The high reinforcement demand in the end corner comes from the large bending moments that arise from the horizontal forces acting on the end console. Additionally, the reinforcement needs sufficient anchorage length to overlap with the main longitudinal reinforcement in the superstructure.

The bearing stress perpendicular to the grain is a critical aspect of the timber design and must be addressed in the final design phase. Designing a connection to eliminate this stress is outside the scope of this thesis, but a solution involving dowels and steel plates could be a promising area for further investigation.

5.2.5 Results from gamma factor variations

The case study shows that the three evaluated connection types result in different utilization ratios, each with its own γ-factor. The dowel only connection has the lowest utilization ratio in the bottom of the timber at midspan, and the lowest γ-factor. Conversely, the adhesive and dowel connection yields the highest utilization ratio, along with the highest γ-factor. This indicates that a higher γ-factor does not necessarily lead to a more optimal utilization ratio for the bottom of the timber at midspan.

Figure 4.4 illustrates how the utilization ratio varies with the γ-factor. The lowest utilization occurs when the γ-factor is approximately 30%, and the overall trend suggests that both very low and very high interaction levels lead to higher utilization ratios. The figure also presents utilization ratios for each time stamp. It can be observed that the 0 year time stamp is governing for γ-values up to 70%, after which the end of life time stamp becomes critical. The small difference in results between the 3–7 year and 80 year time stamps indicates that the long term effects are largely formed within the first few years of service life.

It is worth noting that the results in Figure 4.4 indicate a lower utilization ratio for γ-factors around 30% at the bottom of the timber at midspan. This comparison is made with all other parameters constant, such as the cross section, climate conditions and loads. The reduced utilization suggests that there is potential to optimize the structure. However, it is important to consider that other factors may become governing as a result, such as shear stresses, connection design or deflection requirements. Nevertheless, the figure provides valuable insight into the trends associated with varying γ-factors.

It is worth noting that the γ-method calculates the γ-factor without accounting for friction between the concrete and the glulam. Friction arises from both the self weight of the structure and external loads such as wheel pressure. These unac-

counted frictional forces would contribute to a higher effective γ-factor, which may become critical during the design phase. Therefore, it is important to consider multiple γ-factors in the design process to ensure that all potential governing failure modes are properly identified.

Figure 4.5 shows the midspan deflection as a function of γ-factor. As expected, higher γ-factors lead to lower deflections, which is in line with the findings of the case study. Long term effects cause an increase in deflection, which is also anticipated. Similar to the utilization ratios, the difference in deflection between the 3–7 year and 80 year time stamps is minimal, further confirming that most time dependent effects stabilize early in the lifespan of the bridge.

5.2.6 Comparison and Discussion

One important topic to discuss is that the TCC bridge was not fully optimized in this project. The reason is that it was decided in the limitations to have a constant cross section for each connection. This is a disadvantage for the TCC bridge, as the concept uses more materials than necessary. As shown in the results chapter, most capacity checks yield relatively low utilization ratios. However, some checks, such as bearing stress perpendicular to the grain, result in failure. To enable a more accurate comparison between the TCC bridge and the concrete bridge, the TCC design needs to be optimized to better reflect its true performance potential. The concrete bridge, in contrast, was optimized by Inhouse Tech AB, which led to a more material efficient structure and, consequently, a lower climate impact according to the LCA.

Key optimization opportunities for the TCC bridge include the glulam beams and the connections. For the glulam beams, the optimization should aim to bring the utilization ratios for bending capacity, shear capacity, and bearing stress perpendicular to the grain closer to full capacity. There are reinforcement methods available which would increase the shear stress capacity of glulam beams, which increases the beam design possibilities. The optimization of the connections depend on the specific connection type. For example, dowels can be optimized by adjusting the quantity, spacing, diameter, and embedment depth. Notches can similarly be optimized with respect to spacing and geometry.

5.3 Evaluation of the LCA

The LCA results show that the conventional concrete bridge emits 34 tonnes or 18% more CO_2e, than the TCC bridge. In contrast, the TCC bridge consumes 218 GJ, or 11% more energy than the concrete bridge.

5.3.1 Evaluation of LCA results

The largest contributor to climate impact for both bridges is the predefined measure, which includes maintenance and replacement of the edge beam and pavement. This accounts for 75% of total emissions in the TCC bridge and 63% in the concrete bridge. These values reflect emissions from materials, transport, and the construction site over the bridges service life. While the construction materials of the TCC bridge produce roughly half the emissions of the concrete bridge, this alone is not as big of a decisive factor as the life cycle maintenance. Still, the TCC bridge achieves a net saving of 34 tonnes CO_2e.

The higher energy use of the TCC bridge is harder to interpret, as energy related climate impact depends on the energy source. Renewable energy produces significantly lower CO_2e than fossil fuels. Since renewable energy and timber is accessible in northern Sweden, the environmental impact of the TCC bridge energy use may be less significant. For a more comprehensive comparison, site specific factors such as geographical location and the origin of construction materials should be taken into account.

A key difference between the bridges lies in their design life: 80 years for the TCC bridge (maximum in Eurocode 5) and 120 years for the concrete bridge. Though this complicates comparisons, the predefined measure in the LCA assumes an 80 year lifespan for both bridges. The actual design difference between 80 and 120 years in concrete structures is typically minor, with often just an increase of 10 mm in cover thickness. There are two ways to compare the bridges. One is to assume equal design life by slightly reducing the concrete bridge durability requirements.

The other is to accept the 120 year design life of the concrete bridge and compare it to the 80 year life span of the TCC bridge, factoring in the additional maintenance needed during the extra 40 years. This would lower the annual climate impact emissions for the construction materials of the concrete bridge. Since maintenance is a significant contributor of emissions, the longer lifespan of the concrete bridge does not necessarily translate to proportionally lower emissions per year, but it has to be considered to ensure a fair and comprehensive comparison.

Timber structures could one day be certified for 120 year lifespans, but this remains speculative. More research is needed to determine the long term viability and sustainability potential of extended life timber structures.

5.3.2 Evaluation of LCA method

The LCA was conducted using Klimatkalkyl, a tool developed by the Swedish Transport Administration. This tool was chosen partly due to its user friendly interface and partly because its data sources are transparent and easy to verify. Additionally, as an official tool provided by the Swedish Transport Administration, it can be considered credible and reliable. One limitation of the tool is that it does not allow the inclusion of specific components such as dowels, notches, or adhesives, which could have provided valuable insights if included. Moreover, the predefined measures do not offer a TCC bridge as an option, a limitation that is understandable given that TCC bridges are still an emerging concept. The analysis could also be improved by introducing an option to account specifically for the maintenance of the glulam beams without having to classify the entire structure as a glulam bridge. Allowing for such an addition, supported by relevant sources, would lead to a more accurate and comprehensive LCA.

5.3.3 Limitations of the LCA

One limitation of the LCA results is that the climate impact of the structural connections was not included. This was due to the case study evaluating three different connection types. Furthermore, the environmental impact of the adhesive connection, both the material itself and the application process, was also excluded from the assessment.

Another limitation lies in the scope of the analysis. The LCA only evaluates the superstructure rather than the entire bridge system. As a result, the assessment may not provide a complete picture. While the TCC bridge shows clear environmental advantages in terms of its superstructure, this may not be true if the substructure or full bridge system were included.

Additionally, a decision was made early in the thesis to use the existing end console geometries from the concrete bridge. This was done partly to ensure a consistent basis for the LCA comparison, and partly due to the limitation of only evaluating the superstructure. It is worth discussing whether the end console should be considered part of the superstructure or substructure. The height of the end console depends on the thermal expansion coefficients of the materials, and this factor would actually benefit the TCC bridge. Because the TCC bridge has a lower overall thermal coefficient than the concrete bridge, it would require a smaller end console, thereby reducing material usage which is beneficial in regard to the climate impact of the TCC bridge.

5.4 Evaluation of the LCC

The results from the LCC assessment show that the TCC bridge has the potential to be a more economical alternative compared to the concrete bridge, while also carrying the risk of being more expensive. The interpretation of the results depends on the assumptions and perspective, adn should be considered as an rough estimation. The complete LCC results are presented in Appendix C. To better understand the outcome, the costs are discussed under four main categories.

In the design category, the TCC bridge is expected to have a higher cost than the concrete integral bridge, with a wider range due to uncertainties. This is as anticipated, as new concepts often require more time to develop compared to traditional projects. In contrast, concrete bridges benefit from numerous reference projects, which contribute to a more efficient design process. As a result, the design costs for the concrete integral bridge are lower and have a narrower cost range. However, one could argue that if the TCC concept becomes more established in the industry, the design costs could decrease over time.

The construction cost results indicate that the TCC bridge could be more economical than the concrete bridge. The cost of site establishment is assumed to be equal or slightly lower for the TCC bridge, which seems reasonable since the use of glulam beams and less reinforcement may shorten the construction time. This has a direct impact on site related expenses. The TCC bridge also requires less material overall, which reduces material costs. However, glulam beams may come with higher production and transportation costs, which creates uncertainties that varies between projects.

The TCC bridge also includes costs related to bearings, which are not needed for the concrete bridge. On the other hand, the concrete bridge is expected to have lower formwork costs but higher costs for structural support during construction. This aligns with the expectations, as the glulam beams in the TCC bridge can partly function as structural support during casting. The TCC bridge also requires the use of a crane to place the glulam beams, which introduces further uncertainty. The cost of crane rental depends on site conditions, accessibility and local demand. In summary, the construction costs for the two bridge types may be similar, with the TCC bridge appearing more economical in the lower cost estimates. However, the concrete bridge may be more favorable in the higher cost scenarios. The actual cost is expected to fall somewhere in between. A reasonable conclusion is that while the overall construction costs are comparable, the TCC bridge carries higher uncertainty.

Maintenance costs are nearly identical for both bridge types, with the only difference being the additional cost of repainting required for the glulam beams on the TCC bridge. This is a relatively minor addition to the total maintenance cost. These findings are similar to the maintenance related results from the LCA, discussed in Section 5.3, where the two alternatives also showed similar performance. The end of life category considers the net present value, with a discount rate of 3.5 percent

applied. This results in a minimal cost contribution for both bridge types.

To conclude, the LCC assessment shows that the TCC concept involves greater uncertainty in cost estimation compared to the concrete integral bridge. Design related costs are predicted to be higher for the TCC bridge, while construction costs are expected to be similar or slightly more favorable.

The LCC assessment was conducted in collaboration with industry professionals who have extensive experience in cost related to tendering, production, and construction. This approach is considered effective, as these professionals have hands on knowledge of construction related costs. Given the fluctuation in material and construction prices over time, consulting experts can be regarded as a more realistic method than relying only on literature, which may be outdated.

One limitation of the LCC method used in this thesis is that the total cost estimates were reviewed and refined by only one company, Inhouse Tech AB. To get a more comprehensive result, insights from professionals across multiple companies could be included.

6
Conclusion

The case study conducted in this thesis indicates that TCC bridges have then potential to be a competitive alternative to conventional concrete bridges, both environmentally and economically. The outcome of the LCA shows clear environmental advantage for the TCC bridge. The LCC assessment show mixed results for the TCC bridge. The cost could be both lower and higher compared to the concrete bridge. However, the uncertainties is bigger for cost related to the TCC bridge. This highlights the need for further research and real world implementation to better understand the long term economical aspects.

The results from the γ-factor variations highlight the complexity of the TCC system, where increased interaction does not necessarily lead to improved structural efficiency. This outcome is primarily due to the material properties of timber, which exhibits higher capacity in bending than in normal stresses. As the degree of composite action increases, so do the normal stresses in the timber, leading to a less efficient use of the material. It is also important to note that the calculated γ-factor may vary depending on the level of friction between the timber and concrete. Such frictional effects could influence the degree of interaction and should be considered to ensure that the most critical design scenario is captured.

This project only considers one single TCC bridge design, comparing it to one concrete bridge design. Both bridges is designed based on site specific conditions, geometries and assumptions, meaning that the results are only valid for this specific case. Consequently, no broad conclusions can be drawn about TCC in general. However, it can give valuable insights in how the concept can work. Further research, including other site conditions and geometries is needed to validate and extend the understanding of TCC as a concept in bridge construction.

The aim of this thesis was to deepen the understanding of TCC bridges and their application in bridge construction, and integral bridges in particular. The structural analysis of connection types and evaluation of the short and long term loading, provides an insight into the mechanical behavior of TCC bridge structures. Moreover, the environmental and economical aspects of the concept has been evaluated and the results show competitiveness compared to a corresponding concrete bridge. Limitations were identified and discussed. These things considered, the project has established a strong foundation for further development of of TCC bridges in practice, meaning that the aim of the thesis has been successfully achieved.

6.1 Further research

Further research on the TCC bridge concept could focus on optimizing the connection design for both the dowel only and the combined notch and dowel connections. This includes optimization in terms of quantity, variable spacing, and geometry of the dowels and notches. Additionally, conducting both full scale and localized experimental tests would be valuable for comparing theoretical stiffness calculations with actual performance. While similar studies have been carried out previously, applying them specifically to bridge structures would offer new insights.

Another area of interest is the optimization of the glulam beams themselves, particularly in relation to their structural limitations. This may include reinforcement strategies to improve shear resistance, as well as connection designs that prevent failure due to bearing stress perpendicular to the grain. One possible solution could involve combining dowels with plates or studs to better distribute the normal forces from the end console and the support reactions. Future studies could also explore alternative production methods for the different connection types.

Bibliography

Boverket. (2025, January). Utsläpp av växthusgaser från bygg- och fastighetssektorn. https://www.boverket.se/sv/byggande/hallbart-byggande-och-forvaltning/miljoindikatorer---aktuell-status/vaxthusgaser/

Buka-Vaivade, K., & Serdjuks, D. (2021). Behavior of timber-concrete composite with defects in adhesive connection. *Procedia Structural Integrity*, *37*(100), 563–569. https://doi.org/10.1016/j.prostr.2022.01.123

Ceccotti, A. (2002). Composite concrete-timber structures. *Progress in Structural Engineering and Materials*, *4*(3), 264–275. https://doi.org/10.1002/pse.126

Chang, K.-H. (2015). Fatigue and Fracture Analysis. In *E-design* (pp. 463–521). Elsevier. https://doi.org/10.1016/b978-0-12-382038-9.00009-0

Dias, A., Schänzlin, J., & Dietsch, P. (2018). *Design of timber-concrete composite structures* (tech. rep.).

Dicleli, M. (2016). Integral bridges. In *Innovative bridge design handbook: Construction, rehabilitation and maintenance* (pp. 429–450). Elsevier Inc. https://doi.org/10.1016/B978-0-12-800058-8.00016-5

Duffield Timber. (2019, December). What is the difference between timber, lumber and wood?

Engström, B. (2007). *Restraint cracking of reinforced concrete structures* (tech. rep.).

Fragiacomo, M., Gregori, A., Xue, J., Demartino, C., & Toso, M. (2018, December). Timber-concrete composite bridges: Three case studies. https://doi.org/10.1016/j.jtte.2018.09.001

Harapin, A., Jurišić, M., Bebek, N., & Sunara, M. (2024, March). Long-Term Effects in Structures: Background and Recent Developments. https://doi.org/10.3390/app14062352

Jutila, A. (2003). *Findings and points of interest of the Nordic Timber Bridge Projects Findings and points of interest of the Nordic Timber Bridge Projects Findings and points of interest of the Nordic Timber Bridge Projects* (tech.

rep.). https://doi.org/https://www.forum-holzbau.ch/pdf/findings{_}and{_}points.pdf

Jutila, A., Mäkipuro, R., & Salokangas, L. (1997). Testing a Wood-Concrete Composite Bridge. *Structural Engineering International: Journal of the International Association for Bridge and Structural Engineering (IABSE)*, *7*(4), 275–277. https://doi.org/10.2749/101686697780494635

Mačiulaitis, R., Vaičiene, M., & Žurauskiene, R. (2009). The effect of concrete composition and aggregates properties on performance of concrete. *Journal of Civil Engineering and Management*, *15*(3), 317–324. https://doi.org/10.3846/1392-3730.2009.15.317-324

Marques, A. F. S., Martins, C. E. J., & Dias, A. M. P. G. (2020). Mechanical behavior of dowel connection for timber-concrete composite rural bridges. *Maderas: Ciencia y Tecnologia*, *22*(1). https://doi.org/10.4067/S0718-221X2020005000107

Ong, C. (2015). Glue-laminated timber (Glulam). In *Wood composites* (pp. 123–140). Elsevier. https://doi.org/10.1016/b978-1-78242-454-3.00007-x

Pousette, A., Norén, J., Peñaloza, D., Wikland, U., & Pantze, A. (2014). *LCA för vägbro: Analys av en byggd betongöverbyggnad och en alternativ träöverbyggnad* (tech. rep.). SP Trä & Tyréns.

Ramage, M. H., Burridge, H., Busse-Wicher, M., Fereday, G., Reynolds, T., Shah, D. U., Wu, G., Yu, L., Fleming, P., Densley-Tingley, D., Allwood, J., Dupree, P., Linden, P. F., & Scherman, O. (2017, February). The wood from the trees: The use of timber in construction. https://doi.org/10.1016/j.rser.2016.09.107

Schänzlin, J., & Dias, A. (2022). Design of timber-concrete-composite structures. https://doi.org/10.24451/ehwc-6323

SIS-CEN/TS 19103. (2022). *Eurokod 5: Design of Timber Structures - Structural design of timber - concrete composite structures - Common rules and rules for buildings*. Swedish Standard Institute. www.sis.se

SS-EN 1990. (2002). *Eurocode-Basis of structural design*. Swedish Standards Institute. www.sis.se

SS-EN 1991-2. (2003). *Eurocode 1: Laster på bärverk - Del 2: Trafiklast på broar*. Swedish Standard Institute.

SS-EN 1992-1-1. (2005). *Eurocode 2: Design of concrete structures-Part 1-1: General rules and rules for buildings*. Swedish Standard Institute. www.eurokoder.se,

SS-EN 1994-1-1. (2005). *Eurocode 4: Design of composite steel and concrete structures-Part 1-1: General rules and rules for buildings*. Swedish Standards Institute. www.sis.se

SS-EN 1995-1-1. (2004). *Eurocode 5: Design of timber structures-Part 1-1: General-Common rules and rules for buildings*. Swedish Standards Institute. www.sis.se

SS-EN ISO 14040. (2006). *Miljöledning - Livscykelanalys - Principer och struktur*. Swedish standard institute.

SS-ISO 15686-5. (2022). Byggnader och byggnadsverk - Livslängdsplanering - Del 5: Livscykelkostnader.

Swedish Wood. (n.d.). Moisture-related wood movement.

Swedish Wood. (2019). *Dimensionering av träkonstruktioner Del 1*. www.traguiden.se,

Tannert, T., Endacott, B., Brunner, M., & Vallée, T. (2017). Long-term performance of adhesively bonded timber-concrete composites. *International Journal of Adhesion and Adhesives*, *72*, 51–61. https://doi.org/10.1016/j.ijadhadh.2016.10.005

Teacă, C.-A., Roşu, D., Bodîrlău, R., & Roşu, L. (2013). *Structural Changes in Wood under Artificial UV Light Irradiation Determined by FTIR Spectroscopy and Color Measurements-A Brief Review* (tech. rep. No. 1).

TSFS 2018:57. (2018). *Transportstyrelsens föreskrifter och allmänna råd om tillämpning av eurokoder*. Trafikverket.

Wacker, J. P., Dias, A., & Hosteng, T. K. (2017). *Investigation of Early Timber-Concrete Composite Bridges in the United States* (tech. rep.).

World Economic Forum. (2024, September). Cement is a big problem for the environment. Here's how to make it more sustainable.

A

Calculation example

Appendix A presents the calculations for one time stamp for the notch and dowel connection used in the case study. Only a single calculation is included, as presenting all nine would make the document unnecessarily long. The calculations for the different connections and time stamps are largely similar, with variations primarily in connection properties and long term effects such as creep and shrinkage. Therefore, one representative calculation has been provided.

TCC design 80 years

Geometry and material data

Theoretical span length	$l := 16.4\ \boldsymbol{m}$
Width of bridge	$b := 7.5\ \boldsymbol{m}$
Length of end console	$a := 1.3\ \boldsymbol{m}$
Total length of bridge	$L := l + 2 \cdot a = 19\ \boldsymbol{m}$
Area of bridge deck	$A_{bd} := L \cdot b = 142.5\ \boldsymbol{m}^2$
Distance between beams(c-c)	$C_1 := 4.2\ \boldsymbol{m}$
Distance from end to center of beam	$C_2 := 1.65\ \boldsymbol{m}$
End console	
Height of end console	$h_i := 3.35\ \boldsymbol{m}$
Width of end console	$b_i := b = 7.5\ \boldsymbol{m}$
Thinkness of end console	$t_i := 0.6\ \boldsymbol{m}$
Wing wall	
Length of wing wall	$l_{wing} := 4.85\ \boldsymbol{m}$
Height of wing wall	$h_{wing} := 1.2\ \boldsymbol{m}$
Thickness of wing wall	$t_{wing} := 0.4\ \boldsymbol{m}$
Concrete slab	
Thickness of concrete slab	$t_c := 300\ \boldsymbol{mm}$
Width of concrete slab	$b_c := b \div 2 = 3.75\ \boldsymbol{m}$
Cross-section area of concrete slab	$A_c := 11031.3\ \boldsymbol{cm}^2$
Moment of inertia, concrete slab	$I_c := 880608\ \boldsymbol{cm}^4$
Timber beam	
Width of timber beam	$b_t := 190\ \boldsymbol{mm} \cdot 5 = 950\ \boldsymbol{mm}$
Height of timber beam	$h_t := 1305\ \boldsymbol{mm}$
Cross-section area of timber beams	$A_t := b_t \cdot h_t = 1.24\ \boldsymbol{m}^2$
Moment of inertia, timber beams	$I_t := \frac{b_t \cdot h_t^{\,3}}{12} = \left(1.76 \cdot 10^{-1}\right)\ \boldsymbol{m}^4$
Pavement	
Thickness of pavement	$t_{pavement} := 70\ \boldsymbol{mm}$
Edgebeam (Kantbalk)	
Height edgebeam	$h_{eb} := 0.45\ \boldsymbol{m}$
Width edgebeam	$b_{eb} := 0.45\ \boldsymbol{m}$
Area edgebeam	$A_{eb} := h_{eb} \cdot b_{eb}$

Effective width of transverse concrete console

Outer console length $b_1 := a = 1.3\ \boldsymbol{m}$

Distance between glulam beams $b_2 := C_1 - b_t = 3.25\ \boldsymbol{m}$

Equivalent span length for simply supported beams, Figure 5.1 in 1994-1-1. $l_{e1} := 1.0 \cdot l = 16.4\ \boldsymbol{m}$

$b_0 := b_t = 0.95\ \boldsymbol{m}$

Effective width 1.1 $be_{1.1} := min\left(\frac{l_{e1}}{8}, b_1\right) = 1.3\ \boldsymbol{m}$

Effective width 2.1 $be_{2.1} := min\left(\frac{l_{e1}}{8}, b_2\right) = 2.05\ \boldsymbol{m}$

Effective width 1 $b_{eff.1} := b_0 + be_{1.1} + be_{2.1} = 4.3\ \boldsymbol{m}$

Effective width $b_{eff.1} := min\left(b_{eff.1}, \frac{b}{2}\right) = 3.75\ \boldsymbol{m}$

New moment of inertia, concrete slab $I_c := \frac{\left(b_{eff.1} - 100\ \boldsymbol{mm}\right) \cdot t_c^{\,3}}{12} = \left(8.21 \cdot 10^{-3}\right)\ \boldsymbol{m}^4$

Concrete C35/45

Partial factors for concrete $\gamma_{M.c} := 1.5$ $\alpha_{cc} := 1.0$

$\gamma_{CE} := 1.2$ $\alpha_{ct} := 1.0$

Reinforced concrete density $\gamma_{conc} := 25\ \frac{\boldsymbol{kN}}{\boldsymbol{m}^3}$

Compressive strength $f_{ck} := 35\ \boldsymbol{MPa}$ $f_{cd} := \frac{\alpha_{cc} \cdot f_{ck}}{\gamma_{M.c}} = 23.3\ \boldsymbol{MPa}$

Mean compressive strength $f_{cm} := f_{ck} + 8\ \boldsymbol{MPa} = 43\ \boldsymbol{MPa}$

Mean tensile strength $f_{ctm} := 3.2\ \boldsymbol{MPa}$

Tensile strength, 5 percentile $f_{ctk.0.05} := 2.2 \cdot \boldsymbol{MPa}$ $f_{ctd} := \frac{\alpha_{ct} \cdot f_{ctk.0.05}}{\gamma_{M.c}} = 1.5\ \boldsymbol{MPa}$

Modulus of elasticity $E_{cm} := 34 \cdot \boldsymbol{GPa}$

Reinforcement K500C-T:

Partial factors $\gamma_s := 1.15$

Strength $f_{yk} := 500 \cdot \boldsymbol{MPa}$ $f_{yd} := \frac{f_{yk}}{\gamma_s} = 435\ \boldsymbol{MPa}$

Modulus of elasticity $E_s := 200 \cdot \boldsymbol{GPa}$

Yield strain $\varepsilon_{syd} := \frac{f_{yd}}{E_s} = 2 \cdot 10^{-3}$

Glulam GL30c

Climate + load class factor $k_{mod} := 0.9$

Partial factor $\gamma_{M.t} := 1.25$

Crack factor $k_{cr} := 0.857$

Bending parallel to fiber $f_{m.k} := 30\ \boldsymbol{MPa}$ $f_{m.d} := f_{m.k} \cdot \frac{k_{mod}}{\gamma_{M.t}} = 21.6\ \boldsymbol{MPa}$

Tension paralllel to fiber $f_{t.0.k} := 19.5\ \boldsymbol{MPa}$ $f_{t.0.d} := f_{t.0.k} \cdot \frac{k_{mod}}{\gamma_{M.t}} = 14.04\ \boldsymbol{MPa}$

Tension perpendicular to fiber $f_{t.90.k} := 0.5\ \boldsymbol{MPa}$ $f_{t.90.d} := f_{t.90.k} \cdot \frac{k_{mod}}{\gamma_{M.t}} = 0.36\ \boldsymbol{MPa}$

Compression parallel to fiber	$f_{c.0.k} := 24.5\ \textbf{MPa}$	$f_{c.0.d} := f_{c.0.k} \cdot \frac{k_{mod}}{\gamma_{M.t}} = 17.64\ \textbf{MPa}$
Compression perpendicular to fiber	$f_{c.90.k} := 2.5\ \textbf{MPa}$	$f_{c.90d} := f_{c.90.k} \cdot \frac{k_{mod}}{\gamma_{M.t}} = 1.8\ \textbf{MPa}$
Longitudinal shear	$f_{v.k} := 3.5\ \textbf{MPa}$	$f_{v.d} := f_{v.k} \cdot \frac{k_{mod}}{\gamma_{M.t}} = 2.52\ \textbf{MPa}$
MOE parallell to grain	$E_{t.0.05} := 10.8\ \textbf{GPa}$	$E_{t.0.mean} := 13\ \textbf{GPa}$
MOE perpendicular to grain	$E_{t.90.05} := 250\ \textbf{MPa}$	$E_{t.90.mean} := 300\ \textbf{MPa}$
Shear modulus	$G_{05} := 540\ \textbf{MPa}$	$G_{mean} := 650\ \textbf{MPa}$
Density	$\rho_{t.k} := 390\ \frac{\textbf{kg}}{\textbf{m}^3}$	$\rho_{t.mean} := 430\ \frac{\textbf{kg}}{\textbf{m}^3}$
Timber weight	$\gamma_{tim} := \rho_{t.mean} \cdot 9.82\ \frac{\textbf{m}}{\textbf{s}^2} = 4.22\ \frac{\textbf{kN}}{\textbf{m}^3}$	
Long term coefficient	$k_{def} := 0.8$	

Pavement

Pavement weight	$\gamma_{pav} := 25\ \frac{\textbf{kN}}{\textbf{m}^3}$

Connection properties

Dowels

Number of dowels per row $n_c := 16$

Density timber $\rho := \rho_{t.mean} = 430 \ \frac{kg}{m^3}$

Diameter dowel $d := 20 \ mm$

Stiffness of dowels, SLS $K_{ser.dow} := 2 \cdot \frac{\left(\rho \div \frac{kg}{m^3}\right)^{1.5} \cdot \left(\frac{d}{mm}\right)}{23} \cdot n_c \ \frac{N}{mm} = \left(2.48 \cdot 10^5\right) \ \frac{N}{mm}$

Stiffness of dowels, ULS $K_{u.dow} := \frac{2}{3} \cdot K_{ser.dow} = \left(1.65 \cdot 10^5\right) \ \frac{N}{mm}$

Notches

Width of notches $b_{notches} := b_t$

Height of notches $h_{notches} := 50 \ mm$

Length of notch $l_{notches} := 150 \ mm$

Length of distance between notches $l_{s.notches} := 12.5 \cdot h_{notches} = 625 \ mm$

Stiffness of notches, SLS $K_{ser.notches} := 1500 \cdot \frac{N}{mm^2} \cdot \left(b_{notches}\right) = \left(1.43 \cdot 10^6\right) \ \frac{N}{mm}$

Stiffness of notches, ULS $K_{u.notches} := K_{ser.notches}$

Long term coefficient for connection $k_{def}' := 2 \cdot k_{def}$

Total length of notch and between notch $s := l_{notches} + l_{s.notches} = 775 \ mm$

Total stiffness, SLS $K_{ser} := K_{ser.notches} = \left(1.43 \cdot 10^6\right) \ \frac{N}{mm}$

Total stiffness, ULS $K_u := K_{u.notches} = \left(1.43 \cdot 10^6\right) \ \frac{N}{mm}$

Geotechnical prerequisits

Crushed blasted rock (krossad sprängsten)

Unit weight $\gamma_{flm} := 20 \ \frac{kN}{m^3}$

Characteristic friction angle $\phi_{flm.k} := 45 \ deg$

Partial factor $\gamma_\varphi := 1.3$

Design friction angle $\phi_{flm.d} := \operatorname{atan}\left(\frac{\tan\left(\phi_{flm.k}\right)}{\gamma_\varphi}\right) = 38 \ deg$

Characteristic

Coefficient of earth pressure at rest $K_{0.c} := 1 - \sin\left(\phi_{flm.k}\right) = 0.29$

Passive coefficient of earth pressure $K_{p.c} := \left(1 + \sin\left(\phi_{flm.k}\right)\right) \div \left(1 - \sin\left(\phi_{flm.k}\right)\right) = 5.83$

Characteristic load at rest $P_{0.k} := \left(K_{0.c} \cdot \gamma_{flm} \cdot h_i^{\,2}\right) \div 2 = 33 \ \frac{kN}{m}$

Characteristic passive load $P_{p.k} := \left(K_{p.c} \cdot \gamma_{flm} \cdot h_i^{\,2}\right) \div 2 = 654 \ \frac{kN}{m}$

Force from earth pressure ar rest $F_{0.k} := P_{0.k} \cdot b_i = 246.52 \ kN$

Surcharge

Distributed surcharge $q_{ö} := \frac{6 \cdot 20 + 10 \cdot 1.5}{7.5} \ \frac{kN}{m^2} = 18 \ \frac{kN}{m^2}$

Horisontal force from surcharge $H_{ö} := K_{0.c} \cdot h_i \cdot q_{ö} \cdot b_i = 132.46 \ kN$

Temperature load on end console

Corrigated value for max temperature $T_{e.max} := (34 + 5)\ \boldsymbol{K} = 39\ \boldsymbol{K}$

Corrigated value for min temperature $T_{e.min} := \langle -45 + 8 \rangle\ \boldsymbol{K} = -37\ \boldsymbol{K}$

Difference between max and min temp $\Delta T := \left(T_{e.max} - T_{e.min}\right) = 76\ \boldsymbol{K}$

Thermal coefficient for gluelam beam $\alpha_t := 0.5 \cdot 10^{-5} \cdot \frac{1}{\boldsymbol{K}}$

Thermal coefficient for concrete $\alpha_c := 10 \cdot 10^{-6} \cdot \frac{1}{\boldsymbol{K}}$

Thermal expansion longitudinal $\delta_{temp} := L \cdot \Delta T \cdot \alpha_t \div 2 = 3.61\ \boldsymbol{mm}$

Height of end console $h_{ec} := \max\left(200 \cdot \delta_{temp}, 1.5\ \boldsymbol{m}\right) = 1.5\ \boldsymbol{m}$

We use the same end console dimension (3.35m) as the IHT concrete case study bridge, to recieve a good comparison $h_{ec} := \max\left(h_{ec}, 3.35\ \boldsymbol{m}\right) = 3.35\ \boldsymbol{m}$

Interpolation between passive and at rest coefficient $\Delta P_{temp} := \frac{\delta_{temp} \cdot \left(K_{p.c} - K_{0.c}\right) \cdot 200}{h_{ec}} = 1.19$

Added earth pressure from thermal expansion $q_{th} := -\Delta P_{temp} \cdot h_{ec} \cdot \gamma_{flm} = -79.93\ \boldsymbol{kPa}$

Loads

Self weight

Self weight of concrete $g_c := \gamma_{conc} \cdot t_c \cdot b_c = 28.1 \ \frac{kN}{m}$

Self weight of timber $g_t := \gamma_{tim} \cdot h_t \cdot b_t = 5.2 \ \frac{kN}{m}$

Self weight of pavement $g_{pav} := \gamma_{pav} \cdot \left(t_{pavement} \cdot b_c\right) = 6.56 \ \frac{kN}{m}$

Self weight from edge beam $g_{eb} := A_{eb} \cdot \gamma_{conc} = 5.06 \ \frac{kN}{m}$

Self weight of formwork $g_{form} := g_c \cdot 0.1 = 2.81 \ \frac{kN}{m}$

Total self weight $g_{tot} := \left(g_c + g_t + g_{eb} + g_{form}\right) = 41.2 \ \frac{kN}{m}$

Self weight from wing wall $F_{wing} := 2 \cdot \gamma_{conc} \cdot t_{wing} \cdot l_{wing} \cdot \left(h_{wing} + \left(h_i - h_{wing}\right) \cdot \frac{1}{2}\right) = 270 \ kN$
$+ 2 \cdot g_{eb} \cdot l_{wing}$

Lever arm of wing wall

$$l_{wing.la} := a + \frac{\left(h_{wing} \cdot l_{wing}\right) \cdot \frac{l_{wing}}{2} + \left(\frac{\left(h_i - h_{wing}\right)}{2} \cdot l_{wing}\right) \cdot \frac{l_{wing}}{3}}{\left(h_{wing} \cdot l_{wing}\right) + \left(\frac{\left(h_i - h_{wing}\right)}{2} \cdot l_{wing}\right)} = 3.3 \ m$$

Self weight of end console $F_{int} := \gamma_{conc} \cdot h_i \cdot t_i \cdot b_i = 377 \ kN$

Lever arm of end console $l_{int.la} := 0.7 \ m + \frac{0.6 \ m}{2} = 1 \ m$

Traffic load according to LM1

Adjustment factors for lane 1	$\alpha_{Q1} := 0.9$	$\alpha_{q1} := 0.8$
Adjustment factors for lane 2	$\alpha_{Q2} := 0.9$	$\alpha_{q2} := 1.0$
Adjustment factor for remaining area		$\alpha_{rk} := 1.0$
Width of lane	$w_1 := 3 \ m$	
Width of remaining area	$w_{rk} := 7.5 \ m - 2 \cdot w_1 = 1.5 \ m$	
Wheel width	$b_{wheel} := 0.4 \ m$	

Lane number 1

TS load $Q_{1k} := 300 \ kN \cdot \alpha_{Q1} = 270 \ kN$

UDL load $q_{1k} := 9 \ \frac{kN}{m^2} \cdot \alpha_{q1} = 7.2 \ \frac{kN}{m^2}$

Lane number 2

TS load $Q_{2k} := 200 \ kN \cdot \alpha_{Q2} = 180 \ kN$

UDL load $q_{2k} := 2.5 \ \frac{kN}{m^2} \cdot \alpha_{q2} = 2.5 \ \frac{kN}{m^2}$

Remaining area

TS load $Q_{rk} := 0 \ kN$

UDL area $q_{rk} := 2.5 \ \frac{kN}{m^2}$

Breaking load according to LM1

According to SS-EN 1991-2, 4.4.1

Breaking load equation $Q_{bk} := 0.6 \cdot \alpha_{Q1} \cdot \left(2 \cdot Q_{1k}\right) + 0.10 \cdot \alpha_{q1} \cdot q_{1k} \cdot w_1 \cdot L = 324\ \boldsymbol{kN}$

Maximum criteria for breaking load $Q_{bk} := \max\left(180\ \boldsymbol{kN} \cdot \alpha_{Q1}, Q_{bk}\right) = 324\ \boldsymbol{kN}$

Minimum criteria for breaking load $Q_{bk} := min\left(Q_{bk}, 900\ \boldsymbol{kN}\right) = 324\ \boldsymbol{kN}$

Long-term effects

Creep of concrete

Age of concrete $t := 365 \cdot 80\ \textbf{day} = 29200\ \textbf{day}$

Age when drying starts $t_s := 0\ \textbf{day}$

Age when load is applied $t_0 := 5\ \textbf{day}$

Cement class $Cementclass := 2$

Perimeter of concrete slab $u := 2 \cdot t_c + 2 \cdot b_c = 8.1\ \textbf{m}$

Notional size of cross-section $h_0 := 4 \cdot A_c \div u = 545\ \textbf{mm}$

Relative humidity $RH := 80\%$

Coefficient depending on the ambient relative humidity

$$\beta_h := \begin{cases} \min\left(1.5 \cdot \left(1 + (0.012 \cdot RH \cdot 100)^{18}\right) \cdot \frac{h_0}{\textbf{mm}} + 250\,,\ 1500\right) & \text{if } f_{cm} \le 35\ \textbf{MPa} \\ \min\left(1.5 \cdot \left(1 + (0.012 \cdot RH \cdot 100)^{18}\right) \cdot \frac{h_0}{\textbf{mm}} + 250 \cdot \left(\frac{35}{\frac{f_{cm}}{\textbf{MPa}}}\right)^{0.5},\ 1500 \cdot \left(\frac{35}{\frac{f_{cm}}{\textbf{MPa}}}\right)^{0.5}\right) & \text{else if } f_{cm} > 35\ \textbf{MPa} \end{cases} = 1.35 \cdot 10^3$$

Time function of creep coefficient $\beta_c := \left(\frac{\left\langle (t - t_0) \div \textbf{day} \right\rangle}{\beta_h + \left\langle (t - t_0) \div \textbf{day} \right\rangle}\right)^{0.3} = 0.986$

Factor considering relative humidity

$$\varphi_{RH} := \begin{cases} 1 + \frac{1 - RH}{0.1 \cdot \sqrt[3]{\frac{h_0}{\textbf{mm}}}} & \text{if } f_{cm} \le 35\ \textbf{MPa} \\ \left(1 + \frac{1 - RH}{0.1 \cdot \sqrt[3]{\frac{h_0}{\textbf{mm}}}} \cdot \left(\frac{35}{\frac{f_{cm}}{\textbf{MPa}}}\right)^{0.2}\right) \cdot \left(\frac{35}{\frac{f_{cm}}{\textbf{MPa}}}\right)^{0.2} & \text{else if } f_{cm} > 35\ \textbf{MPa} \end{cases} = 1.19$$

Factor considering concrete strength class $\beta_{fcm} := \frac{16.8}{\sqrt{f_{cm} \div \textbf{MPa}}} = 2.56$

Factor considering the age when load is applied $\beta_{t0} := \frac{1}{\left(0.1 + \left(t_0 \div \textbf{day}\right)^{0.2}\right)} = 0.68$

Notional creep coefficient $\varphi_0 := \varphi_{RH} \cdot \beta_{fcm} \cdot \beta_{t0} = 2.052$

Final creep coefficient $\varphi_{t,t0} := \varphi_0 \cdot \beta_c = 2.024$

Shrinkage of concrete

Reference relative humidity

$$RH_0 := 100\%$$

Factor considering the ambient relative humidity

$$\beta_{RH} := 1.55 \cdot \left(1 - \left(\frac{RH}{RH_0}\right)^3\right) = 0.76$$

Starting value of drying shrinkage strain

$$\varepsilon_{cdi} := 0.335 \cdot 10^{-3} \qquad \text{class N}$$

Factor considering the size of the section

$$k_h := \begin{cases} 1 & \text{if } h_0 < 100\ \textbf{mm} \\ 1 - \frac{1 - 0.85}{100 - 200} \cdot \left(100 - \frac{h_0}{\textbf{mm}}\right) & \text{else if } 100\ \textbf{mm} \le h_0 \le 200\ \textbf{mm} \\ 0.85 - \frac{0.85 - 0.75}{200 - 300} \cdot \left(200 - \frac{h_0}{\textbf{mm}}\right) & \text{else if } 200\ \textbf{mm} \le h_0 \le 300\ \textbf{mm} \\ 0.75 - \frac{0.75 - 0.7}{300 - 500} \cdot \left(300 - \frac{h_0}{\textbf{mm}}\right) & \text{else if } 300\ \textbf{mm} \le h_0 \le 500\ \textbf{mm} \\ 0.7 & \text{else if } h_0 \ge 500\ \textbf{mm} \end{cases}$$

$$k_h = 0.7$$

Final value of drying shrinkage

$$\varepsilon_{cd} := k_h \cdot \beta_{RH} \cdot \varepsilon_{cdi} = 1.77 \cdot 10^{-4}$$

Final value of autogenous shrinkage

$$\varepsilon_{ca} := 2.5 \cdot \left(\frac{f_{ck}}{\textbf{MPa}} - 10\right) \cdot 10^{-6} = 6.25 \cdot 10^{-5}$$

Total shrinkage of concrete

$$\varepsilon_{cs} := \varepsilon_{cd} + \varepsilon_{ca} = 2.4 \cdot 10^{-4}$$

Initial composite factor, required for MOE calculations

Composite factor at t=0

$$\gamma_c := \frac{1}{1 + \frac{\pi^2 \cdot A_c \cdot E_{cm} \cdot I_{s.notches}}{K_{u.notches} \cdot L^2}} = 0.69$$

Effective E-modulus for different loads ULS

Modification of creep considering composite action

Concrete $\Psi_{c.80y} := 1.8 - 0.3 \cdot \gamma_c^{2.5} = 1.68$

Timber $\Psi_{tim.80y} := 1$

Connection $\Psi_{conn.80y} := 1$

Reduction of shrinkage effect $\varepsilon_{c.80y} := 0.9 \cdot \varepsilon_{cs} = 2.16 \cdot 10^{-4}$

MOE temp concrete $E_{c.temp} := \frac{E_{cm}}{1 + 0.3} = 26.15\ \textbf{GPa}$

MOE temp timber $E_{t.temp} := E_{t.0.mean} = 13\ \textbf{GPa}$

MOE creep concrete $E_{c.creep} := \frac{E_{cm}}{1 + \Psi_{c.80y} \cdot \varphi_{t.t0}} = 7.72\ \textbf{GPa}$

MOE timber concrete $E_{t.creep} := \frac{E_{t.0.mean}}{1 + \Psi_{tim.80y} \cdot k_{def}} = 7.22\ \textbf{GPa}$

Slip modulus ULS $K_{u.creep} := \frac{K_u}{1 + \Psi_{conn.80y} \cdot k_{def}'} = \left(5.48 \cdot 10^5\right) \frac{\textbf{N}}{\textbf{mm}}$

Effective E-modulus for different loads SLS

MOE temp concrete $E_{c.temp.sls} := E_{cm} = 34\ \textbf{GPa}$

MOE Temperature timber $E_{t.temp.sls} := E_{t.0.mean}$

MOE creep concrete $E_{c.creep.sls} := \frac{E_{cm}}{1 + \varphi_{t.t0}} = 11.24\ \textbf{GPa}$

MOE timber concrete $E_{t.creep.sls} := \frac{E_{t.0.mean}}{1 + k_{def}} = 7.22\ \textbf{GPa}$

Slip modulus SLS $K_{ser.creep} := \frac{K_{ser}}{1 + \Psi_{conn.80y} \cdot k_{def}'} = \left(5.48 \cdot 10^5\right) \frac{\textbf{N}}{\textbf{mm}}$

Effective bending stiffness

Composite coefficient of concretre cross-section $\gamma_{c.func}(E_c, K) := \dfrac{1}{1 + \dfrac{\pi^2 \cdot A_c \cdot E_c \cdot s}{K \cdot L^2}}$

Composite coefficient of timber cross-section $\gamma_t := 1$

Distance between center of the timber element and the center of gravity $a_{t.func}(\gamma_c, E_{cm}, E_{t.0.mean}) := \dfrac{\gamma_c \cdot E_{cm} \cdot A_c \cdot (t_c + h_t)}{2 \cdot (\gamma_c \cdot E_{cm} \cdot A_c + E_{t.0.mean} \cdot A_t)}$

Distance between center of the concrete element and the center of gravity $a_{c.func}(a_t) := \dfrac{t_c + h_t}{2} - a_t$

Effective bending stiffness $EI_{eff.func}(\gamma_c, E_{cm}, E_{t.0.mean}, a_t, a_c) := E_{cm} \cdot I_c + \gamma_c \cdot E_{cm} \cdot A_c \cdot a_c^2 + E_{t.0.mean} \cdot I_t + E_{t.0.mean} \cdot A_t \cdot a_t^2$

Distance from lower edge to the centroid of the composite cross section $h_{v.func}(a_t) := a_t + \dfrac{h_t}{2}$

γ-method for Notch connection in ULS

$\gamma_{c.temp} := \gamma_{c.func}(E_{c.temp}, K_u) = 0.7$

$\gamma_{c.uls} := \gamma_{c.func}(E_{cm}, K_u) = 0.64$

$\gamma_{c.sw} := \gamma_{c.func}(E_{c.creep}, K_{u.creep}) = 0.75$

$a_{t.temp} := a_{t.func}(\gamma_{c.temp}, E_{c.temp}, E_{t.temp}) = 0.45\ \boldsymbol{m}$

$a_{t.uls} := a_{t.func}(\gamma_{c.uls}, E_{cm}, E_{t.0.mean}) = 0.48\ \boldsymbol{m}$

$a_{t.sw} := a_{t.func}(\gamma_{c.sw}, E_{c.creep}, E_{t.creep}) = 0.33\ \boldsymbol{m}$

$a_{c.temp} := a_{c.func}(a_{t.temp}) = 0.36\ \boldsymbol{m}$

$a_{c.uls} := a_{c.func}(a_{t.uls}) = 0.32\ \boldsymbol{m}$

$a_{c.sw} := a_{c.func}(a_{t.sw}) = 0.47\ \boldsymbol{m}$

$EI_{eff.temp} := EI_{eff.func}(\gamma_{c.temp}, E_{c.temp}, E_{t.temp}, a_{t.temp}, a_{c.temp}) = (8.27 \cdot 10^6)\ \boldsymbol{kN \cdot m^2}$

$EI_{eff.uls} := EI_{eff.func}(\gamma_{c.uls}, E_{cm}, E_{t.0.mean}, a_{t.uls}, a_{c.uls}) = (8.78 \cdot 10^6)\ \boldsymbol{kN \cdot m^2}$

$EI_{eff.sw} := EI_{eff.func}(\gamma_{c.sw}, E_{c.creep}, E_{t.creep}, a_{c.temp}, a_{c.sw}) = (3.87 \cdot 10^6)\ \boldsymbol{kN \cdot m^2}$

$h_{v.t.temp} := h_{v.func}(a_{t.temp}) = 1.1\ \boldsymbol{m}$

$h_{v.t.uls} := h_{v.func}(a_{t.uls}) = 1.13\ \boldsymbol{m}$

$h_{v.t.sw} := h_{v.func}(a_{t.sw}) = 0.99\ \boldsymbol{m}$

γ-method for Notch connection in SLS

$\gamma_{c.temp.sls} := \gamma_{c.func}(E_{c.temp.sls}, K_{ser}) = 0.64$

$\gamma_{c.sls} := \gamma_{c.func}(E_{cm}, K_{ser}) = 0.64$

$\gamma_{c.sw.sls} := \gamma_{c.func}(E_{c.creep.sls}, K_{ser.creep}) = 0.68$

$a_{t.temp.sls} := a_{t.func}(\gamma_{c.temp.sls}, E_{c.temp.sls}, E_{t.temp.sls}) = 0.48\ \boldsymbol{m}$

$a_{t.sls} := a_{t.func}(\gamma_{c.sls}, E_{cm}, E_{t.0.mean}) = 0.48\ \boldsymbol{m}$

$a_{t.sw.sls} := a_{t.func}(\gamma_{c.sw.sls}, E_{c.creep.sls}, E_{t.creep.sls}) = 0.39\ \boldsymbol{m}$

$a_{c.temp.sls} := a_{c.func}(a_{t.temp.sls}) = 0.32\ \boldsymbol{m}$

$a_{c.sls} := a_{c.func}(a_{t.sls}) = 0.32\ \boldsymbol{m}$

$a_{c.sw.sls} := a_{c.func}(a_{t.sw.sls}) = 0.41\ \boldsymbol{m}$

$EI_{eff.temp.sls} := EI_{eff.func}(\gamma_{c.temp}, E_{c.temp}, E_{t.temp.sls}, a_{t.temp.sls}, a_{c.temp.sls}) = (8.32 \cdot 10^6)\ \boldsymbol{kN \cdot m^2}$

$EI_{eff.sls} := EI_{eff.func}(\gamma_{c.sls}, E_{cm}, E_{t.0.mean}, a_{t.sls}, a_{c.sls}) = (8.78 \cdot 10^6)\ \boldsymbol{kN \cdot m^2}$

$EI_{eff.sw.sls} := EI_{eff.func}(\gamma_{c.sw.sls}, E_{c.creep.sls}, E_{t.creep.sls}, a_{t.sw.sls}, a_{c.sw.sls}) = (4.15 \cdot 10^6)\ \boldsymbol{kN \cdot m^2}$

$h_{v.temp.sls} := h_{v.func}(a_{t.temp.sls})$

$h_{v.sls} := h_{v.func}(a_{t.sls})$

$h_{v.t.sw.sls} := h_{v.func}(a_{t.sw.sls})$

Effect of inelastic strains SLS

Distance from center of gravity of timberbeam and concrete slab

$$z := \frac{h_t + t_c}{2} = 0.8\ \boldsymbol{m}$$

Coeffficient for inelastic strains

$$C_{p.func}\left(E_{cm}, E_{t.0.mean}, \gamma_c\right) := \overrightarrow{\pi^2 \cdot \frac{E_{cm} \cdot A_c \cdot E_{t.0.mean} \cdot A_t \cdot z \cdot \gamma_c}{\left(E_{cm} \cdot A_c + E_{t.0.mean} \cdot A_t\right) \cdot l^2}}$$

$$C_{p.sls.creep} := C_{p.func}\left(E_{c.creep.sls}, E_{t.creep.sls}, \gamma_{c.sw.sls}\right) = \left(1.03 \cdot 10^8\right)\ \frac{\boldsymbol{kg}}{\boldsymbol{s}^2}$$

Inelastic strain of concrete

Shrinkage of concrete from creep

$$\varepsilon_{c.shrinkage} := -\varepsilon_{c.80y} = -2.16 \cdot 10^{-4}$$

Reference temperature

$$T_0 := 10\ \boldsymbol{K}$$

Difference in max temp and ref temp

$$\Delta T_{c.max} := T_{e.max} - T_0 = 29\ \boldsymbol{K}$$

Difference in min temp and ref temp

$$\Delta T_{c.min} := \left(T_{e.min} - T_0\right) = -47\ \boldsymbol{K}$$

Moisture related strain

Yearly variation of timber moisture content

$$\Delta mc := 2.5$$

Moisture expansion coefficient parallell grain

$$\alpha_{t.u} := 10^{-5}$$

Maximum strain moisture, expansion

$$\varepsilon_{t.u.max} := \Delta mc \cdot \alpha_{t.u} = 2.5 \cdot 10^{-5}$$

Minimum strain moisture, contraction

$$\varepsilon_{t.u.min} := -\Delta mc \cdot \alpha_{t.u} = -2.5 \cdot 10^{-5}$$

Temperature related strain

Shrinkage of concrete from thermal contraction

$$\varepsilon_{c.temp.min} := \alpha_c \cdot \Delta T_{c.min} = -4.7 \cdot 10^{-4}$$

$$\varepsilon_{c.temp.max} := \alpha_c \cdot \Delta T_{c.max} = 2.9 \cdot 10^{-4}$$

Shrinkage of timber from thermal and moisture strain

$$\varepsilon_{t.min} := \alpha_t \cdot \Delta T_{c.min} + \varepsilon_{t.u.min} = -2.6 \cdot 10^{-4}$$

$$\varepsilon_{t.max} := \alpha_t \cdot \Delta T_{c.max} + \varepsilon_{t.u.max} = 1.7 \cdot 10^{-4}$$

Total strain from min temp

$$\Delta\varepsilon_{temp.min} := \varepsilon_{t.min} - \varepsilon_{c.temp.min} = 2.1 \cdot 10^{-4}$$

Total strain from max temp

$$\Delta\varepsilon_{temp.max} := \varepsilon_{t.max} - \varepsilon_{c.temp.max} = -1.2 \cdot 10^{-4}$$

Max strain from temperature

$$\Delta\varepsilon_{temp} := \max\left(\text{abs}\left(\Delta\varepsilon_{temp.min}\right), \text{abs}\left(\Delta\varepsilon_{temp.max}\right)\right) = 2.1 \cdot 10^{-4}$$

Difference in inelastic strain between timber and concrete

$$\Delta\varepsilon := \Delta\varepsilon_{temp} - \varepsilon_{c.shrinkage} = 4.26 \cdot 10^{-4}$$

Fictitious vertical load equivalent to inelastic strains

$$p_{sls.creep} := C_{p.sls.creep} \cdot \Delta\varepsilon = 44.08\ \frac{\boldsymbol{kN}}{\boldsymbol{m}}$$

Partial factor for shirnkage

$$\gamma_{F.sls} := 1$$

Design value of fictitious load

$$p_{sls.d.creep} := \gamma_{F.sls} \cdot p_{sls.creep} = 44.08\ \frac{\boldsymbol{kN}}{\boldsymbol{m}}$$

Permanent uniformly distributed load

$$q_d := g_{tot} = 41.23\ \frac{\boldsymbol{kN}}{\boldsymbol{m}}$$

Modification coefficient of the bending stiffness

$$C_{J.func}\left(E_{cm}, E_{t.0.mean}, \gamma_c, p_{sls.d}, p_{sls}, q_d\right) := \overrightarrow{\frac{q_d + p_{sls.d}}{\frac{E_{cm} \cdot A_c + E_{t.0.mean} \cdot A_t}{\gamma_c \cdot E_{cm} \cdot A_c + E_{t.0.mean} \cdot A_t} \cdot p_{sls} + q_d}}$$

$$C_{J.sls.creep} := C_{J.func}\left(E_{c.creep.sls}, E_{t.creep.sls}, \gamma_{c.sw.sls}, p_{sls.d.creep}, p_{sls.creep}, q_d\right) = 0.89$$

Effective bending stiffness with respect to inelastic strains

$$EI_{eff.sw.sls} := C_{J.sls.creep} \cdot EI_{eff.sw.sls} = 3.71\ \boldsymbol{m^4 \cdot GPa}$$

Bending moment at support caused by the fictitious load

$$\Delta M_{fic.uls.2} := -\frac{0.8 \cdot p_{sls.creep} \cdot a^2}{2} = -29.8\ \boldsymbol{kNm}$$

Bending moment in mid span caused by the fictitious load

$$\Delta M_{fic.uls.1} := \frac{0.8 \cdot p_{sls.creep} \cdot l^2}{8} = 1185.55\ \boldsymbol{kNm}$$

Effect of inelastic strains ULS

$$C_{p.uls.creep} := C_{p.func}\left(E_{c.creep}, E_{t.creep}, \gamma_{c.sw}\right) = \left(9.67 \cdot 10^{7}\right)\ \frac{kg}{s^2}$$

Fictitious vertical load equivalent to inelastic strains

$$p_{uls.creep} := C_{p.uls.creep} \cdot \Delta\varepsilon = 41.18\ \frac{kN}{m}$$

Partial factor for shirnkage

$$\gamma_{F.uls} := 1.5$$

Design value of fictitious load

$$p_{uls.d.creep} := \gamma_{F.uls} \cdot p_{uls.creep} = 61.77\ \frac{kN}{m}$$

Permanent uniformly distributed load

$$q_d := 1.35 \cdot g_{tot} = 55.67\ \frac{kN}{m}$$

$$C_{J.uls.creep} := C_{J.func}\left(E_{c.creep}, E_{t.creep}, \gamma_{c.sw}, p_{uls.d.creep}, p_{uls.creep}, q_d\right) = 1.15$$

Effective bending stiffness with respect to inelastic strains

$$EI_{eff.sw} := C_{J.uls.creep} \cdot EI_{eff.sw} = 4.44\ m^4 \cdot GPa$$

Bending moment at support caused by the fictitious load

$$\Delta M_{fic.uls.2} := -\frac{0.8 \cdot p_{uls.creep} \cdot a^2}{2} = -27.84\ kNm$$

Bending moment in mid span caused by the fictitious load

$$\Delta M_{fic.uls.1} := \frac{0.8 \cdot p_{uls.creep} \cdot l^2}{8} = 1107.66\ kNm$$

Forces

Forces from self weight

Support moment from self weight

$$M_{s.g} := \frac{\left(-l_{wing.la} \cdot F_{wing} - l_{int.la} \cdot F_{int}\right)}{2} = -639\ kNm$$

Span moment from self weight

$$M_{f.g} := \frac{g_{tot} \cdot l^2}{8} + M_{s.g} = 747\ kNm$$

Shear force from self weight

$$V_{g.max} := \frac{g_{tot} \cdot \left(l - 2 \cdot \left(h_t - t_c\right)\right)}{2} = 297\ kN$$

Support moment from self weigh of pavement

$$M_{s.g.pav.base} := -\frac{g_{pav} \cdot a^2}{2} = -5.55\ kNm$$

Support moment from self weigh of pavement including fictitous load

$$M_{s.g.pav} := -M_{s.g.pav.base} + \Delta M_{fic.uls.2} = -22.29\ kNm$$

Span moment from self weight of pavement

$$M_{f.g.pav} := \frac{g_{pav} \cdot l^2}{8} + M_{s.g.pav} + \Delta M_{fic.uls.1} = 1306\ kNm$$

Shear force from self weight of pavement

$$V_{g.max.pav} := \frac{g_{pav} \cdot \left(l - 2 \cdot \left(h_t - t_c\right)\right)}{2} = 47.22\ kN$$

Mid span - stresses from selfweight

Total stress in top of concrete

$$\sigma_{g.c.top.1} := \begin{bmatrix} 0 \\ 0 \end{bmatrix} MPa$$

Total stress in bottom of concrete

$$\sigma_{g.c.bot.1} := \begin{bmatrix} 0 \\ 0 \end{bmatrix} MPa$$

Stress in top of timber

$$\sigma_{t.top.1} := \frac{-M_{f.g}}{I_t} \cdot \frac{h_t}{2} = -2.77\ MPa$$

Stress in bottom of timber

$$\sigma_{t.bot.1} := \frac{M_{f.g}}{I_t} \cdot \frac{h_t}{2} = 2.77\ MPa$$

Total stress in top of timber

$$\sigma_{g.t.top.1} := \begin{bmatrix} 0 \\ \sigma_{t.top.1} \end{bmatrix} = \begin{bmatrix} 0 \\ -2.77 \end{bmatrix} MPa$$

Total stress in bottom of timber

$$\sigma_{g.t.bot.1} := \begin{bmatrix} 0 \\ \sigma_{t.bot.1} \end{bmatrix} = \begin{bmatrix} 0 \\ 2.77 \end{bmatrix} MPa$$

Mid span - stresses from self weight of pavement ULS

Normal stress from composite action $\sigma_{g.pav.c.1} := \frac{\gamma_{c.sw} \cdot E_{c.creep} \cdot a_{c.sw}}{EI_{eff.sw}} \cdot M_{f.g.pav} = 0.8$ ***MPa***

Stress from bending $\sigma_{g.pav.m.c.1} := \frac{0.5 \cdot E_{c.creep} \cdot t_c}{EI_{eff.sw}} \cdot M_{f.g.pav} = 0.341$ ***MPa***

Total stress in top of concrete $\sigma_{g.pav.c.top.1} := \begin{bmatrix} -\sigma_{g.pav.c.1} \\ -\sigma_{g.pav.m.c.1} \end{bmatrix} = \begin{bmatrix} -0.8 \\ -0.34 \end{bmatrix}$ ***MPa***

Total stress in bottom of concrete $\sigma_{g.pav.c.bot.1} := \begin{bmatrix} -\sigma_{g.pav.c.1} \\ \sigma_{g.pav.m.c.1} \end{bmatrix} = \begin{bmatrix} -0.8 \\ 0.34 \end{bmatrix}$ ***MPa***

Normal stress from composite action $\sigma_{g.pav.t.1} := \frac{\gamma_t \cdot E_{t.creep} \cdot a_{t.sw}}{EI_{eff.sw}} \cdot M_{f.g.pav} = 0.712$ ***MPa***

Stress from bending $\sigma_{g.pav.m.t.1} := \frac{0.5 \cdot E_{t.creep} \cdot h_t}{EI_{eff.sw}} \cdot M_{f.g.pav} = 1.387$ ***MPa***

Total stress in top of timber $\sigma_{g.pav.t.top.1} := \begin{bmatrix} \sigma_{g.pav.t.1} \\ -\sigma_{g.pav.m.t.1} \end{bmatrix} = \begin{bmatrix} 0.71 \\ -1.39 \end{bmatrix}$ ***MPa***

Total stress in bottom of timber $\sigma_{g.pav.t.bot.1} := \begin{bmatrix} \sigma_{g.pav.t.1} \\ \sigma_{g.pav.m.t.1} \end{bmatrix} = \begin{bmatrix} 0.71 \\ 1.39 \end{bmatrix}$ ***MPa***

Mid span - stresses from self weight of pavement SLS

Normal stress from composite action $\sigma_{g.pav.c.sls.1} := \frac{\gamma_{c.sw.sls} \cdot E_{c.creep.sls} \cdot a_{c.sw.sls}}{EI_{eff.sw.sls}} \cdot M_{f.g.pav} = 1.11$ ***MPa***

Stress from bending $\sigma_{g.pav.m.c.sls.1} := \frac{0.5 \cdot E_{c.creep.sls} \cdot t_c}{EI_{eff.sw.sls}} \cdot M_{f.g.pav} = 0.594$ ***MPa***

Total stress in top of concrete $\sigma_{g.pav.c.top.sls.1} := \begin{bmatrix} -\sigma_{g.pav.c.sls.1} \\ -\sigma_{g.pav.m.c.sls.1} \end{bmatrix} = \begin{bmatrix} -1.11 \\ -0.59 \end{bmatrix}$ ***MPa***

Total stress in bottom of concrete $\sigma_{g.pav.c.bot.sls.1} := \begin{bmatrix} -\sigma_{g.pav.c.sls.1} \\ \sigma_{g.pav.m.c.sls.1} \end{bmatrix} = \begin{bmatrix} -1.11 \\ 0.59 \end{bmatrix}$ ***MPa***

Normal stress from composite action $\sigma_{g.pav.t.sls.1} := \frac{\gamma_t \cdot E_{t.creep.sls} \cdot a_{t.sw.sls}}{EI_{eff.sw.sls}} \cdot M_{f.g.pav} = 0.987$ ***MPa***

Stress from bending $\sigma_{g.pav.m.t.sls.1} := \frac{0.5 \cdot E_{t.creep.sls} \cdot h_t}{EI_{eff.sw.sls}} \cdot M_{f.g.pav} = 1.66$ ***MPa***

Total stress in top of timber $\sigma_{g.pav.t.top.sls.1} := \begin{bmatrix} \sigma_{g.pav.t.sls.1} \\ -\sigma_{g.pav.m.t.sls.1} \end{bmatrix} = \begin{bmatrix} 0.99 \\ -1.66 \end{bmatrix}$ ***MPa***

Total stress in bottom of timber $\sigma_{g.pav.t.bot.sls.1} := \begin{bmatrix} \sigma_{g.pav.t.sls.1} \\ \sigma_{g.pav.m.t.sls.1} \end{bmatrix} = \begin{bmatrix} 0.99 \\ 1.66 \end{bmatrix}$ ***MPa***

Forces from traffic load

File factor for point loads in LM1

$$f_{Q.LM1} := \frac{Q_{1k} + Q_{1k} \cdot \left(\frac{C_2 - 0.5\ \boldsymbol{m}}{C_1} \right) + Q_{1k} \cdot \left(\frac{C_1 - \left(2.5\ \boldsymbol{m} - C_2 \right)}{C_1} \right)}{2 \cdot Q_{1k}} = 1.25$$

$$+ \frac{Q_{2k} \cdot \left(\frac{C_1 - \left(3.5\ \boldsymbol{m} - C_2 \right)}{C_1} \right) + Q_{2k} \cdot \left(\frac{C_1 - \left(5.5\ \boldsymbol{m} - C_2 \right)}{C_1} \right)}{2 \cdot Q_{1k}}$$

File factor for distributed loads in LM1

$$f_{q.LM1} := \frac{q_{1k} \cdot w_1 + \frac{q_{1k} \cdot w_1 \cdot \left(C_2 - \frac{w_1}{2} \right)}{C_1}}{q_{1k} \cdot w_1} + \frac{\frac{q_{2k} \cdot w_1 \cdot \left(C_1 - \left(\frac{w_1}{2} + 3\ \boldsymbol{m} - C_2 \right) \right)}{C_1}}{q_{1k} \cdot w_1} = 1.147$$

Minimum support moment from traffic load

$$M_{Q.s.min} := -f_{Q.LM1} \cdot \left(a - \frac{b_{wheel}}{2} \right) \cdot Q_{1k} = -371\ \boldsymbol{kNm}$$

$$M_{q.s.min} := -f_{q.LM1} \cdot a^2\ \frac{\left(q_{1k} \cdot w_1 \right)}{2} = -20.94\ \boldsymbol{kNm}$$

Minimum span moment from traffic load

$$M_{Q.f.min} := -f_{Q.LM1} \cdot \frac{1}{2} \cdot \left(a - \frac{b_{wheel}}{2} \right) Q_{1k} = -186\ \boldsymbol{kNm}$$

$$M_{q.f.min} := -f_{q.LM1} \cdot a^2\ \frac{\left(q_{1k} \cdot w_1 \right)}{2} = -20.94\ \boldsymbol{kNm}$$

Maximum span moment from traffic load

$$M_{Q.f.max} := f_{Q.LM1} \cdot \frac{Q_{1k} \cdot \left(\frac{l}{2} + 0.6\ \boldsymbol{m} \right) \cdot \left(\frac{l}{2} - 0.6\ \boldsymbol{m} \right) \cdot 2}{l} = 2753\ \boldsymbol{kNm}$$

$$M_{q.f.max} := f_{q.LM1} \cdot \frac{\left(q_{1k} \cdot w_1 \right) \cdot l^2}{8} = 833.18\ \boldsymbol{kNm}$$

Maximum shear force from traffic load

$$V_{Q.max} := f_{Q.LM1} \cdot Q_{1k} \cdot \frac{\left(l - 2 \cdot \left(h_t - t_c \right) \right)}{l} + f_{Q.LM1} \cdot Q_{1k} \cdot \frac{\left(l - 2 \cdot \left(h_t - t_c \right) \right) - 1.2\ \boldsymbol{m}}{l} = 568\ \boldsymbol{kN}$$

$$V_{q.max} := f_{q.LM1} \cdot \left(q_{1k} \cdot w_1 \right) \cdot \frac{l}{2} = 203.21\ \boldsymbol{kN}$$

Mid span - Max stresses from traffic load (TS) ULS

Normal stress from composite action $\sigma_{Q.c.1} := \frac{\gamma_{c.uls} \cdot E_{cm} \cdot a_{c.uls}}{EI_{eff.uls}} \cdot M_{Q.f.max} = 2.2$ ***MPa***

Stress from bending $\sigma_{Q.m.c.1} := \frac{0.5 \cdot E_{cm} \cdot t_c}{EI_{eff.uls}} \cdot M_{Q.f.max} = 1.6$ ***MPa***

Total stress in top of concrete $\sigma_{Q.c.top.1} := \begin{bmatrix} -\sigma_{Q.c.1} \\ -\sigma_{Q.m.c.1} \end{bmatrix} = \begin{bmatrix} -2.2 \\ -1.6 \end{bmatrix}$ ***MPa***

Total stress in bottom of concrete $\sigma_{Q.c.bot.1} := \begin{bmatrix} -\sigma_{Q.c.1} \\ \sigma_{Q.m.c.1} \end{bmatrix} = \begin{bmatrix} -2.2 \\ 1.6 \end{bmatrix}$ ***MPa***

Normal stress from composite action $\sigma_{Q.t.1} := \frac{\gamma_t \cdot E_{t.0.mean} \cdot a_{t.uls}}{EI_{eff.uls}} \cdot M_{Q.f.max} = 2$ ***MPa***

Stress from bending $\sigma_{Q.m.t.1} := \frac{0.5 \cdot E_{t.0.mean} \cdot h_t}{EI_{eff.uls}} \cdot M_{Q.f.max} = 2.7$ ***MPa***

Total stress in top of timber $\sigma_{Q.t.top.1} := \begin{bmatrix} \sigma_{Q.t.1} \\ -\sigma_{Q.m.t.1} \end{bmatrix} = \begin{bmatrix} 2 \\ -2.7 \end{bmatrix}$ ***MPa***

Total stress in bottom of timber $\sigma_{Q.t.bot.1} := \begin{bmatrix} \sigma_{Q.t.1} \\ \sigma_{Q.m.t.1} \end{bmatrix} = \begin{bmatrix} 2 \\ 2.7 \end{bmatrix}$ ***MPa***

Mid span - Max stresses from traffic load (UDL) ULS

Normal stress from composite action $\sigma_{q.c.1} := \frac{\gamma_{c.uls} \cdot E_{cm} \cdot a_{c.uls}}{EI_{eff.uls}} \cdot M_{q.f.max} = 0.7$ ***MPa***

Stress from bending $\sigma_{q.m.c.1} := \frac{0.5 \cdot E_{cm} \cdot t_c}{EI_{eff.uls}} \cdot M_{q.f.max} = 0.5$ ***MPa***

Total stress in top of concrete $\sigma_{q.c.top.1} := \begin{bmatrix} -\sigma_{q.c.1} \\ -\sigma_{q.m.c.1} \end{bmatrix} = \begin{bmatrix} -0.67 \\ -0.48 \end{bmatrix}$ ***MPa***

Total stress in bottom of concrete $\sigma_{q.c.bot.1} := \begin{bmatrix} -\sigma_{q.c.1} \\ \sigma_{q.m.c.1} \end{bmatrix} = \begin{bmatrix} -0.7 \\ 0.5 \end{bmatrix}$ ***MPa***

Normal stress from composite action $\sigma_{q.t.1} := \frac{\gamma_t \cdot E_{t.0.mean} \cdot a_{t.uls}}{EI_{eff.uls}} \cdot M_{q.f.max} = 0.6$ ***MPa***

Stress from bending $\sigma_{q.m.t.1} := \frac{0.5 \cdot E_{t.0.mean} \cdot h_t}{EI_{eff.uls}} \cdot M_{q.f.max} = 0.8$ ***MPa***

Total stress in top of timber $\sigma_{q.t.top.1} := \begin{bmatrix} \sigma_{q.t.1} \\ -\sigma_{q.m.c.1} \end{bmatrix} = \begin{bmatrix} 0.6 \\ -0.5 \end{bmatrix}$ ***MPa***

Total stress in bottom of timber $\sigma_{q.t.bot.1} := \begin{bmatrix} \sigma_{q.t.1} \\ \sigma_{q.m.c.1} \end{bmatrix} = \begin{bmatrix} 0.6 \\ 0.5 \end{bmatrix}$ ***MPa***

Mid span - Max stresses from traffic load (TS) SLS

Normal stress from composite action $\sigma_{Q.c.1.sls} := \frac{\gamma_{c.sls} \cdot E_{cm} \cdot a_{c.sls}}{EI_{eff.sls}} \cdot M_{Q.f.max} = 2.2$ **MPa**

Stress from bending $\sigma_{Q.m.c.1.sls} := \frac{0.5 \cdot E_{cm} \cdot t_c}{EI_{eff.sls}} \cdot M_{Q.f.max} = 1.6$ **MPa**

Total stress in top of concrete $\sigma_{Q.c.top.1.sls} := \begin{bmatrix} -\sigma_{Q.c.1.sls} \\ -\sigma_{Q.m.c.1.sls} \end{bmatrix} = \begin{bmatrix} -2.2 \\ -1.6 \end{bmatrix}$ **MPa**

Total stress in bottom of concrete $\sigma_{Q.c.bot.1.sls} := \begin{bmatrix} -\sigma_{Q.c.1.sls} \\ \sigma_{Q.m.c.1.sls} \end{bmatrix} = \begin{bmatrix} -2.2 \\ 1.6 \end{bmatrix}$ **MPa**

Normal stress from composite action $\sigma_{Q.t.1.sls} := \frac{\gamma_t \cdot E_{t.0.mean} \cdot a_{t.sls}}{EI_{eff.sls}} \cdot M_{Q.f.max} = 2$ **MPa**

Stress from bending $\sigma_{Q.m.t.1.sls} := \frac{0.5 \cdot E_{t.0.mean} \cdot h_t}{EI_{eff.sls}} \cdot M_{Q.f.max} = 2.7$ **MPa**

Total stress in top of timber $\sigma_{Q.t.top.1.sls} := \begin{bmatrix} \sigma_{Q.t.1.sls} \\ -\sigma_{Q.m.t.1.sls} \end{bmatrix} = \begin{bmatrix} 2 \\ -2.7 \end{bmatrix}$ **MPa**

Total stress in bottom of timber $\sigma_{Q.t.bot.1.sls} := \begin{bmatrix} \sigma_{Q.t.1.sls} \\ \sigma_{Q.m.t.1.sls} \end{bmatrix} = \begin{bmatrix} 2 \\ 2.7 \end{bmatrix}$ **MPa**

Mid span - Max stresses from traffic load (UDL) SLS

Normal stress from composite action $\sigma_{q.c.1.sls} := \frac{\gamma_{c.sls} \cdot E_{cm} \cdot a_{c.sls}}{EI_{eff.sls}} \cdot M_{q.f.max} = 0.7$ **MPa**

Stress from bending $\sigma_{q.m.c.1.sls} := \frac{0.5 \cdot E_{cm} \cdot t_c}{EI_{eff.sls}} \cdot M_{q.f.max} = 0.5$ **MPa**

Total stress in top of concrete $\sigma_{q.c.top.1.sls} := \begin{bmatrix} -\sigma_{q.c.1.sls} \\ -\sigma_{q.m.c.1.sls} \end{bmatrix} = \begin{bmatrix} -0.67 \\ -0.48 \end{bmatrix}$ **MPa**

Total stress in bottom of concrete $\sigma_{q.c.bot.1.sls} := \begin{bmatrix} -\sigma_{q.c.1.sls} \\ \sigma_{q.m.c.1.sls} \end{bmatrix} = \begin{bmatrix} -0.7 \\ 0.5 \end{bmatrix}$ **MPa**

Normal stress from composite action $\sigma_{q.t.1.sls} := \frac{\gamma_t \cdot E_{t.0.mean} \cdot a_{t.sls}}{EI_{eff.sls}} \cdot M_{q.f.max} = 0.6$ **MPa**

Stress from bending $\sigma_{q.m.t.1.sls} := \frac{0.5 \cdot E_{t.0.mean} \cdot h_t}{EI_{eff.sls}} \cdot M_{q.f.max} = 0.8$ **MPa**

Total stress in top of timber $\sigma_{q.t.top.1.sls} := \begin{bmatrix} \sigma_{q.t.1.sls} \\ -\sigma_{q.m.c.1.sls} \end{bmatrix} = \begin{bmatrix} 0.6 \\ -0.5 \end{bmatrix}$ **MPa**

Total stress in bottom of timber $\sigma_{q.t.bot.1.sls} := \begin{bmatrix} \sigma_{q.t.1.sls} \\ \sigma_{q.m.c.1.sls} \end{bmatrix} = \begin{bmatrix} 0.6 \\ 0.5 \end{bmatrix}$ **MPa**

Horizontal forces

Normal stresses from horizontal forces

Normal stress from surcharge

$$\sigma_{ö} := \begin{bmatrix} \frac{-H_{ö}}{2 \cdot (A_t + A_c)} \\ 0 \end{bmatrix} = \begin{bmatrix} -28.3 \\ 0 \end{bmatrix} \textbf{kPa}$$

Normal stress from earth pressure

$$\sigma_{0.k} := \begin{bmatrix} \frac{-F_{0.k}}{2 \cdot (A_t + A_c)} \\ 0 \end{bmatrix} = \begin{bmatrix} -52.61 \\ 0 \end{bmatrix} \textbf{kPa}$$

Stresses caused by breaking force

$$\sigma_{Break} := \begin{bmatrix} \frac{-Q_{bk}}{2 \cdot (A_t + A_c)} \\ 0 \end{bmatrix} = \begin{bmatrix} -69.24 \\ 0 \end{bmatrix} \textbf{kPa}$$

Normal stress from thermal expansion

$$\sigma_{th} := \begin{bmatrix} q_{th} \\ 0 \end{bmatrix} = \begin{bmatrix} -79.93 \\ 0 \end{bmatrix} \textbf{kPa}$$

Moment from horizontal forces

Distance between traingular pressure and neutral axis

$$l_{tri} := \frac{2}{3} \cdot h_{ec} - \left(a_{c.sls} + \frac{t_c}{2} \right) = 1.76 \textbf{ m}$$

Distance between rectangular pressure and neutral axis

$$l_{rec} := \frac{h_{ec}}{2} - \left(a_{c.sls} + \frac{t_c}{2} \right) = 1.2 \textbf{ m}$$

Moment from surcharge

$$M_{sur} := -\frac{H_{ö}}{2} \cdot l_{rec} = -79.69 \textbf{ kNm}$$

Moment from earth pressure

$$M_{ep} := -\frac{F_{0.k}}{2} \cdot l_{tri} = -217.13 \textbf{ kNm}$$

Moment from breaking force

$$M_{bk} := -\frac{Q_{bk}}{2} \cdot l_{tri} = -285.75 \textbf{ kNm}$$

Moment from thermal expansion

$$M_{thermal} := \frac{q_{th} \cdot t_i \cdot h_i}{2} \cdot l_{tri} = -141.51 \textbf{ kNm}$$

Load combinations

Taken from SS-EN 1990:2023, Annex A, Table A.1.8

ULS

Unfavourable resulting effects

Permanent load	$\gamma_G := 1.35$		
Variable load	$\gamma_Q := 1.5$		
Favourable resulting effects			
Permanent load	$\gamma_{G.f} := 1.0$		
Variable load	$\gamma_{Q.f} := 0$		
SLS	Combined	Frequent	Quasi
LM1- Boggie load	$\psi_{0.Q} := 0.75$	$\psi_{1.Q} := 0.75$	$\psi_{2.Q} := 0$
LM1- Distibuted load	$\psi_{0.q} := 0.40$	$\psi_{1.q} := 0.40$	$\psi_{2.q} := 0$
LM1- Breaking load	$\psi_{0.B} := 0.70$	$\psi_{1.B} := 0.70$	$\psi_{2.B} := 0$
LM1- Other horizontal load	$\psi_{0.Ö} := 0.75$	$\psi_{1.Ö} := 0.75$	$\psi_{2.Ö} := 0$
Temperature load	$\psi_{0.th} := 0.60$	$\psi_{1.th} := 0.60$	$\psi_{2.th} := 0.50$
Safety class 3	$\gamma_d := 1$		
Factor according to 6.10b	$\xi := 0.89$		
Gamma factor for earth pressure	$\gamma_E := 1.35$		
Factor for self weight of pavement			
Superior	$\gamma_{sup} := 1.1$		
Inferior	$\gamma_{inf} := 0.9$		

$$zeros := \begin{bmatrix} 0 \\ 0 \end{bmatrix} \textbf{MPa}$$

$\sigma_{sur.c.top.1} := \sigma_{ö}$
$\sigma_{sur.c.bot.1} := \sigma_{ö}$
$\sigma_{sur.t.top.1} := \sigma_{ö}$
$\sigma_{sur.t.bot.1} := \sigma_{ö}$

$\sigma_{sur.c.top.sls.1} := \sigma_{ö}$
$\sigma_{sur.c.bot.sls.1} := \sigma_{ö}$
$\sigma_{sur.t.top.sls.1} := \sigma_{ö}$
$\sigma_{sur.t.bot.sls.1} := \sigma_{ö}$

$\sigma_{bk.c.top.1} := \sigma_{Break}$
$\sigma_{bk.c.bot.1} := \sigma_{Break}$
$\sigma_{bk.t.top.1} := \sigma_{Break}$
$\sigma_{bk.t.bot.1} := \sigma_{Break}$

$\sigma_{bk.c.top.sls.1} := \sigma_{Break}$
$\sigma_{bk.c.bot.sls.1} := \sigma_{Break}$
$\sigma_{bk.t.top.sls.1} := \sigma_{Break}$
$\sigma_{bk.t.bot.sls.1} := \sigma_{Break}$

$\sigma_{ep.c.top.1} := \sigma_{0.k}$
$\sigma_{ep.c.bot.1} := \sigma_{0.k}$
$\sigma_{ep.t.top.1} := \sigma_{0.k}$
$\sigma_{ep.t.bot.1} := \sigma_{0.k}$

$\sigma_{ep.c.top.sls.1} := \sigma_{0.k}$
$\sigma_{ep.c.bot.sls.1} := \sigma_{0.k}$
$\sigma_{ep.t.top.sls.1} := \sigma_{0.k}$
$\sigma_{ep.t.bot.sls.1} := \sigma_{0.k}$

$\sigma_{th.c.top.1} := zeros$
$\sigma_{th.c.bot.1} := zeros$
$\sigma_{th.t.top.1} := zeros$
$\sigma_{th.t.bot.1} := zeros$

$\sigma_{th.c.top.sls.1} := zeros$
$\sigma_{th.c.bot.sls.1} := zeros$
$\sigma_{th.t.top.sls.1} := zeros$
$\sigma_{th.t.bot.sls.1} := zeros$

ULS - 6.10a Mis span

$$\sum_{j\geq 1}\gamma_{G,j,sup}G_{k,j,sup}" + "\gamma_{G,j,inf}G_{k,j,inf}" + "\gamma_{Q,1}\Psi_{0,1}Q_{k,1}" + "\sum_{i\geq 1}\gamma_{Q,i}\Psi_{0,i}Q_{k,i} \qquad 6.10a$$

$$\sum_{j\geq 1}\xi_{G,j,sup}\gamma_{G,j,sup}G_{k,j,sup}" + "\gamma_{G,j,inf}G_{k,j,inf}" + "\gamma_{Q,1}Q_{k,1}" + "\sum_{i\geq 1}\gamma_{Q,i}\Psi_{0,i}Q_{k,i} \qquad 6.10b$$

Total stress in top of concrete

Min $\sigma_{min.c.top.ULS.6.10a.1} := \gamma_d \cdot \left(\gamma_G \cdot \left(\sigma_{g.c.top.1} + \gamma_{sup} \cdot \sigma_{g.pav.c.top.1}\right) + \gamma_E \cdot \sigma_{ep.c.top.1}\right) \dots = \begin{bmatrix} -4.2 \\ -2.59 \end{bmatrix}$ ***MPa***

$\dots + \gamma_d \cdot \gamma_Q \cdot \left(\psi_{0.Q} \cdot \sigma_{Q.c.top.1} + \psi_{0.q} \cdot \sigma_{q.c.top.1}\right) \dots$

$+ 0.6 \cdot \gamma_d \cdot \gamma_Q \cdot \left(\psi_{0.B} \cdot \sigma_{bk.c.top.1} + \psi_{0.\ddot{O}} \cdot \sigma_{sur.c.top.1}\right) + \gamma_d \cdot \psi_{0.th} \cdot \sigma_{th.c.top.1}$

Max $\sigma_{max.c.top.ULS.6.10a.1} := \gamma_d \cdot \gamma_{G.f} \cdot \left(\sigma_{g.c.top.1} + \gamma_{inf} \cdot \sigma_{g.pav.c.top.1} + \sigma_{ep.c.top.1}\right) \dots = \begin{bmatrix} -3.65 \\ -2.4 \end{bmatrix}$ ***MPa***

$+ \gamma_d \cdot \gamma_Q \cdot \left(\psi_{0.Q} \cdot \sigma_{Q.c.top.1} + \psi_{0.q} \cdot \sigma_{q.c.top.1}\right)$

Total stress in bottom of concrete

Min $\sigma_{min.c.bot.ULS.6.10a.1} := \gamma_d \cdot \left(\gamma_G \cdot \left(\sigma_{g.c.bot.1} + \gamma_{sup} \cdot \sigma_{g.pav.c.bot.1}\right) + \gamma_E \cdot \sigma_{ep.c.bot.1}\right) \dots = \begin{bmatrix} -4.2 \\ 2.59 \end{bmatrix}$ ***MPa***

$\dots + \gamma_d \cdot \gamma_Q \cdot \left(\psi_{0.Q} \cdot \sigma_{Q.c.bot.1} + \psi_{0.q} \cdot \sigma_{q.c.bot.1}\right) \dots$

$+ 0.6 \cdot \gamma_d \cdot \gamma_Q \cdot \left(\psi_{0.B} \cdot \sigma_{bk.c.bot.1} + \psi_{0.\ddot{O}} \cdot \sigma_{sur.c.bot.1}\right) + \gamma_d \cdot \psi_{0.th} \cdot \sigma_{th.c.bot.1}$

Max $\sigma_{max.c.bot.ULS.6.10a.1} := \gamma_d \cdot \gamma_{G.f} \cdot \left(\sigma_{g.c.bot.1} + \gamma_{inf} \cdot \sigma_{g.pav.c.bot.1} + \sigma_{ep.c.bot.1}\right) \dots = \begin{bmatrix} -3.65 \\ 2.4 \end{bmatrix}$ ***MPa***

$+ \gamma_d \cdot \gamma_Q \cdot \left(\psi_{0.Q} \cdot \sigma_{Q.c.bot.1} + \psi_{0.q} \cdot \sigma_{q.c.bot.1}\right)$

Total stress in top of timber

Min $\sigma_{min.t.top.ULS.6.10a.1} := \gamma_d \cdot \left(\gamma_G \cdot \left(\sigma_{g.t.top.1} + \gamma_{sup} \cdot \sigma_{g.pav.t.top.1}\right) + \gamma_E \cdot \sigma_{ep.t.top.1}\right) \dots = \begin{bmatrix} 3.48 \\ -9.08 \end{bmatrix}$ ***MPa***

$\dots + \gamma_d \cdot \gamma_Q \cdot \left(\psi_{0.Q} \cdot \sigma_{Q.t.top.1} + \psi_{0.q} \cdot \sigma_{q.t.top.1}\right) \dots$

$+ 0.6 \cdot \gamma_d \cdot \gamma_Q \cdot \left(\psi_{0.B} \cdot \sigma_{bk.t.top.1} + \psi_{0.\ddot{O}} \cdot \sigma_{sur.t.top.1}\right) + \gamma_d \cdot \psi_{0.th} \cdot \sigma_{th.t.top.1}$

Max $\sigma_{max.t.top.ULS.6.10a.1} := \gamma_d \cdot \gamma_{G.f} \cdot \left(\sigma_{g.t.top.1} + \gamma_{inf} \cdot \sigma_{g.pav.t.top.1} + \sigma_{ep.t.top.1}\right) \dots = \begin{bmatrix} 3.15 \\ -7.3 \end{bmatrix}$ ***MPa***

$+ \gamma_d \cdot \gamma_Q \cdot \left(\psi_{0.Q} \cdot \sigma_{Q.t.top.1} + \psi_{0.q} \cdot \sigma_{q.t.top.1}\right)$

Total stress in bottom of timber

Min $\sigma_{min.t.bot.ULS.6.10a.1} := \gamma_d \cdot \gamma_{G.f} \cdot \left(\sigma_{g.t.bot.1} + \gamma_{inf} \cdot \sigma_{g.pav.t.bot.1} + \sigma_{ep.t.bot.1}\right) \dots = \begin{bmatrix} 3.15 \\ 7.3 \end{bmatrix}$ ***MPa***

$+ \gamma_d \cdot \gamma_Q \cdot \left(\psi_{0.Q} \cdot \sigma_{Q.t.bot.1} + \psi_{0.q} \cdot \sigma_{q.t.bot.1}\right)$

Max $\sigma_{max.t.bot.ULS.6.10a.1} := \gamma_d \cdot \left(\gamma_G \cdot \left(\sigma_{g.t.bot.1} + \gamma_{sup} \cdot \sigma_{g.pav.t.bot.1}\right) + \gamma_E \cdot \sigma_{ep.t.bot.1}\right) \dots = \begin{bmatrix} 3.48 \\ 9.08 \end{bmatrix}$ ***MPa***

$\dots + \gamma_d \cdot \gamma_Q \cdot \left(\psi_{0.Q} \cdot \sigma_{Q.t.bot.1} + \psi_{0.q} \cdot \sigma_{q.t.bot.1}\right) \dots$

$+ 0.6 \cdot \gamma_d \cdot \gamma_Q \cdot \left(\psi_{0.B} \cdot \sigma_{bk.t.bot.1} + \psi_{0.\ddot{O}} \cdot \sigma_{sur.t.bot.1}\right) + \gamma_d \cdot \psi_{0.th} \cdot \sigma_{th.t.bot.1}$

Capacity check

$\sigma_{c.Rd}(\sigma_{Ed}) :=$ for $i \in 1 .. \text{cols}(\sigma_{Ed})$

  if $\sigma_{Ed_{1,i}} + \sigma_{Ed_{2,i}} < 0$ ***Pa***

    $\sigma_{Rd_{1,i}} \leftarrow f_{cd}$

  else

    $\sigma_{Rd_{1,i}} \leftarrow f_{ctd}$

  σ_{Rd}

$\sigma_{Rd}(\sigma_{Ed}) :=$ for $i \in 1 .. \text{cols}(\sigma_{Ed})$

  if $\sigma_{Ed_{1,i}} < 0$ ***Pa***

    $\sigma_{Rd_{1,i}} \leftarrow f_{c.0.d}$

    $\sigma_{Rd_{2,i}} \leftarrow f_{m.d}$

  else

    $\sigma_{Rd_{1,i}} \leftarrow f_{t.0.d}$

    $\sigma_{Rd_{2,i}} \leftarrow f_{m.d}$

  σ_{Rd}

Total stress in top of concrete - min

$$\sigma_{Rd\_min.c.top.ULS.6.10a.1} := \sigma_{c.Rd}\left(\sigma_{min.c.top.ULS.6.10a.1}\right) = [23.33]\ \textbf{MPa}$$

$$\eta_{min.c.top.ULS.6.10a.1} := \frac{\text{abs}\left(\sigma_{min.c.top.ULS.6.10a.1}(0,0) + \sigma_{min.c.top.ULS.6.10a.1}(1,0)\right)}{\sigma_{Rd\_min.c.top.ULS.6.10a.1}(0,0)} = 29\%$$

Total stress in top of concrete - max

$$\sigma_{Rd\_max.c.top.ULS.6.10a.1} := \sigma_{c.Rd}\left(\sigma_{max.c.top.ULS.6.10a.1}\right) = [23.33]\ \textbf{MPa}$$

$$\eta_{max.c.top.ULS.6.10a.1} := \frac{\text{abs}\left(\sigma_{max.c.top.ULS.6.10a.1}(0,0) + \sigma_{max.c.top.ULS.6.10a.1}(1,0)\right)}{\sigma_{Rd\_max.c.top.ULS.6.10a.1}(0,0)}$$

Total stress in bottom of concrete - min

$$\sigma_{Rd\_min.c.bot.ULS.6.10a.1} := \sigma_{c.Rd}\left(\sigma_{min.c.bot.ULS.6.10a.1}\right) = [23.33]\ \textbf{MPa}$$

$$\eta_{min.c.bot.ULS.6.10a.1} := \frac{\text{abs}\left(\sigma_{min.c.bot.ULS.6.10a.1}(0,0) + \sigma_{min.c.bot.ULS.6.10a.1}(1,0)\right)}{\sigma_{Rd\_min.c.bot.ULS.6.10a.1}(0,0)} = 7\%$$

Total stress in bottom of concrete - max

$$\sigma_{Rd\_max.c.bot.ULS.6.10a.1} := \sigma_{c.Rd}\left(\sigma_{max.c.bot.ULS.6.10a.1}\right) = [23.33]\ \textbf{MPa}$$

$$\eta_{max.c.bot.ULS.6.10a.1} := \frac{\text{abs}\left(\sigma_{max.c.bot.ULS.6.10a.1}(0,0) + \sigma_{max.c.bot.ULS.6.10a.1}(1,0)\right)}{\sigma_{Rd\_max.c.bot.ULS.6.10a.1}(0,0)} = 5\%$$

Total stress in top of timber - min

$$\sigma_{Rd\_min.t.top.ULS.6.10a.1} := \sigma_{Rd}\left(\sigma_{min.t.top.ULS.6.10a.1}\right) = \begin{bmatrix} 14.04 \\ 21.6 \end{bmatrix}\ \textbf{MPa}$$

$$\eta_{min.t.top.ULS.6.10a.1} := \text{abs}\left(\frac{\sigma_{min.t.top.ULS.6.10a.1}(0,0)}{\sigma_{Rd\_min.t.top.ULS.6.10a.1}(0,0)} + \frac{\sigma_{min.t.top.ULS.6.10a.1}(1,0)}{\sigma_{Rd\_min.t.top.ULS.6.10a.1}(1,0)}\right) = 17\%$$

Total stress in top of timber - max

$$\sigma_{Rd\_max.t.top.ULS.6.10a.1} := \sigma_{Rd}\left(\sigma_{max.t.top.ULS.6.10a.1}\right) = \begin{bmatrix} 14.04 \\ 21.6 \end{bmatrix}\ \textbf{MPa}$$

$$\eta_{max.t.top.ULS.6.10a.1} := \text{abs}\left(\frac{\sigma_{max.t.top.ULS.6.10a.1}(0,0)}{\sigma_{Rd\_max.t.top.ULS.6.10a.1}(0,0)} + \frac{\sigma_{max.t.top.ULS.6.10a.1}(1,0)}{\sigma_{Rd\_max.t.top.ULS.6.10a.1}(1,0)}\right) = 11\%$$

Total stress in bottom of timber - min

$$\sigma_{Rd\_min.t.bot.ULS.6.10a.1} := \sigma_{Rd}\left(\sigma_{min.t.bot.ULS.6.10a.1}\right) = \begin{bmatrix} 14.04 \\ 21.6 \end{bmatrix}\ \textbf{MPa}$$

$$\eta_{min.t.bot.ULS.6.10a.1} := \text{abs}\left(\frac{\sigma_{min.t.bot.ULS.6.10a.1}(0,0)}{\sigma_{Rd\_min.t.bot.ULS.6.10a.1}(0,0)} + \frac{\sigma_{min.t.bot.ULS.6.10a.1}(1,0)}{\sigma_{Rd\_min.t.bot.ULS.6.10a.1}(1,0)}\right) = 56\%$$

Total stress in bottom of timber - max

$$\sigma_{Rd\_max.t.bot.ULS.6.10a.1} := \sigma_{Rd}\left(\sigma_{max.t.bot.ULS.6.10a.1}\right) = \begin{bmatrix} 14.04 \\ 21.6 \end{bmatrix}\ \textbf{MPa}$$

$$\eta_{max.t.bot.ULS.6.10a.1} := \text{abs}\left(\frac{\sigma_{max.t.bot.ULS.6.10a.1}(0,0)}{\sigma_{Rd\_max.t.bot.ULS.6.10a.1}(0,0)} + \frac{\sigma_{max.t.bot.ULS.6.10a.1}(1,0)}{\sigma_{Rd\_max.t.bot.ULS.6.10a.1}(1,0)}\right) = 67\%$$

ULS - 6.10b Mid span

$$\sum_{j\geq 1}\gamma_{G,j,sup}G_{k,j,sup}\text{"}+\text{"}\gamma_{G,j,inf}G_{k,j,inf}\text{"}+\text{"}\gamma_{Q,1}\Psi_{0,1}Q_{k,1}\text{"}+\text{"}\sum_{i\geq 1}\gamma_{Q,i}\Psi_{0,i}Q_{k,i} \qquad \text{6.10a}$$

$$\text{6.10b}$$

$$\sum_{j\geq 1}\xi_{G,j,sup}\gamma_{G,j,sup}G_{k,j,sup}\text{"}+\text{"}\gamma_{G,j,inf}G_{k,j,inf}\text{"}+\text{"}\gamma_{Q,1}Q_{k,1}\text{"}+\text{"}\sum_{i\geq 1}\gamma_{Q,i}\Psi_{0,i}Q_{k,i}$$

Total stress in top of concrete

Min $\sigma_{min.c.top.ULS.6.10b.1} := \gamma_d \cdot \xi \cdot \left(\gamma_G \cdot \left(\sigma_{g.c.top.1} + \gamma_{sup} \cdot \sigma_{g.pav.c.top.1}\right) + \gamma_E \cdot \sigma_{ep.c.top.1}\right) \dashv$
$+ \gamma_d \cdot \gamma_Q \cdot \left(\sigma_{Q.c.top.1} + \sigma_{q.c.top.1}\right) \dashv$
$+ 0.6 \cdot \gamma_d \cdot \gamma_Q \cdot \left(\psi_{0.B} \cdot \sigma_{bk.c.top.1} + \psi_{0.\ddot{O}} \cdot \sigma_{sur.c.top.1}\right) + \gamma_d \cdot \psi_{0.th} \cdot \sigma_{th.c.top.1}$
$= \begin{bmatrix} -5.48 \\ -3.57 \end{bmatrix}$ ***MPa***

Max $\sigma_{max.c.top.ULS.6.10b.1} := \gamma_d \cdot \gamma_{G.f} \cdot \left(\sigma_{g.c.top.1} + \sigma_{g.pav.c.top.1} + \sigma_{ep.c.top.1}\right) \dashv = \begin{bmatrix} -5.15 \\ -3.46 \end{bmatrix}$ ***MPa***
$+ \gamma_d \cdot \gamma_Q \cdot \left(\sigma_{Q.c.top.1} + \sigma_{q.c.top.1}\right)$

Total stress in bottom of concrete

Min $\sigma_{min.c.bot.ULS.6.10b.1} := \gamma_d \cdot \xi \cdot \left(\gamma_G \cdot \left(\sigma_{g.c.bot.1} + \gamma_{sup} \cdot \sigma_{g.pav.c.bot.1}\right) + \gamma_E \cdot \sigma_{ep.c.bot.1}\right) \dashv$
$+ \gamma_d \cdot \gamma_Q \cdot \left(\sigma_{Q.c.bot.1} + \sigma_{q.c.bot.1}\right) \dashv$
$+ 0.6 \cdot \gamma_d \cdot \gamma_Q \cdot \left(\psi_{0.B} \cdot \sigma_{bk.c.bot.1} + \psi_{0.\ddot{O}} \cdot \sigma_{sur.c.bot.1}\right) + \gamma_d \cdot \psi_{0.th} \cdot \sigma_{th.c.bot.1}$
$= \begin{bmatrix} -5.48 \\ 3.57 \end{bmatrix}$ ***MPa***

Max $\sigma_{max.c.bot.ULS.6.10b.1} := \gamma_d \cdot \gamma_{G.f} \cdot \left(\sigma_{g.c.bot.1} + \gamma_{inf} \cdot \sigma_{g.pav.c.bot.1} + \sigma_{ep.c.bot.1}\right) \dashv = \begin{bmatrix} -5.07 \\ 3.43 \end{bmatrix}$ ***MPa***
$+ \gamma_d \cdot \gamma_Q \cdot \left(\sigma_{Q.c.bot.1} + \sigma_{q.c.bot.1}\right)$

Total stress in top of timber

Min $\sigma_{min.t.top.ULS.6.10b.1} := \gamma_d \cdot \xi \cdot \left(\gamma_G \cdot \left(\sigma_{g.t.top.1} + \gamma_{sup} \cdot \sigma_{g.pav.t.top.1}\right) + \gamma_E \cdot \sigma_{ep.t.top.1}\right) \dashv$
$+ \gamma_d \cdot \gamma_Q \cdot \left(\sigma_{Q.t.top.1} + \sigma_{q.t.top.1}\right) \dashv$
$+ 0.6 \cdot \gamma_d \cdot \gamma_Q \cdot \left(\psi_{0.B} \cdot \sigma_{bk.t.top.1} + \psi_{0.\ddot{O}} \cdot \sigma_{sur.t.top.1}\right) + \gamma_d \cdot \psi_{0.th} \cdot \sigma_{th.t.top.1}$
$= \begin{bmatrix} 4.64 \\ -9.87 \end{bmatrix}$ ***MPa***

Max $\sigma_{max.t.top.ULS.6.10b.1} := \gamma_d \cdot \gamma_{G.f} \cdot \left(\sigma_{g.t.top.1} + \gamma_{inf} \cdot \sigma_{g.pav.t.top.1} + \sigma_{ep.t.top.1}\right) \dashv = \begin{bmatrix} 4.41 \\ -8.73 \end{bmatrix}$ ***MPa***
$+ \gamma_d \cdot \gamma_Q \cdot \left(\sigma_{Q.t.top.1} + \sigma_{q.t.top.1}\right)$

Total stress in bottom of timber

Min $\sigma_{min.t.bot.ULS.6.10b.1} := \gamma_d \cdot \gamma_{G.f} \cdot \left(\sigma_{g.t.bot.1} + \gamma_{inf} \cdot \sigma_{g.pav.t.bot.1} + \sigma_{ep.t.bot.1}\right) \dashv = \begin{bmatrix} 4.41 \\ 8.73 \end{bmatrix}$ ***MPa***
$+ \gamma_d \cdot \gamma_Q \cdot \left(\sigma_{Q.t.bot.1} + \sigma_{q.t.bot.1}\right)$

Max $\sigma_{max.t.bot.ULS.6.10b.1} := \gamma_d \cdot \xi \cdot \left(\gamma_G \cdot \left(\sigma_{g.t.bot.1} + \gamma_{sup} \cdot \sigma_{g.pav.t.bot.1}\right) + \gamma_E \cdot \sigma_{ep.t.bot.1}\right) \dashv$
$+ \gamma_d \cdot \gamma_Q \cdot \left(\sigma_{Q.t.bot.1} + \sigma_{q.t.bot.1}\right) \dashv$
$+ 0.6 \cdot \gamma_d \cdot \gamma_Q \cdot \left(\psi_{0.B} \cdot \sigma_{bk.t.bot.1} + \psi_{0.\ddot{O}} \cdot \sigma_{sur.t.bot.1}\right) + \gamma_d \cdot \psi_{0.th} \cdot \sigma_{th.t.bot.1}$
$= \begin{bmatrix} 4.64 \\ 9.87 \end{bmatrix}$ ***MPa***

Capacity check

Total stress in top of concrete - min

$$\sigma_{Rd\_min.c.top.ULS.6.10b.1} := \sigma_{c.Rd}\left(\sigma_{min.c.top.ULS.6.10b.1}\right) = [\,23.33\,]\ \textbf{\textit{MPa}}$$

$$\eta_{min.c.top.ULS.6.10b.1} := \frac{\mathrm{abs}\left(\sigma_{min.c.top.ULS.6.10b.1}(0,0) + \sigma_{min.c.top.ULS.6.10b.1}(1,0)\right)}{\sigma_{Rd\_min.c.top.ULS.6.10b.1}(0,0)} = 39\%$$

Total stress in top of concrete - max

$$\sigma_{Rd\_max.c.top.ULS.6.10b.1} := \sigma_{c.Rd}\left(\sigma_{max.c.top.ULS.6.10b.1}\right) = [\,23.33\,]\ \textbf{\textit{MPa}}$$

$$\eta_{max.c.top.ULS.6.10b.1} := \frac{\mathrm{abs}\left(\sigma_{max.c.top.ULS.6.10b.1}(0,0) + \sigma_{max.c.top.ULS.6.10b.1}(1,0)\right)}{\sigma_{Rd\_max.c.top.ULS.6.10b.1}(0,0)} = 37\%$$

Total stress in bottom of concrete - min

$$\sigma_{Rd\_min.c.bot.ULS.6.10b.1} := \sigma_{c.Rd}\left(\sigma_{min.c.bot.ULS.6.10b.1}\right) = [\,23.33\,]\ \textbf{\textit{MPa}}$$

$$\eta_{min.c.bot.ULS.6.10b.1} := \frac{\mathrm{abs}\left(\sigma_{min.c.bot.ULS.6.10b.1}(0,0) + \sigma_{min.c.bot.ULS.6.10b.1}(1,0)\right)}{\sigma_{Rd\_min.c.bot.ULS.6.10b.1}(0,0)} = 8\%$$

Total stress in bottom of concrete - max

$$\sigma_{Rd\_max.c.bot.ULS.6.10b.1} := \sigma_{c.Rd}\left(\sigma_{max.c.bot.ULS.6.10b.1}\right) = [\,23.33\,]\ \textbf{\textit{MPa}}$$

$$\eta_{max.c.bot.ULS.6.10b.1} := \frac{\mathrm{abs}\left(\sigma_{max.c.bot.ULS.6.10b.1}(0,0) + \sigma_{max.c.bot.ULS.6.10b.1}(1,0)\right)}{\sigma_{Rd\_max.c.bot.ULS.6.10b.1}(0,0)} = 7\%$$

Total stress in top of timber - min

$$\sigma_{Rd\_min.t.top.ULS.6.10b.1} := \sigma_{Rd}\left(\sigma_{min.t.top.ULS.6.10b.1}\right) = \begin{bmatrix} 14.04 \\ 21.6 \end{bmatrix}\ \textbf{\textit{MPa}}$$

$$\eta_{min.t.top.ULS.6.10b.1} := \mathrm{abs}\left(\frac{\sigma_{min.t.top.ULS.6.10b.1}(0,0)}{\sigma_{Rd\_min.t.top.ULS.6.10b.1}(0,0)} + \frac{\sigma_{min.t.top.ULS.6.10b.1}(1,0)}{\sigma_{Rd\_min.t.top.ULS.6.10b.1}(1,0)}\right) = 13\%$$

Total stress in top of timber - max

$$\sigma_{Rd\_max.t.top.ULS.6.10b.1} := \sigma_{Rd}\left(\sigma_{max.t.top.ULS.6.10b.1}\right) = \begin{bmatrix} 14.04 \\ 21.6 \end{bmatrix}\ \textbf{\textit{MPa}}$$

$$\eta_{max.t.top.ULS.6.10b.1} := \mathrm{abs}\left(\frac{\sigma_{max.t.top.ULS.6.10b.1}(0,0)}{\sigma_{Rd\_max.t.top.ULS.6.10b.1}(0,0)} + \frac{\sigma_{max.t.top.ULS.6.10b.1}(1,0)}{\sigma_{Rd\_max.t.top.ULS.6.10b.1}(1,0)}\right) = 9\%$$

Total stress in bottom of timber - min

$$\sigma_{Rd\_min.t.bot.ULS.6.10b.1} := \sigma_{Rd}\left(\sigma_{min.t.bot.ULS.6.10b.1}\right) = \begin{bmatrix} 14.04 \\ 21.6 \end{bmatrix}\ \textbf{\textit{MPa}}$$

$$\eta_{min.t.bot.ULS.6.10b.1} := \mathrm{abs}\left(\frac{\sigma_{min.t.bot.ULS.6.10b.1}(0,0)}{\sigma_{Rd\_min.t.bot.ULS.6.10b.1}(0,0)} + \frac{\sigma_{min.t.bot.ULS.6.10b.1}(1,0)}{\sigma_{Rd\_min.t.bot.ULS.6.10b.1}(1,0)}\right) = 72\%$$

Total stress in bottom of timber - max

$$\sigma_{Rd\_max.t.bot.ULS.6.10b.1} := \sigma_{Rd}\left(\sigma_{max.t.bot.ULS.6.10b.1}\right) = \begin{bmatrix} 14.04 \\ 21.6 \end{bmatrix}\ \textbf{\textit{MPa}}$$

$$\eta_{max.t.bot.ULS.6.10b.1} := \mathrm{abs}\left(\frac{\sigma_{max.t.bot.ULS.6.10b.1}(0,0)}{\sigma_{Rd\_max.t.bot.ULS.6.10b.1}(0,0)} + \frac{\sigma_{max.t.bot.ULS.6.10b.1}(1,0)}{\sigma_{Rd\_max.t.bot.ULS.6.10b.1}(1,0)}\right) = 79\%$$

SLS - Characteristic combination

Total stress in top of concrete

Min $\sigma_{min.c.top.SLS.kar.1} := \sigma_{g.c.top.1} + \gamma_{sup} \cdot \sigma_{g.pav.c.top.sls.1} + \sigma_{ep.c.top.sls.1} + \left(\sigma_{Q.c.top.1.sls} + \sigma_{q.c.top.1.sls}\right) + 0.6 \cdot \left(\psi_{0.B} \cdot \sigma_{bk.c.top.sls.1} + \psi_{0.Ö} \cdot \sigma_{sur.c.top.sls.1}\right) + \gamma_d \cdot \psi_{0.th} \cdot \sigma_{th.c.top.sls.1} = \begin{bmatrix} -4.18 \\ -2.74 \end{bmatrix}$ ***MPa***

Max $\sigma_{max.c.top.SLS.kar.1} := \sigma_{g.c.top.1} + \gamma_{inf} \cdot \sigma_{g.pav.c.top.sls.1} + \sigma_{ep.c.top.sls.1} + \sigma_{Q.c.top.1.sls} + \sigma_{q.c.top.1.sls} = \begin{bmatrix} -3.92 \\ -2.62 \end{bmatrix}$ ***MPa***

Total stress in bottom of concrete

Min $\sigma_{min.c.bot.SLS.kar.1} := \sigma_{g.c.bot.1} + \gamma_{sup} \cdot \sigma_{g.pav.c.bot.sls.1} + \sigma_{ep.c.bot.sls.1} + \left(\sigma_{Q.c.bot.1.sls} + \sigma_{q.c.bot.1.sls}\right) + 0.6 \cdot \left(\psi_{0.B} \cdot \sigma_{bk.c.bot.sls.1} + \psi_{0.Ö} \cdot \sigma_{sur.c.bot.sls.1}\right) + \gamma_d \cdot \psi_{0.th} \cdot \sigma_{th.c.bot.sls.1} = \begin{bmatrix} -4.18 \\ 2.74 \end{bmatrix}$ ***MPa***

Max $\sigma_{max.c.bot.SLS.kar.1} := \sigma_{g.c.bot.1} + \gamma_{inf} \cdot \sigma_{g.pav.c.bot.sls.1} + \sigma_{ep.c.bot.sls.1} + \left(\sigma_{Q.c.bot.1.sls} + \sigma_{q.c.bot.1.sls}\right) = \begin{bmatrix} -3.92 \\ 2.62 \end{bmatrix}$ ***MPa***

Total stress in top of timber

Min $\sigma_{min.t.top.SLS.kar.1} := \sigma_{g.t.top.1} + \gamma_{sup} \cdot \sigma_{g.pav.t.top.sls.1} + \sigma_{ep.t.top.sls.1} + \left(\sigma_{Q.t.top.1.sls} + \sigma_{q.t.top.1.sls}\right) + 0.6 \cdot \left(\psi_{0.B} \cdot \sigma_{bk.t.top.sls.1} + \psi_{0.Ö} \cdot \sigma_{sur.t.top.sls.1}\right) + \gamma_d \cdot \psi_{0.th} \cdot \sigma_{th.t.top.sls.1} = \begin{bmatrix} 3.54 \\ -7.74 \end{bmatrix}$ ***MPa***

Max $\sigma_{max.t.top.SLS.kar.1} := \sigma_{g.t.top.1} + \gamma_{inf} \cdot \sigma_{g.pav.t.top.sls.1} + \sigma_{ep.t.top.sls.1} + \left(\sigma_{Q.t.top.1.sls} + \sigma_{q.t.top.1.sls}\right) = \begin{bmatrix} 3.39 \\ -7.41 \end{bmatrix}$ ***MPa***

Total stress in bottom of timber

Min $\sigma_{min.t.bot.SLS.kar.1} := \sigma_{g.t.bot.1} + \gamma_{inf} \cdot \sigma_{g.pav.t.bot.sls.1} + \sigma_{ep.t.bot.sls.1} + \left(\sigma_{Q.t.bot.1.sls} + \sigma_{q.t.bot.1.sls}\right) = \begin{bmatrix} 3.39 \\ 7.41 \end{bmatrix}$ ***MPa***

Max $\sigma_{max.t.bot.SLS.kar.1} := \sigma_{g.t.bot.1} + \gamma_{sup} \cdot \sigma_{g.pav.t.bot.sls.1} + \sigma_{ep.t.bot.sls.1} + \left(\sigma_{Q.t.bot.1.sls} + \sigma_{q.t.bot.1.sls}\right) + 0.6 \cdot \left(\psi_{0.B} \cdot \sigma_{bk.t.bot.sls.1} + \psi_{0.Ö} \cdot \sigma_{sur.t.bot.sls.1}\right) + \gamma_d \cdot \psi_{0.th} \cdot \sigma_{th.t.bot.sls.1} = \begin{bmatrix} 3.54 \\ 7.74 \end{bmatrix}$ ***MPa***

SLS - Frequent combination

Total stress in top of concrete

Min $\sigma_{min.c.top.SLS.freq.1} := \sigma_{g.c.top.1} + \gamma_{sup} \cdot \sigma_{g.pav.c.top.sls.1} + \sigma_{ep.c.top.sls.1} + \psi_{1.Q} \cdot \sigma_{Q.c.top.1.sls} + \psi_{1.q} \cdot \sigma_{q.c.top.1.sls} + \psi_{1.th} \cdot \sigma_{th.c.top.sls.1} = \begin{bmatrix} -3.19 \\ -2.05 \end{bmatrix}$ ***MPa***

Max $\sigma_{max.c.top.SLS.freq.1} := \sigma_{g.c.top.1} + \gamma_{inf} \cdot \sigma_{g.pav.c.top.sls.1} + \sigma_{ep.c.top.sls.1} + \psi_{1.Q} \cdot \sigma_{Q.c.top.1.sls} + \psi_{1.q} \cdot \sigma_{q.c.top.1.sls} = \begin{bmatrix} -2.97 \\ -1.93 \end{bmatrix}$ ***MPa***

Total stress in bottom of concrete

Min $\sigma_{min.c.bot.SLS.freq.1} := \sigma_{g.c.bot.1} + \gamma_{sup} \cdot \sigma_{g.pav.c.bot.sls.1} + \sigma_{ep.c.bot.sls.1} + \psi_{1.Q} \cdot \sigma_{Q.c.bot.1.sls} + \psi_{1.q} \cdot \sigma_{q.c.bot.1.sls} + \psi_{1.th} \cdot \sigma_{th.c.bot.sls.1} = \begin{bmatrix} -3.19 \\ 2.05 \end{bmatrix}$ ***MPa***

Max $\sigma_{max.c.bot.SLS.freq.1} := \sigma_{g.c.bot.1} + \gamma_{inf} \cdot \sigma_{g.pav.c.bot.sls.1} + \sigma_{ep.c.bot.sls.1} + \psi_{1.Q} \cdot \sigma_{Q.c.bot.1.sls} + \psi_{1.q} \cdot \sigma_{q.c.bot.1.sls} = \begin{bmatrix} -2.97 \\ 1.93 \end{bmatrix}$ ***MPa***

Total stress in top of timber

Min $\sigma_{min.t.top.SLS.freq.1} := \sigma_{g.t.top.1} + \gamma_{sup} \cdot \sigma_{g.pav.t.top.sls.1} + \sigma_{ep.t.top.sls.1} + \psi_{1.Q} \cdot \sigma_{Q.t.top.1.sls} + \psi_{1.q} \cdot \sigma_{q.t.top.1.sls} + \psi_{1.th} \cdot \sigma_{th.t.top.sls.1} = \begin{bmatrix} 2.74 \\ -6.78 \end{bmatrix}$ ***MPa***

Max $\sigma_{max.t.top.SLS.freq.1} := \sigma_{g.t.top.1} + \gamma_{inf} \cdot \sigma_{g.pav.t.top.sls.1} + \sigma_{ep.t.top.sls.1} + \psi_{1.Q} \cdot \sigma_{Q.t.top.1.sls} + \psi_{1.q} \cdot \sigma_{q.t.top.1.sls} = \begin{bmatrix} 2.54 \\ -6.45 \end{bmatrix}$ ***MPa***

Total stress in bottom of timber

Min $\sigma_{min.t.bot.SLS.freq.1} := \sigma_{g.t.bot.1} + \gamma_{inf} \cdot \sigma_{g.pav.t.bot.sls.1} + \sigma_{ep.t.bot.sls.1} + \psi_{1.Q} \cdot \sigma_{Q.t.bot.1.sls} + \psi_{1.q} \cdot \sigma_{q.t.bot.1.sls} = \begin{bmatrix} 2.54 \\ 6.45 \end{bmatrix}$ ***MPa***

Max $\sigma_{max.t.bot.SLS.freq.1} := \sigma_{g.t.bot.1} + \gamma_{sup} \cdot \sigma_{g.pav.t.bot.sls.1} + \sigma_{ep.t.bot.sls.1} + \psi_{1.Q} \cdot \sigma_{Q.t.bot.1.sls} + \psi_{1.q} \cdot \sigma_{q.t.bot.1.sls} + \psi_{1.th} \cdot \sigma_{th.t.bot.sls.1} = \begin{bmatrix} 2.74 \\ 6.78 \end{bmatrix}$ ***MPa***

Quasi permanent

Total stress in top of concrete $\sigma_{min.c.top.SLS.quasi.1} := \sigma_{g.c.top.1} + \psi_{1.th} \cdot \sigma_{th.c.top.sls.1} = \begin{bmatrix} 0 \\ 0 \end{bmatrix}$ ***MPa***

Total stress in bottom of concrete $\sigma_{min.c.bot.SLS.quasi.1} := \sigma_{g.c.bot.1} + \psi_{1.th} \cdot \sigma_{th.c.bot.sls.1} = \begin{bmatrix} 0 \\ 0 \end{bmatrix}$ ***MPa***

Total stress in top of timber $\sigma_{min.t.top.SLS.quasi.1} := \sigma_{g.t.top.1} + \psi_{1.th} \cdot \sigma_{th.t.top.sls.1} = \begin{bmatrix} 0 \\ -2.77 \end{bmatrix}$ ***MPa***

Total stress in bottom of timber $\sigma_{min.t.bot.SLS.quasi.1} := \sigma_{g.t.bot.1} + \psi_{1.th} \cdot \sigma_{th.t.bot.sls.1} = \begin{bmatrix} 0 \\ 2.77 \end{bmatrix}$ ***MPa***

Support analysis
Effective bending stiffness

Area reinforcement fi20 s100 $A_{s.20} := \frac{b_c}{100\ mm} \cdot \frac{(20\ mm)^2}{4} \cdot \pi = 0.01\ m^2$

Area reinforcement fi12 s200 $A_{s.12} := \frac{b_c}{200\ mm} \cdot \frac{(12\ mm)^2}{4} \cdot \pi = (2.12 \cdot 10^{-3})\ m^2$

Total reinforcement area $A_{s.tot} := A_{s.20} + A_{s.12} = 0.01\ m^2$

Height top reinforcement $h_{s.20} := t_c - 40\ mm = 0.26\ m$

Effective height reinforcement $h_s := \frac{(t_c - 40\ mm - 16 \cdot mm) \cdot A_{s.20} + (40\ mm + 16 \cdot mm) \cdot A_{s.12}}{A_{s.tot}} = 0.22\ m$

Composite coefficient of concretre cross-section $\gamma_{s.func}(E_s, K) := \overrightarrow{\frac{1}{1 + \frac{\pi^2 \cdot A_{s.tot} \cdot E_s \cdot s}{K \cdot L^2}}}$

Composite coefficient of timber cross-section $\gamma_t := 1$

Distance between center of the timber element and the center of gravity $a_{t.func}(\gamma_s, E_s, E_{t.0.mean}) := \overrightarrow{\frac{\gamma_s \cdot A_{s.tot} \cdot E_s \cdot (h_s + h_t)}{2 \cdot (\gamma_s \cdot A_{s.tot} \cdot E_s + E_{t.0.mean} \cdot A_t)}}$

Distance between center of the concrete element and the center of gravity $a_{s.func}(a_t) := \overrightarrow{\frac{h_s + h_t}{2} - a_t}$

Effective bending stiffness $EI_{eff.func}(\gamma_s, E_s, E_{t.0.mean}, a_t, a_s) := \overrightarrow{\gamma_s \cdot E_s \cdot A_{s.tot} \cdot a_s^2 + E_{t.0.mean} \cdot I_t + E_{t.0.mean} \cdot A_t \cdot a_t^2}$

Distance from lower edge to the centroid of the composite cross section $h_{v.func}(a_t) := a_t + \frac{h_t}{2}$

γ-method for Notch connection in ULS

$\gamma_{s.temp} := \gamma_{s.func}(E_{c.temp}, K_u) = 0.99$

$\gamma_{s.uls} := \gamma_{s.func}(E_s, K_u) = 0.96$

$\gamma_{s.sw} := \gamma_{s.func}(E_s, K_{u.creep}) = 0.9$

$a_{t.temp} := a_{t.func}(\gamma_{s.temp}, E_s, E_{t.temp}) = 0.11\ m$

$a_{t.uls} := a_{t.func}(\gamma_{s.uls}, E_s, E_{t.0.mean}) = 0.11\ m$

$a_{t.sw} := a_{t.func}(\gamma_{s.sw}, E_s, E_{t.creep}) = 0.17\ m$

$a_{s.temp} := a_{s.func}(a_{t.temp}) = 0.65\ m$

$a_{s.uls} := a_{s.func}(a_{t.uls}) = 0.65\ m$

$a_{s.sw} := a_{s.func}(a_{t.sw}) = 0.59\ m$

$EI_{eff.temp} := EI_{eff.func}(\gamma_{s.temp}, E_s, E_{t.temp}, a_{t.temp}, a_{s.temp}) = (3.65 \cdot 10^6)\ kN \cdot m^2$

$EI_{eff.uls} := EI_{eff.func}(\gamma_{s.uls}, E_s, E_{t.0.mean}, a_{t.uls}, a_{s.uls}) = (3.61 \cdot 10^6)\ kN \cdot m^2$

$EI_{eff.sw} := EI_{eff.func}(\gamma_{s.sw}, E_s, E_{t.creep}, a_{t.temp}, a_{s.sw}) = (2.27 \cdot 10^6)\ kN \cdot m^2$

$h_{v.t.temp} := h_{v.func}(a_{t.temp}) = 0.76\ m$

$h_{v.t.uls} := h_{v.func}(a_{t.uls}) = 0.76\ m$

$h_{v.t.sw} := h_{v.func}(a_{t.sw}) = 0.82\ m$

γ-method for Notch connection in SLS

$\gamma_{s.temp.sls} := \gamma_{s.func}\left(E_s, K_{ser}\right) = 0.96$

$\gamma_{s.sls} := \gamma_{s.func}\left(E_s, K_{ser}\right) = 0.96$

$\gamma_{s.sw.sls} := \gamma_{s.func}\left(E_s, K_{ser.creep}\right) = 0.9$

$a_{t.temp.sls} := a_{t.func}\left(\gamma_{s.temp.sls}, E_s, E_{t.temp.sls}\right) = 0.11\ \boldsymbol{m}$

$a_{t.sls} := a_{t.func}\left(\gamma_{s.sls}, E_s, E_{t.0.mean}\right) = 0.11\ \boldsymbol{m}$

$a_{t.sw.sls} := a_{t.func}\left(\gamma_{s.sw.sls}, E_s, E_{t.creep.sls}\right) = 0.17\ \boldsymbol{m}$

$a_{s.temp.sls} := a_{s.func}\left(a_{t.temp.sls}\right) = 0.65\ \boldsymbol{m}$

$a_{s.sls} := a_{s.func}\left(a_{t.sls}\right) = 0.65\ \boldsymbol{m}$

$a_{s.sw.sls} := a_{s.func}\left(a_{t.sw.sls}\right) = 0.59\ \boldsymbol{m}$

$EI_{eff.temp.sls} := EI_{eff.func}\left(\gamma_{s.temp}, E_s, E_{t.temp.sls}, a_{t.temp.sls}, a_{s.temp.sls}\right) = \left(3.65 \cdot 10^6\right)\ \boldsymbol{kN \cdot m^2}$

$EI_{eff.sls} := EI_{eff.func}\left(\gamma_{s.sls}, E_s, E_{t.0.mean}, a_{t.sls}, a_{s.sls}\right) = \left(3.61 \cdot 10^6\right)\ \boldsymbol{kN \cdot m^2}$

$EI_{eff.sw.sls} := EI_{eff.func}\left(\gamma_{s.sw.sls}, E_s, E_{t.creep.sls}, a_{t.sw.sls}, a_{s.sw.sls}\right) = \left(2.4 \cdot 10^6\right)\ \boldsymbol{kN \cdot m^2}$

$h_{v.temp.sls} := h_{v.func}\left(a_{t.temp.sls}\right)$

$h_{v.sls} := h_{v.func}\left(a_{t.sls}\right)$

$h_{v.t.sw.sls} := h_{v.func}\left(a_{t.sw.sls}\right)$

Effect of inelastic strains

Distance from center of gravity of timberbeam and concrete slab

$z := \frac{h_t + h_s}{2} = 0.76\ \boldsymbol{m}$

Coeffficient for inelastic strains

$C_{p.func}\left(E_s, E_{t.0.mean}, \gamma_{s.sls}\right) := \overrightarrow{\pi^2 \cdot \frac{E_s \cdot A_{s.tot} \cdot E_{t.0.mean} \cdot A_t \cdot z \cdot \gamma_{s.sls}}{\left(E_s \cdot A_{s.tot} + E_{t.0.mean} \cdot A_t\right) \cdot l^2}}$

$C_{p.sls} := C_{p.func}\left(E_s, E_{t.creep.sls}, \gamma_{s.sls}\right) = \left(5.68 \cdot 10^7\right)\ \frac{\boldsymbol{kg}}{\boldsymbol{s^2}}$

Reference temperature

$T_0 := 10\ \boldsymbol{K}$

Difference in max temp and ref temp

$\Delta T_{c.max} := T_{e.max} - T_0 = 29\ \boldsymbol{K}$

Difference in min temp and ref temp

$\Delta T_{c.min} := \left(T_{e.min} - T_0\right) = -47\ \boldsymbol{K}$

Moisture related strain

Yearly variation of timber moisture content

$\Delta mc := 2.5$ Table 6.1, Annex A in SIS-CEN/TS 19103:2022

Moisture expansion coefficient parallell grain

$\alpha_{t.u} := 10^{-5}$

Maximum strain moisture, expansion

$\varepsilon_{t.u.max} := \Delta mc \cdot \alpha_{t.u} = 2.5 \cdot 10^{-5}$

Minimum strain moisture, contraction

$\varepsilon_{t.u.min} := -\Delta mc \cdot \alpha_{t.u} = -2.5 \cdot 10^{-5}$

Temperature related strain

Shrinkage of timber from thermal and moisture strain

$\varepsilon_{t.min} := \alpha_t \cdot \Delta T_{c.min} + \varepsilon_{t.u.min} = -2.6 \cdot 10^{-4}$

$\varepsilon_{t.max} := \alpha_t \cdot \Delta T_{c.max} + \varepsilon_{t.u.max} = 1.7 \cdot 10^{-4}$

Total strain from min temp

$\Delta\varepsilon_{temp.min} := \varepsilon_{t.min} = -2.6 \cdot 10^{-4}$

Total strain from max temp

$\Delta\varepsilon_{temp.max} := \varepsilon_{t.max} = 1.7 \cdot 10^{-4}$

Max strain from temperature

$\Delta\varepsilon_{temp} := \max\left(\text{abs}\left(\Delta\varepsilon_{temp.min}\right), \text{abs}\left(\Delta\varepsilon_{temp.max}\right)\right) = 2.6 \cdot 10^{-4}$

Fictitious vertical load equivalent to inelastic strains

$p_{sls} := C_{p.sls}\ \Delta\varepsilon_{temp} = 14.78\ \frac{\boldsymbol{kN}}{\boldsymbol{m}}$

Partial factor for shirnkage

$\gamma_{F.shrinkage} := 1$

Design value of fictitious load

$p_{sls.d} := \gamma_{F.shrinkage} \cdot p_{sls} = 14.78\ \frac{\boldsymbol{kN}}{\boldsymbol{m}}$

Permanent uniformly distributed load

$q_d := g_{tot} = 41.23\ \frac{\boldsymbol{kN}}{\boldsymbol{m}}$

Modification coefficient of the bending stiffness

$$C_{J.func}\left(E_s, E_{t.0.mean}, \gamma_{s.sls}, p_{sls.d}, p_{sls}, q_d\right) := \frac{q_d + p_{sls.d}}{\frac{E_s \cdot A_{s.tot} + E_{t.0.mean} \cdot A_t}{\gamma_{s.sls} \cdot E_s \cdot A_{s.tot} + E_{t.0.mean} \cdot A_t} \cdot p_{sls} + q_d}$$

$$C_{J.sls} := C_{J.func}\left(E_s, E_{t.creep.sls}, \gamma_{s.sls}, p_{sls.d}, p_{sls}, q_d\right) = 1$$

Effective bending stiffness with respect to inelastic strains

$$EI_{eff.sw.sls} := C_{J.sls} \cdot EI_{eff.sw.sls} = 2.4\ \boldsymbol{m^4 \cdot GPa}$$

Bending moment at support caused by the fictitious load

$$\Delta M_{fic.sls.2} := -\frac{0.8 \cdot p_{sls} \cdot a^2}{2} = -9.99\ \boldsymbol{kNm}$$

Moment from self weight of pavement and fictious load

$$M_{s.g.pav.sls} := M_{s.g.pav.base} + \Delta M_{fic.sls.2} = -15.53\ \boldsymbol{kNm}$$

Effect of inelastic strains ULS

Coeffficient for inelastic strains

$$C_{p.uls} := C_{p.func}\left(E_s, E_{t.creep}, \gamma_{s.uls}\right) = \left(5.68 \cdot 10^4\right) \frac{\boldsymbol{N}}{\boldsymbol{mm}}$$

Fictitious vertical load equivalent to inelastic strains

$$p_{uls} := C_{p.uls}\ \Delta\varepsilon_{temp} = 14.78\ \frac{\boldsymbol{kN}}{\boldsymbol{m}}$$

Partial factor for shirnkage

$$\gamma_{F.uls} := 1.5$$

Design value of fictitious load

$$p_{uls.d} := \gamma_{F.uls} \cdot p_{uls} = 22.16\ \frac{\boldsymbol{kN}}{\boldsymbol{m}}$$

Permanent uniformly distributed load

$$q_d := 1.35 \cdot g_{tot} = 55.67\ \frac{\boldsymbol{kN}}{\boldsymbol{m}}$$

Modification coefficient of the bending stiffness

$$C_{J.uls} := C_{J.func}\left(E_{c.creep}, E_{t.creep}, \gamma_{c.uls}, p_{uls.d}, p_{uls}, q_d\right) = 1.1$$

Effective bending stiffness with respect to inelastic strains

$$EI_{eff.sw} := C_{J.uls} \cdot EI_{eff.sw} = 2.5\ \boldsymbol{m^4 \cdot GPa}$$

Bending moment at support caused by the fictitious load

$$\Delta M_{fic.uls.2} := -\frac{0.8 \cdot p_{uls} \cdot a^2}{2} = -9.99\ \boldsymbol{kNm}$$

Moment from self weight of pavement and fictious load

$$M_{s.g.pav} := M_{s.g.pav.base} + \Delta M_{fic.uls.2} = -15.53\ \boldsymbol{kNm}$$

Support - stresses from selfweight in timber

Total stress in top of concrete

$$\sigma_{g.s.top.2} := \begin{bmatrix} 0 \\ 0 \end{bmatrix} \boldsymbol{MPa}$$

Total stress in bottom of concrete

$$\sigma_{g.s.bot.2} := \begin{bmatrix} 0 \\ 0 \end{bmatrix} \boldsymbol{MPa}$$

Stress in top of timber

$$\sigma_{t.top.2} := \frac{-M_{s.g}}{I_t} \cdot \frac{h_t}{2} = 2.37\ \boldsymbol{MPa}$$

Stress in bottom of timber

$$\sigma_{t.bot.2} := \frac{M_{s.g}}{I_t} \cdot \frac{h_t}{2} = -2.37\ \boldsymbol{MPa}$$

Total stress in top of timber

$$\sigma_{g.t.top.2} := \begin{bmatrix} 0 \\ \sigma_{t.top.2} \end{bmatrix} = \begin{bmatrix} 0 \\ 2.37 \end{bmatrix} \boldsymbol{MPa}$$

Total stress in bottom of timber

$$\sigma_{g.t.bot.2} := \begin{bmatrix} 0 \\ \sigma_{t.bot.2} \end{bmatrix} = \begin{bmatrix} 0 \\ -2.37 \end{bmatrix} \boldsymbol{MPa}$$

Shear stress

$$\tau_g := \frac{1.5}{A_t \cdot k_{cr}}\ V_{g.max} = 0.42\ \boldsymbol{MPa}$$

Support - stresses from self weight of pavement

Normal stress from composite action $\sigma_{g.pav.s..2} := \frac{\gamma_{s.sw} \cdot E_s \cdot a_{s.sw}}{EI_{eff.sw}} \cdot M_{s.g.pav} = -665.639$ **kPa**

Stress from bending $\sigma_{g.pav.m.s.2} := \frac{E_s \cdot h_{s.20}}{EI_{eff.sw}} \cdot M_{s.g.pav} = -322.837$ **kPa**

Total stress in top of concrete $\sigma_{g.pav.s.top.2} := \begin{bmatrix} -\sigma_{g.pav.s..2} \\ -\sigma_{g.pav.m.s.2} \end{bmatrix} = \begin{bmatrix} 665.64 \\ 322.84 \end{bmatrix}$ **kPa**

Total stress in bottom of concrete $\sigma_{g.pav.s.bot.2} := \begin{bmatrix} -\sigma_{g.pav.s..2} \\ \sigma_{g.pav.m.s.2} \end{bmatrix} = \begin{bmatrix} 665.64 \\ -322.84 \end{bmatrix}$ **kPa**

Normal stress from composite action $\sigma_{g.pav.t.2} := \frac{\gamma_t \cdot E_{t.creep} \cdot a_{t.sw}}{EI_{eff.sw}} \cdot M_{s.g.pav} = -7.464$ **kPa**

Stress from bending $\sigma_{g.pav.m.t.2} := \frac{0.5 \cdot E_{t.creep} \cdot h_t}{EI_{eff.sw}} \cdot M_{s.g.pav} = -29.257$ **kPa**

Total stress in top of timber $\sigma_{g.pav.t.top.2} := \begin{bmatrix} \sigma_{g.pav.t.2} \\ -\sigma_{g.pav.m.t.2} \end{bmatrix} = \begin{bmatrix} -7.46 \\ 29.26 \end{bmatrix}$ **kPa**

Total stress in bottom of timber $\sigma_{g.pav.t.bot.2} := \begin{bmatrix} \sigma_{g.pav.t.2} \\ \sigma_{g.pav.m.t.2} \end{bmatrix} = \begin{bmatrix} -7.46 \\ -29.26 \end{bmatrix}$ **kPa**

Maximum shear stress $\tau_{g.pav} := \frac{0.5 \cdot E_{t.creep} \cdot h_{v.t.sw}^2}{EI_{eff.sw}} \cdot \frac{V_{g.max.pav}}{k_{cr}} = 53.33$ **kPa**

Fastener load $F_{conn.g.pav} := E_{cm} \cdot A_c \cdot \gamma_{c.uls} \cdot s \cdot \frac{a_{c.uls}}{EI_{eff.sw}} \cdot V_{g.max.pav} = 113.31$ **kN**

Support - stresses from self weight of pavement SLS

Normal stress from composite action $\sigma_{g.pav.s.sls.2} := \frac{\gamma_{s.sw.sls} \cdot E_s \cdot a_{s.sw.sls}}{EI_{eff.sw.sls}} \cdot M_{s.g.pav.sls} = -694.608$ **kPa**

Stress from bending $\sigma_{g.pav.m.s.sls.2} := \frac{E_s \cdot h_{s.20}}{EI_{eff.sw.sls}} \cdot M_{s.g.pav.sls} = -336.887$ **kPa**

Total stress in top of concrete $\sigma_{g.pav.s.top.sls.2} := \begin{bmatrix} -\sigma_{g.pav.s.sls.2} \\ -\sigma_{g.pav.m.s.sls.2} \end{bmatrix} = \begin{bmatrix} 694.61 \\ 336.89 \end{bmatrix}$ **kPa**

Total stress in bottom of concrete $\sigma_{g.pav.s.bot.sls.2} := \begin{bmatrix} -\sigma_{g.pav.s.sls.2} \\ \sigma_{g.pav.m.s.sls.2} \end{bmatrix} = \begin{bmatrix} 694.61 \\ -336.89 \end{bmatrix}$ **kPa**

Normal stress from composite action $\sigma_{g.pav.t.sls.2} := \frac{\gamma_t \cdot E_{t.creep.sls} \cdot a_{t.sw.sls}}{EI_{eff.sw.sls}} \cdot M_{s.g.pav.sls} = -7.789$ **kPa**

Stress from bending $\sigma_{g.pav.m.t.sls.2} := \frac{0.5 \cdot E_{t.creep.sls} \cdot h_t}{EI_{eff.sw.sls}} \cdot M_{s.g.pav.sls} = -30.53$ **kPa**

Total stress in top of timber $\sigma_{g.pav.t.top.sls.2} := \begin{bmatrix} \sigma_{g.pav.t.sls.2} \\ -\sigma_{g.pav.m.t.sls.2} \end{bmatrix} = \begin{bmatrix} -7.79 \\ 30.53 \end{bmatrix}$ **kPa**

Total stress in bottom of timber $\sigma_{g.pav.t.bot.sls.2} := \begin{bmatrix} \sigma_{g.pav.t.sls.2} \\ \sigma_{g.pav.m.t.sls.2} \end{bmatrix} = \begin{bmatrix} -7.79 \\ -30.53 \end{bmatrix}$ **kPa**

Maximum shear stress $\tau_{g.pav.sls} := \frac{0.5 \cdot E_{t.creep.sls} \cdot h_{v.t.sw.sls}^2}{EI_{eff.sw.sls}} \cdot \frac{V_{g.max.pav}}{k_{cr}} = 55.65$ **kPa**

Fastener load $F_{conn.g.pav.sls} := E_{cm} \cdot A_c \cdot \gamma_{c.sls} \cdot s \cdot \frac{a_{c.sls}}{EI_{eff.sw.sls}} \cdot V_{g.max.pav} = 118.25$ **kN**

Support - Min stresses from traffic load (TS) - ULS

Normal stress from composite action $\sigma_{Q.s.2} := \frac{\gamma_{s.uls} \cdot E_s \cdot a_{s.uls}}{EI_{eff.uls}} \cdot M_{Q.s.min} = -12.877$ **MPa**

Stress from bending $\sigma_{Q.m.s.2} := \frac{E_s \cdot h_{s.20}}{EI_{eff.uls}} \cdot M_{Q.s.min} = -5.346$ **MPa**

Total stress in top of concrete $\sigma_{Q.s.top.2} := \begin{bmatrix} -\sigma_{Q.s.2} \\ -\sigma_{Q.m.s.2} \end{bmatrix} = \begin{bmatrix} 12.877 \\ 5.346 \end{bmatrix}$ **MPa**

Total stress in bottom of concrete $\sigma_{Q.s.bot.2} := \begin{bmatrix} -\sigma_{Q.s.2} \\ \sigma_{Q.m.s.2} \end{bmatrix} = \begin{bmatrix} 12.877 \\ -5.346 \end{bmatrix}$ **MPa**

Normal stress from composite action $\sigma_{Q.t.2} := \frac{\gamma_t \cdot E_{t.0.mean} \cdot a_{t.uls}}{EI_{eff.uls}} \cdot M_{Q.s.min} = -0.144$ **MPa**

Stress from bending $\sigma_{Q.m.t.2} := \frac{0.5 \cdot E_{t.0.mean} \cdot h_t}{EI_{eff.uls}} \cdot M_{Q.s.min} = -0.872$ **MPa**

Total stress in top of timber $\sigma_{Q.t.top.2} := \begin{bmatrix} \sigma_{Q.t.2} \\ -\sigma_{Q.m.t.2} \end{bmatrix} = \begin{bmatrix} -0.144 \\ 0.872 \end{bmatrix}$ **MPa**

Total stress in bottom of timber $\sigma_{Q.t.bot.2} := \begin{bmatrix} \sigma_{Q.t.2} \\ \sigma_{Q.m.t.2} \end{bmatrix} = \begin{bmatrix} -0.144 \\ -0.872 \end{bmatrix}$ **MPa**

Maximum shear stress $\tau_Q := \frac{0.5 \cdot E_{t.0.mean} \cdot h_{v.t.uls}^2}{EI_{eff.uls}} \cdot \frac{V_{Q.max}}{k_{cr}} = 0.69$ **MPa**

Fastener load $F_{conn.Q} := E_{cm} \cdot A_c \cdot \gamma_{c.uls} \cdot s \cdot \frac{a_{c.uls}}{EI_{eff.uls}} \cdot V_{Q.max} = 943.84$ **kN**

Support - Min stresses from traffic load (UDL) - ULS

Normal stress from composite action $\sigma_{q.s.2} := \frac{\gamma_{s.uls} \cdot E_s \cdot a_{s.uls}}{EI_{eff.uls}} \cdot M_{q.s.min} = -726.375$ **kPa**

Stress from bending $\sigma_{q.m.s.2} := \frac{E_s \cdot h_{s.20}}{EI_{eff.uls}} \cdot M_{q.s.min} = -301.574$ **kPa**

Total stress in top of concrete $\sigma_{q.s.top.2} := \begin{bmatrix} -\sigma_{q.s.2} \\ -\sigma_{q.m.s.2} \end{bmatrix} = \begin{bmatrix} 726.375 \\ 301.574 \end{bmatrix}$ **kPa**

Total stress in bottom of concrete $\sigma_{q.s.bot.2} := \begin{bmatrix} -\sigma_{q.s.2} \\ \sigma_{q.m.s.2} \end{bmatrix} = \begin{bmatrix} 726.375 \\ -301.574 \end{bmatrix}$ **kPa**

Normal stress from composite action $\sigma_{q.t.2} := \frac{\gamma_t \cdot E_{t.0.mean} \cdot a_{t.uls}}{EI_{eff.uls}} \cdot M_{q.s.min} = -8.145$ **kPa**

Stress from bending $\sigma_{q.m.t.2} := \frac{0.5 \cdot E_{t.0.mean} \cdot h_t}{EI_{eff.uls}} \cdot M_{q.s.min} = -49.194$ **kPa**

Total stress in top of timber $\sigma_{q.t.top.2} := \begin{bmatrix} \sigma_{q.t.2} \\ -\sigma_{q.m.t.2} \end{bmatrix} = \begin{bmatrix} -8.145 \\ 49.194 \end{bmatrix}$ **kPa**

Total stress in bottom of timber $\sigma_{q.t.bot.2} := \begin{bmatrix} \sigma_{q.t.2} \\ \sigma_{q.m.t.2} \end{bmatrix} = \begin{bmatrix} -8.145 \\ -49.194 \end{bmatrix}$ **kPa**

Maximum shear stress $\tau_q := \frac{0.5 \cdot E_{t.0.mean} \cdot h_{v.t.uls}^2}{EI_{eff.uls}} \cdot \frac{V_{q.max}}{k_{cr}} = 246.9$ **kPa**

Fastener load $F_{conn.q} := E_{cm} \cdot A_c \cdot \gamma_{c.uls} \cdot s \cdot \frac{a_{c.uls}}{EI_{eff.uls}} \cdot V_{q.max} = 337.93$ **kN**

Support - Min stresses from traffic load (TS) SLS

Normal stress from composite action $\sigma_{Q.s.2.sls} := \frac{\gamma_{s.sls} \cdot E_s \cdot a_{s.sls}}{EI_{eff.sls}} \cdot M_{Q.s.min} = -12.877$ ***MPa***

Stress from bending $\sigma_{Q.m.s.2.sls} := \frac{E_s \cdot h_{s.20}}{EI_{eff.sls}} \cdot M_{Q.s.min} = -5.346$ ***MPa***

Total stress in top of concrete $\sigma_{Q.s.top.2.sls} := \begin{bmatrix} -\sigma_{Q.s.2.sls} \\ -\sigma_{Q.m.s.2.sls} \end{bmatrix} = \begin{bmatrix} 12.877 \\ 5.346 \end{bmatrix}$ ***MPa***

Total stress in bottom of concrete $\sigma_{Q.s.bot.2.sls} := \begin{bmatrix} -\sigma_{Q.s.2.sls} \\ \sigma_{Q.m.s.2.sls} \end{bmatrix} = \begin{bmatrix} 12.877 \\ -5.346 \end{bmatrix}$ ***MPa***

Normal stress from composite action $\sigma_{Q.t.2.sls} := \frac{\gamma_t \cdot E_{t.0.mean} \cdot a_{t.sls}}{EI_{eff.sls}} \cdot M_{Q.s.min} = -0.144$ ***MPa***

Stress from bending $\sigma_{Q.m.t.2.sls} := \frac{0.5 \cdot E_{t.0.mean} \cdot h_t}{EI_{eff.sls}} \cdot M_{Q.s.min} = -0.872$ ***MPa***

Total stress in top of timber $\sigma_{Q.t.top.2.sls} := \begin{bmatrix} \sigma_{Q.t.2.sls} \\ -\sigma_{Q.m.t.2.sls} \end{bmatrix} = \begin{bmatrix} -0.144 \\ 0.872 \end{bmatrix}$ ***MPa***

Total stress in bottom of timber $\sigma_{Q.t.bot.2.sls} := \begin{bmatrix} \sigma_{Q.t.2.sls} \\ \sigma_{Q.m.t.2.sls} \end{bmatrix} = \begin{bmatrix} -0.144 \\ -0.872 \end{bmatrix}$ ***MPa***

Maximum shear stress $\tau_{Q.sls} := \frac{0.5 \cdot E_{t.0.mean} \cdot h_{v.sls}^{\ 2}}{EI_{eff.sls}} \cdot \frac{V_{Q.max}}{k_{cr}} = 0.69$ ***MPa***

Fastener load $F_{conn.Q.sls} := E_{cm} \cdot A_c \cdot \gamma_{c.sls} \cdot s \cdot \frac{a_{c.sls}}{EI_{eff.sls}} \cdot V_{Q.max} = 943.84$ ***kN***

Support - Min stresses from traffic load (UDL) SLS

Normal stress from composite action $\sigma_{q.s.2.sls} := \frac{\gamma_{s.sls} \cdot E_s \cdot a_{s.sls}}{EI_{eff.sls}} \cdot M_{q.s.min} = -726.375$ ***kPa***

Stress from bending $\sigma_{q.m.s.2.sls} := \frac{E_s \cdot h_{s.20}}{EI_{eff.sls}} \cdot M_{q.s.min} = -301.574$ ***kPa***

Total stress in top of concrete $\sigma_{q.s.top.2.sls} := \begin{bmatrix} -\sigma_{q.s.2.sls} \\ -\sigma_{q.m.s.2.sls} \end{bmatrix} = \begin{bmatrix} 726.375 \\ 301.574 \end{bmatrix}$ ***kPa***

Total stress in bottom of concrete $\sigma_{q.s.bot.2.sls} := \begin{bmatrix} -\sigma_{q.s.2.sls} \\ \sigma_{q.m.s.2.sls} \end{bmatrix} = \begin{bmatrix} 726.375 \\ -301.574 \end{bmatrix}$ ***kPa***

Normal stress from composite action $\sigma_{q.t.2.sls} := \frac{\gamma_t \cdot E_{t.0.mean} \cdot a_{t.sls}}{EI_{eff.sls}} \cdot M_{q.s.min} = -8.145$ ***kPa***

Stress from bending $\sigma_{q.m.t.2.sls} := \frac{0.5 \cdot E_{t.0.mean} \cdot h_t}{EI_{eff.sls}} \cdot M_{q.s.min} = -49.194$ ***kPa***

Total stress in top of timber $\sigma_{q.t.top.2.sls} := \begin{bmatrix} \sigma_{q.t.2.sls} \\ -\sigma_{q.m.t.2.sls} \end{bmatrix} = \begin{bmatrix} -8.145 \\ 49.194 \end{bmatrix}$ ***kPa***

Total stress in bottom of timber $\sigma_{q.t.bot.2.sls} := \begin{bmatrix} \sigma_{q.t.2.sls} \\ \sigma_{q.m.t.2.sls} \end{bmatrix} = \begin{bmatrix} -8.145 \\ -49.194 \end{bmatrix}$ ***kPa***

Maximum shear stress $\tau_{q.sls} := \frac{0.5 \cdot E_{t.0.mean} \cdot h_{v.sls}^{\ 2}}{EI_{eff.sls}} \cdot \frac{V_{q.max}}{k_{cr}} = 246.9$ ***kPa***

Fastener load $F_{conn.q.sls} := E_{cm} \cdot A_c \cdot \gamma_{c.sls} \cdot s \cdot \frac{a_{c.sls}}{EI_{eff.sls}} \cdot V_{q.max} = 337.93$ ***kN***

Support - Min stresses from surcharge ULS

Normal stress from composite action $\sigma_{sur.s.2} := \frac{\gamma_{s.uls} \cdot E_s \cdot a_{s.uls}}{EI_{eff.uls}} \cdot M_{sur} = -2.764$ ***MPa***

Stress from bending $\sigma_{sur.m.s.2} := \frac{E_s \cdot h_{s.20}}{EI_{eff.uls}} \cdot M_{sur} = -1.148$ ***MPa***

Total stress in top of concrete $\sigma_{sur.s.top.2} := \sigma_{ö} + \begin{bmatrix} -\sigma_{sur.s.2} \\ -\sigma_{sur.m.s.2} \end{bmatrix} = \begin{bmatrix} 2.736 \\ 1.148 \end{bmatrix}$ ***MPa***

Total stress in bottom of concrete $\sigma_{sur.s.bot.2} := \sigma_{ö} + \begin{bmatrix} -\sigma_{sur.s.2} \\ \sigma_{sur.m.s.2} \end{bmatrix} = \begin{bmatrix} 2.736 \\ -1.148 \end{bmatrix}$ ***MPa***

Normal stress from composite action $\sigma_{sur.t.2} := \frac{\gamma_t \cdot E_{t.0.mean} \cdot a_{t.uls}}{EI_{eff.uls}} \cdot M_{sur} = -0.031$ ***MPa***

Stress from bending $\sigma_{sur.m.t.2} := \frac{0.5 \cdot E_{t.0.mean} \cdot h_t}{EI_{eff.uls}} \cdot M_{sur} = -0.187$ ***MPa***

Total stress in top of timber $\sigma_{sur.t.top.2} := \sigma_{ö} + \begin{bmatrix} \sigma_{sur.t.2} \\ -\sigma_{sur.m.t.2} \end{bmatrix} = \begin{bmatrix} -0.059 \\ 0.187 \end{bmatrix}$ ***MPa***

Total stress in bottom of timber $\sigma_{sur.t.bot.2} := \sigma_{ö} + \begin{bmatrix} \sigma_{sur.t.2} \\ \sigma_{sur.m.t.2} \end{bmatrix} = \begin{bmatrix} -0.059 \\ -0.187 \end{bmatrix}$ ***MPa***

Support - Min stresses from earth pressure ULS

Normal stress from composite action $\sigma_{ep.s.2} := \frac{\gamma_{s.sw} \cdot E_s \cdot a_{s.sw}}{EI_{eff.sw}} \cdot M_{ep} = -9.304$ ***MPa***

Stress from bending $\sigma_{ep.m.s.2} := \frac{E_s \cdot h_{s.20}}{EI_{eff.sw}} \cdot M_{ep} = -4.513$ ***MPa***

Total stress in top of concrete $\sigma_{ep.s.top.2} := \sigma_{0.k} + \begin{bmatrix} -\sigma_{ep.s.2} \\ -\sigma_{ep.m.s.2} \end{bmatrix} = \begin{bmatrix} 9.252 \\ 4.513 \end{bmatrix}$ ***MPa***

Total stress in bottom of concrete $\sigma_{ep.s.bot.2} := \sigma_{0.k} + \begin{bmatrix} -\sigma_{ep.s.2} \\ \sigma_{ep.m.s.2} \end{bmatrix} = \begin{bmatrix} 9.252 \\ -4.513 \end{bmatrix}$ ***MPa***

Normal stress from composite action $\sigma_{ep.t.2} := \frac{\gamma_t \cdot E_{t.creep} \cdot a_{t.sw}}{EI_{eff.sw}} \cdot M_{ep} = -0.104$ ***MPa***

Stress from bending $\sigma_{ep.m.t.2} := \frac{0.5 \cdot E_{t.creep} \cdot h_t}{EI_{eff.sw}} \cdot M_{ep} = -0.409$ ***MPa***

Total stress in top of timber $\sigma_{ep.t.top.2} := \sigma_{0.k} + \begin{bmatrix} \sigma_{ep.t.2} \\ -\sigma_{ep.m.t.2} \end{bmatrix} = \begin{bmatrix} -0.157 \\ 0.409 \end{bmatrix}$ ***MPa***

Total stress in bottom of timber $\sigma_{ep.t.bot.2} := \sigma_{0.k} + \begin{bmatrix} \sigma_{ep.t.2} \\ \sigma_{ep.m.t.2} \end{bmatrix} = \begin{bmatrix} -0.157 \\ -0.409 \end{bmatrix}$ ***MPa***

Support - Min stresses from breaking force ULS

Normal stress from composite action $\sigma_{bk.s.2} := \frac{\gamma_{s.uls} \cdot E_s \cdot a_{s.uls}}{EI_{eff.uls}} \cdot M_{bk} = -9.912$ ***MPa***

Stress from bending $\sigma_{bk.m.s.2} := \frac{E_s \cdot h_{s.20}}{EI_{eff.uls}} \cdot M_{bk} = -4.115$ ***MPa***

Total stress in top of concrete $\sigma_{bk.s.top.2} := \sigma_{Break} + \begin{bmatrix} -\sigma_{bk.s.2} \\ -\sigma_{bk.m.s.2} \end{bmatrix} = \begin{bmatrix} 9.843 \\ 4.115 \end{bmatrix}$ ***MPa***

Total stress in bottom of concrete $\sigma_{bk.s.bot.2} := \sigma_{Break} + \begin{bmatrix} -\sigma_{bk.s.2} \\ \sigma_{bk.m.s.2} \end{bmatrix} = \begin{bmatrix} 9.843 \\ -4.115 \end{bmatrix}$ ***MPa***

Normal stress from composite action $\sigma_{bk.t.2} := \frac{\gamma_t \cdot E_{t.0.mean} \cdot a_{t.uls}}{EI_{eff.uls}} \cdot M_{bk} = -0.111$ ***MPa***

Stress from bending $\sigma_{bk.m.t.2} := \frac{0.5 \cdot E_{t.0.mean} \cdot h_t}{EI_{eff.uls}} \cdot M_{bk} = -0.671$ ***MPa***

Total stress in top of timber $\sigma_{bk.t.top.2} := \sigma_{Break} + \begin{bmatrix} \sigma_{bk.t.2} \\ -\sigma_{bk.m.t.2} \end{bmatrix} = \begin{bmatrix} -0.18 \\ 0.671 \end{bmatrix}$ ***MPa***

Total stress in bottom of timber $\sigma_{bk.t.bot.2} := \sigma_{Break} + \begin{bmatrix} \sigma_{bk.t.2} \\ \sigma_{bk.m.t.2} \end{bmatrix} = \begin{bmatrix} -0.18 \\ -0.671 \end{bmatrix}$ ***MPa***

Support - Min stresses from thermal force ULS

Normal stress from composite action $\sigma_{th.s.2} := \frac{\gamma_{s.temp} \cdot E_s \cdot a_{s.temp}}{EI_{eff.temp}} \cdot M_{thermal} = -5.002$ ***MPa***

Stress from bending $\sigma_{th.m.s.2} := \frac{E_s \cdot h_{s.20}}{EI_{eff.temp}} \cdot M_{thermal} = -2.015$ ***MPa***

Total stress in top of concrete $\sigma_{th.s.top.2} := \sigma_{th} + \begin{bmatrix} -\sigma_{th.s.2} \\ -\sigma_{th.m.s.2} \end{bmatrix} = \begin{bmatrix} 4.922 \\ 2.015 \end{bmatrix}$ ***MPa***

Total stress in bottom of concrete $\sigma_{th.s.bot.2} := \sigma_{th} + \begin{bmatrix} -\sigma_{th.s.2} \\ \sigma_{th.m.s.2} \end{bmatrix} = \begin{bmatrix} 4.922 \\ -2.015 \end{bmatrix}$ ***MPa***

Normal stress from composite action $\sigma_{th.t.2} := \frac{\gamma_t \cdot E_{t.0.mean} \cdot a_{t.temp}}{EI_{eff.temp}} \cdot M_{thermal} = -0.056$ ***MPa***

Stress from bending $\sigma_{th.m.t.2} := \frac{0.5 \cdot E_{t.0.mean} \cdot h_t}{EI_{eff.temp}} \cdot M_{thermal} = -0.329$ ***MPa***

Total stress in top of timber $\sigma_{th.t.top.2} := \sigma_{th} + \begin{bmatrix} \sigma_{th.t.2} \\ -\sigma_{th.m.t.2} \end{bmatrix} = \begin{bmatrix} -0.136 \\ 0.329 \end{bmatrix}$ ***MPa***

Total stress in bottom of timber $\sigma_{th.t.bot.2} := \sigma_{th} + \begin{bmatrix} \sigma_{th.t.2} \\ \sigma_{th.m.t.2} \end{bmatrix} = \begin{bmatrix} -0.136 \\ -0.329 \end{bmatrix}$ ***MPa***

Support - Min stresses from surcharge SLS

Normal stress from composite action $\sigma_{sur.s.2.sls} := \frac{\gamma_{s.sls} \cdot E_s \cdot a_{s.sls}}{EI_{eff.sls}} \cdot M_{sur} = -2.764$ ***MPa***

Stress from bending $\sigma_{sur.m.s.2.sls} := \frac{E_s \cdot h_{s.20}}{EI_{eff.sls}} \cdot M_{sur} = -1.148$ ***MPa***

Total stress in top of concrete $\sigma_{sur.s.top.2.sls} := \sigma_{ö} + \begin{bmatrix} -\sigma_{sur.s.2.sls} \\ -\sigma_{sur.m.s.2.sls} \end{bmatrix} = \begin{bmatrix} 2.736 \\ 1.148 \end{bmatrix}$ ***MPa***

Total stress in bottom of concrete $\sigma_{sur.s.bot.2.sls} := \sigma_{ö} + \begin{bmatrix} -\sigma_{sur.s.2.sls} \\ \sigma_{sur.m.s.2.sls} \end{bmatrix} = \begin{bmatrix} 2.736 \\ -1.148 \end{bmatrix}$ ***MPa***

Normal stress from composite action $\sigma_{sur.t.2.sls} := \frac{\gamma_t \cdot E_{t.0.mean} \cdot a_{t.sls}}{EI_{eff.sls}} \cdot M_{sur} = -0.031$ ***MPa***

Stress from bending $\sigma_{sur.m.t.2.sls} := \frac{0.5 \cdot E_{t.0.mean} \cdot h_t}{EI_{eff.sls}} \cdot M_{sur} = -0.187$ ***MPa***

Total stress in top of timber $\sigma_{sur.t.top.2.sls} := \sigma_{ö} + \begin{bmatrix} \sigma_{sur.t.2.sls} \\ -\sigma_{sur.m.t.2.sls} \end{bmatrix} = \begin{bmatrix} -0.059 \\ 0.187 \end{bmatrix}$ ***MPa***

Total stress in bottom of timber $\sigma_{sur.t.bot.2.sls} := \sigma_{ö} + \begin{bmatrix} \sigma_{sur.t.2.sls} \\ \sigma_{sur.m.t.2.sls} \end{bmatrix} = \begin{bmatrix} -0.059 \\ -0.187 \end{bmatrix}$ ***MPa***

Support - Min stresses from earth pressure SLS

Normal stress from composite action $\sigma_{ep.s.2.sls} := \frac{\gamma_{s.sw.sls} \cdot E_s \cdot a_{s.sw.sls}}{EI_{eff.sw.sls}} \cdot M_{ep} = -9.709$ ***MPa***

Stress from bending $\sigma_{ep.m.s.2.sls} := \frac{E_s \cdot h_{s.20}}{EI_{eff.sw.sls}} \cdot M_{ep} = -4.709$ ***MPa***

Total stress in top of concrete $\sigma_{ep.s.top.2.sls} := \sigma_{0.k} + \begin{bmatrix} -\sigma_{ep.s.2.sls} \\ -\sigma_{ep.m.s.2.sls} \end{bmatrix} = \begin{bmatrix} 9.657 \\ 4.709 \end{bmatrix}$ ***MPa***

Total stress in bottom of concrete $\sigma_{ep.s.bot.2.sls} := \sigma_{0.k} + \begin{bmatrix} -\sigma_{ep.s.2.sls} \\ \sigma_{ep.m.s.2.sls} \end{bmatrix} = \begin{bmatrix} 9.657 \\ -4.709 \end{bmatrix}$ ***MPa***

Normal stress from composite action $\sigma_{ep.t.2.sls} := \frac{\gamma_t \cdot E_{t.creep.sls} \cdot a_{t.sw.sls}}{EI_{eff.sw.sls}} \cdot M_{ep} = -0.109$ ***MPa***

Stress from bending $\sigma_{ep.m.t.2.sls} := \frac{0.5 \cdot E_{t.creep.sls} \cdot h_t}{EI_{eff.sw.sls}} \cdot M_{ep} = -0.427$ ***MPa***

Total stress in top of timber $\sigma_{ep.t.top.2.sls} := \sigma_{0.k} + \begin{bmatrix} \sigma_{ep.t.2.sls} \\ -\sigma_{ep.m.t.2.sls} \end{bmatrix} = \begin{bmatrix} -0.161 \\ 0.427 \end{bmatrix}$ ***MPa***

Total stress in bottom of timber $\sigma_{ep.t.bot.2.sls} := \sigma_{0.k} + \begin{bmatrix} \sigma_{ep.t.2.sls} \\ \sigma_{ep.m.t.2.sls} \end{bmatrix} = \begin{bmatrix} -0.161 \\ -0.427 \end{bmatrix}$ ***MPa***

Support - Min stresses from breaking force SLS

Normal stress from composite action $\sigma_{bk.s.2.sls} := \frac{\gamma_{s.sls} \cdot E_s \cdot a_{s.sls}}{EI_{eff.sls}} \cdot M_{bk} = -9.912$ ***MPa***

Stress from bending $\sigma_{bk.m.s.2.sls} := \frac{E_s \cdot h_{s.20}}{EI_{eff.sls}} \cdot M_{bk} = -4.115$ ***MPa***

Total stress in top of concrete $\sigma_{bk.s.top.2.sls} := \sigma_{Break} + \begin{bmatrix} -\sigma_{bk.s.2.sls} \\ -\sigma_{bk.m.s.2.sls} \end{bmatrix} = \begin{bmatrix} 9.843 \\ 4.115 \end{bmatrix}$ ***MPa***

Total stress in bottom of concrete $\sigma_{bk.s.bot.2.sls} := \sigma_{Break} + \begin{bmatrix} -\sigma_{bk.s.2.sls} \\ \sigma_{bk.m.s.2.sls} \end{bmatrix} = \begin{bmatrix} 9.843 \\ -4.115 \end{bmatrix}$ ***MPa***

Normal stress from composite action $\sigma_{bk.t.2.sls} := \frac{\gamma_t \cdot E_{t.0.mean} \cdot a_{t.sls}}{EI_{eff.sls}} \cdot M_{bk} = -0.111$ ***MPa***

Stress from bending $\sigma_{bk.m.t.2.sls} := \frac{0.5 \cdot E_{t.0.mean} \cdot h_t}{EI_{eff.sls}} \cdot M_{bk} = -0.671$ ***MPa***

Total stress in top of timber $\sigma_{bk.t.top.2.sls} := \sigma_{Break} + \begin{bmatrix} \sigma_{bk.t.2.sls} \\ -\sigma_{bk.m.t.2.sls} \end{bmatrix} = \begin{bmatrix} -0.18 \\ 0.671 \end{bmatrix}$ ***MPa***

Total stress in bottom of timber $\sigma_{bk.t.bot.2.sls} := \sigma_{Break} + \begin{bmatrix} \sigma_{bk.t.2.sls} \\ \sigma_{bk.m.t.2.sls} \end{bmatrix} = \begin{bmatrix} -0.18 \\ -0.671 \end{bmatrix}$ ***MPa***

Support - Min stresses from thermal force SLS

Normal stress from composite action $\sigma_{th.s.2.sls} := \frac{\gamma_{s.temp.sls} \cdot E_s \cdot a_{s.temp.sls}}{EI_{eff.temp.sls}} \cdot M_{thermal} = -4.854$ ***MPa***

Stress from bending $\sigma_{th.m.s.2.sls} := \frac{E_s \cdot h_{s.20}}{EI_{eff.temp.sls}} \cdot M_{thermal} = -2.015$ ***MPa***

Total stress in top of concrete $\sigma_{th.s.top.2.sls} := \sigma_{th} + \begin{bmatrix} -\sigma_{th.s.2.sls} \\ -\sigma_{th.m.s.2.sls} \end{bmatrix} = \begin{bmatrix} 4.774 \\ 2.015 \end{bmatrix}$ ***MPa***

Total stress in bottom of concrete $\sigma_{th.s.bot.2.sls} := \sigma_{th} + \begin{bmatrix} -\sigma_{th.s.2.sls} \\ \sigma_{th.m.s.2.sls} \end{bmatrix} = \begin{bmatrix} 4.774 \\ -2.015 \end{bmatrix}$ ***MPa***

Normal stress from composite action $\sigma_{th.t.2.sls} := \frac{\gamma_t \cdot E_{t.0.mean} \cdot a_{t.temp.sls}}{EI_{eff.temp.sls}} \cdot M_{thermal} = -0.054$ ***MPa***

Stress from bending $\sigma_{th.m.t.2.sls} := \frac{0.5 \cdot E_{t.0.mean} \cdot h_t}{EI_{eff.temp.sls}} \cdot M_{thermal} = -0.329$ ***MPa***

Total stress in top of timber $\sigma_{th.t.top.2.sls} := \sigma_{th} + \begin{bmatrix} \sigma_{th.t.2.sls} \\ -\sigma_{th.m.t.2.sls} \end{bmatrix} = \begin{bmatrix} -0.134 \\ 0.329 \end{bmatrix}$ ***MPa***

Total stress in bottom of timber $\sigma_{th.t.bot.2.sls} := \sigma_{th} + \begin{bmatrix} \sigma_{th.t.2.sls} \\ \sigma_{th.m.t.2.sls} \end{bmatrix} = \begin{bmatrix} -0.134 \\ -0.329 \end{bmatrix}$ ***MPa***

ULS - 6.10a Support

$$\sum_{j\geq 1}\gamma_{G,j,sup}G_{k,j,sup}" + "\gamma_{G,j,inf}G_{k,j,inf}" + "\gamma_{Q,1}\Psi_{0,1}Q_{k,1}" + "\sum_{i\geq 1}\gamma_{Q,i}\Psi_{0,i}Q_{k,i} \quad \text{6.10a}$$

$$\sum_{j\geq 1}\xi_{G,j,sup}\gamma_{G,j,sup}G_{k,j,sup}" + "\gamma_{G,j,inf}G_{k,j,inf}" + "\gamma_{Q,1}Q_{k,1}" + "\sum_{i\geq 1}\gamma_{Q,i}\Psi_{0,i}Q_{k,i} \quad \text{6.10b}$$

Total stress in top of concrete

Min $\sigma_{min.s.top.ULS.6.10a.2} := \gamma_d \cdot \left(\gamma_G \cdot \left(\sigma_{g.s.top.2} + \gamma_{sup} \cdot \sigma_{g.pav.s.top.2}\right) + \gamma_E \cdot \sigma_{ep.s.top.2}\right) \dots = \begin{bmatrix} 39.4 \\ 17.34 \end{bmatrix}$ ***MPa***

$\dots + \gamma_d \cdot \gamma_Q \cdot \left(\psi_{0.Q} \cdot \sigma_{Q.s.top.2} + \psi_{0.q} \cdot \sigma_{q.s.top.2}\right) \dots$

$+ 0.6 \cdot \gamma_d \cdot \gamma_Q \cdot \left(\psi_{0.B} \cdot \sigma_{bk.s.top.2} + \psi_{0.\ddot{O}} \cdot \sigma_{sur.s.top.2}\right) + \gamma_d \cdot \psi_{0.th} \cdot \sigma_{th.s.top.2}$

Max $\sigma_{max.s.top.ULS.6.10a.2} := \gamma_d \cdot \gamma_{G.f} \cdot \left(\sigma_{g.s.top.2} + \gamma_{inf} \cdot \sigma_{g.pav.s.top.2} + \sigma_{ep.s.top.2}\right) \dots = \begin{bmatrix} 24.77 \\ 11 \end{bmatrix}$ ***MPa***

$+ \gamma_d \cdot \gamma_Q \cdot \left(\psi_{0.Q} \cdot \sigma_{Q.s.top.2} + \psi_{0.q} \cdot \sigma_{q.s.top.2}\right)$

Total stress in bottom of concrete

Min $\sigma_{min.s.bot.ULS.6.10a.2} := \gamma_d \cdot \left(\gamma_G \cdot \left(\sigma_{g.s.bot.2} + \gamma_{sup} \cdot \sigma_{g.pav.s.bot.2}\right) + \gamma_E \cdot \sigma_{ep.s.bot.2}\right) \dots = \begin{bmatrix} 39.4 \\ -17.34 \end{bmatrix}$ ***MPa***

$\dots + \gamma_d \cdot \gamma_Q \cdot \left(\psi_{0.Q} \cdot \sigma_{Q.s.bot.2} + \psi_{0.q} \cdot \sigma_{q.s.bot.2}\right) \dots$

$+ 0.6 \cdot \gamma_d \cdot \gamma_Q \cdot \left(\psi_{0.B} \cdot \sigma_{bk.s.bot.2} + \psi_{0.\ddot{O}} \cdot \sigma_{sur.s.bot.2}\right) + \gamma_d \cdot \psi_{0.th} \cdot \sigma_{th.s.bot.2}$

Max $\sigma_{max.s.bot.ULS.6.10a.2} := \gamma_d \cdot \gamma_{G.f} \cdot \left(\sigma_{g.s.bot.2} + \gamma_{inf} \cdot \sigma_{g.pav.s.bot.2} + \sigma_{ep.s.bot.2}\right) \dots = \begin{bmatrix} 24.77 \\ -11 \end{bmatrix}$ ***MPa***

$+ \gamma_d \cdot \gamma_Q \cdot \left(\psi_{0.Q} \cdot \sigma_{Q.s.bot.2} + \psi_{0.q} \cdot \sigma_{q.s.bot.2}\right)$

Total stress in top of timber

Min $\sigma_{min.t.top.ULS.6.10a.2} := \gamma_d \cdot \left(\gamma_G \cdot \left(\sigma_{g.t.top.2} + \gamma_{sup} \cdot \sigma_{g.pav.t.top.2}\right) + \gamma_E \cdot \sigma_{ep.t.top.2}\right) \dots = \begin{bmatrix} -0.63 \\ 5.55 \end{bmatrix}$ ***MPa***

$\dots + \gamma_d \cdot \gamma_Q \cdot \left(\psi_{0.Q} \cdot \sigma_{Q.t.top.2} + \psi_{0.q} \cdot \sigma_{q.t.top.2}\right) \dots$

$+ 0.6 \cdot \gamma_d \cdot \gamma_Q \cdot \left(\psi_{0.B} \cdot \sigma_{bk.t.top.2} + \psi_{0.\ddot{O}} \cdot \sigma_{sur.t.top.2}\right) + \gamma_d \cdot \psi_{0.th} \cdot \sigma_{th.t.top.2}$

Max $\sigma_{max.t.top.ULS.6.10a.2} := \gamma_d \cdot \gamma_{G.f} \cdot \left(\sigma_{g.t.top.2} + \gamma_{inf} \cdot \sigma_{g.pav.t.top.2} + \sigma_{ep.t.top.2}\right) \dots = \begin{bmatrix} -0.33 \\ 3.82 \end{bmatrix}$ ***MPa***

$+ \gamma_d \cdot \gamma_Q \cdot \left(\psi_{0.Q} \cdot \sigma_{Q.t.top.2} + \psi_{0.q} \cdot \sigma_{q.t.top.2}\right)$

Total stress in bottom of timber

Min $\sigma_{min.t.bot.ULS.6.10a.2} := \gamma_d \cdot \gamma_{G.f} \cdot \left(\sigma_{g.t.bot.2} + \gamma_{inf} \cdot \sigma_{g.pav.t.bot.2} + \sigma_{ep.t.bot.2}\right) \dots = \begin{bmatrix} -0.33 \\ -3.82 \end{bmatrix}$ ***MPa***

$+ \gamma_d \cdot \gamma_Q \cdot \left(\psi_{0.Q} \cdot \sigma_{Q.t.bot.2} + \psi_{0.q} \cdot \sigma_{q.t.bot.2}\right)$

Max $\sigma_{max.t.bot.ULS.6.10a.2} := \gamma_d \cdot \left(\gamma_G \cdot \left(\sigma_{g.t.bot.2} + \gamma_{sup} \cdot \sigma_{g.pav.t.bot.2}\right) + \gamma_E \cdot \sigma_{ep.t.bot.2}\right) \dots = \begin{bmatrix} -0.63 \\ -5.55 \end{bmatrix}$ ***MPa***

$\dots + \gamma_d \cdot \gamma_Q \cdot \left(\psi_{0.Q} \cdot \sigma_{Q.t.bot.2} + \psi_{0.q} \cdot \sigma_{q.t.bot.2}\right) \dots$

$+ 0.6 \cdot \gamma_d \cdot \gamma_Q \cdot \left(\psi_{0.B} \cdot \sigma_{bk.t.bot.2} + \psi_{0.\ddot{O}} \cdot \sigma_{sur.t.bot.2}\right) + \gamma_d \cdot \psi_{0.th} \cdot \sigma_{th.t.bot.2}$

Shear stress

$$\tau_{ULS.6.10a} := \gamma_d \cdot \gamma_G \cdot \left(\tau_g + \gamma_{sup} \cdot \tau_{g.pav}\right) + \gamma_d \cdot \gamma_Q \cdot \left(\psi_{0.Q} \cdot \tau_Q + \psi_{0.q} \cdot \tau_q\right) = 1.57 \ \textbf{MPa}$$

Fastener load

$$F_{conn.ULS.6.10a} := \gamma_d \cdot \gamma_G \cdot \gamma_{sup} \cdot F_{conn.g.pav} + \gamma_d \cdot \gamma_Q \cdot \left(\psi_{0.Q} \cdot F_{conn.Q} + \psi_{0.q} \cdot F_{conn.q}\right) = \left(1.43 \cdot 10^3\right) \ \textbf{kN}$$

Capacity check

Total stress in top of concrete - min

$$\eta_{min.s.top.ULS.6.10a.2} := \frac{\text{abs}\left(\sigma_{min.s.top.ULS.6.10a.2}(0,0) + \sigma_{min.s.top.ULS.6.10a.2}(1,0)\right)}{f_{yd}} = 13\%$$

Total stress in top of concrete - max

$$\eta_{max.s.top.ULS.6.10a.2} := \frac{\text{abs}\left(\sigma_{max.s.top.ULS.6.10a.2}(0,0) + \sigma_{max.s.top.ULS.6.10a.2}(1,0)\right)}{f_{yd}} = 8\%$$

Total stress in bottom of concrete - min

$$\eta_{min.s.bot.ULS.6.10a.2} := \frac{\text{abs}\left(\sigma_{min.s.bot.ULS.6.10a.2}(0,0) + \sigma_{min.s.bot.ULS.6.10a.2}(1,0)\right)}{f_{yd}} = 5\%$$

Total stress in bottom of concrete - max

$$\eta_{max.s.bot.ULS.6.10a.2} := \frac{\text{abs}\left(\sigma_{max.s.bot.ULS.6.10a.2}(0,0) + \sigma_{max.s.bot.ULS.6.10a.2}(1,0)\right)}{f_{yd}} = 3\%$$

Total stress in top of timber - min

$$\sigma_{Rd\_min.t.top.ULS.6.10a.2} := \sigma_{Rd}\left(\sigma_{min.t.top.ULS.6.10a.2}\right) = \begin{bmatrix} 17.64 \\ 21.6 \end{bmatrix} \textbf{\textit{MPa}}$$

$$\eta_{min.t.top.ULS.6.10a.2} := \text{abs}\left(\frac{\sigma_{min.t.top.ULS.6.10a.2}(0,0)}{\sigma_{Rd\_min.t.top.ULS.6.10a.2}(0,0)} + \frac{\sigma_{min.t.top.ULS.6.10a.2}(1,0)}{\sigma_{Rd\_min.t.top.ULS.6.10a.2}(1,0)}\right) = 22\%$$

Total stress in top of timber - max

$$\sigma_{Rd\_max.t.top.ULS.6.10a.2} := \sigma_{Rd}\left(\sigma_{max.t.top.ULS.6.10a.2}\right) = \begin{bmatrix} 17.64 \\ 21.6 \end{bmatrix} \textbf{\textit{MPa}}$$

$$\eta_{max.t.top.ULS.6.10a.2} := \text{abs}\left(\frac{\sigma_{max.t.top.ULS.6.10a.2}(0,0)}{\sigma_{Rd\_max.t.top.ULS.6.10a.2}(0,0)} + \frac{\sigma_{max.t.top.ULS.6.10a.2}(1,0)}{\sigma_{Rd\_max.t.top.ULS.6.10a.2}(1,0)}\right) = 16\%$$

Total stress in bottom of timber - min

$$\sigma_{Rd\_min.t.bot.ULS.6.10a.2} := \sigma_{Rd}\left(\sigma_{min.t.bot.ULS.6.10a.2}\right) = \begin{bmatrix} 17.64 \\ 21.6 \end{bmatrix} \textbf{\textit{MPa}}$$

$$\eta_{min.t.bot.ULS.6.10a.2} := \text{abs}\left(\frac{\sigma_{min.t.bot.ULS.6.10a.2}(0,0)}{\sigma_{Rd\_min.t.bot.ULS.6.10a.2}(0,0)} + \frac{\sigma_{min.t.bot.ULS.6.10a.2}(1,0)}{\sigma_{Rd\_min.t.bot.ULS.6.10a.2}(1,0)}\right) = 20\%$$

Total stress in bottom of timber - max

$$\sigma_{Rd\_max.t.bot.ULS.6.10a.2} := \sigma_{Rd}\left(\sigma_{max.t.bot.ULS.6.10a.2}\right) = \begin{bmatrix} 17.64 \\ 21.6 \end{bmatrix} \textbf{\textit{MPa}}$$

$$\eta_{max.t.bot.ULS.6.10a.2} := \text{abs}\left(\frac{\sigma_{max.t.bot.ULS.6.10a.2}(0,0)}{\sigma_{Rd\_max.t.bot.ULS.6.10a.2}(0,0)} + \frac{\sigma_{max.t.bot.ULS.6.10a.2}(1,0)}{\sigma_{Rd\_max.t.bot.ULS.6.10a.2}(1,0)}\right) = 29\%$$

Shear capacity check

$$\eta_{V.ULS.6.10a} := \frac{\tau_{ULS.6.10a}}{f_{v.d}} = 62\%$$

ULS - 6.10b Support

$$\sum_{j\geq 1}\gamma_{G,j,sup}G_{k,j,sup}\text{"}+\text{"}\gamma_{G,j,inf}G_{k,j,inf}\text{"}+\text{"}\gamma_{Q,1}\Psi_{0,1}Q_{k,1}\text{"}+\text{"}\sum_{i\geq 1}\gamma_{Q,i}\Psi_{0,i}Q_{k,i} \quad \text{6.10a}$$

$$\sum_{j\geq 1}\xi_{G,j,sup}\gamma_{G,j,sup}G_{k,j,sup}\text{"}+\text{"}\gamma_{G,j,inf}G_{k,j,inf}\text{"}+\text{"}\gamma_{Q,1}Q_{k,1}\text{"}+\text{"}\sum_{i\geq 1}\gamma_{Q,i}\Psi_{0,i}Q_{k,i} \quad \text{6.10b}$$

Total stress in top of concrete

Min $\sigma_{min.s.top.ULS.6.10b.2} := \gamma_d \cdot \xi \cdot \left(\gamma_G \cdot \left(\sigma_{g.s.top.2} + \gamma_{sup} \cdot \sigma_{g.pav.s.top.2}\right) + \gamma_E \cdot \sigma_{ep.s.top.2}\right) \dots = \begin{bmatrix} 43.4 \\ 18.9 \end{bmatrix}$ ***MPa***

$\dots + \gamma_d \cdot \gamma_Q \cdot \left(\sigma_{Q.s.top.2} + \sigma_{q.s.top.2}\right) \dots$

$+ 0.6 \cdot \gamma_d \cdot \gamma_Q \cdot \left(\psi_{0.B} \cdot \sigma_{bk.s.top.2} + \psi_{0.Ö} \cdot \sigma_{sur.s.top.2}\right) + \gamma_d \cdot \psi_{0.th} \cdot \sigma_{th.s.top.2}$

Max $\sigma_{max.s.top.ULS.6.10b.2} := \gamma_d \cdot \gamma_{G.f} \cdot \left(\sigma_{g.s.top.2} + \sigma_{g.pav.s.top.2} + \sigma_{ep.s.top.2}\right) \dots = \begin{bmatrix} 30.32 \\ 13.31 \end{bmatrix}$ ***MPa***

$+ \gamma_d \cdot \gamma_Q \cdot \left(\sigma_{Q.s.top.2} + \sigma_{q.s.top.2}\right)$

Total stress in bottom of concrete

Min $\sigma_{min.s.bot.ULS.6.10b.2} := \gamma_d \cdot \xi \cdot \left(\gamma_G \cdot \left(\sigma_{g.s.bot.2} + \gamma_{sup} \cdot \sigma_{g.pav.s.bot.2}\right) + \gamma_E \cdot \sigma_{ep.s.bot.2}\right) \dots = \begin{bmatrix} 43.4 \\ -18.9 \end{bmatrix}$ ***MPa***

$\dots + \gamma_d \cdot \gamma_Q \cdot \left(\sigma_{Q.s.bot.2} + \sigma_{q.s.bot.2}\right) \dots$

$+ 0.6 \cdot \gamma_d \cdot \gamma_Q \cdot \left(\psi_{0.B} \cdot \sigma_{bk.s.bot.2} + \psi_{0.Ö} \cdot \sigma_{sur.s.bot.2}\right) + \gamma_d \cdot \psi_{0.th} \cdot \sigma_{th.s.bot.2}$

Max $\sigma_{max.s.bot.ULS.6.10b.2} := \gamma_d \cdot \gamma_{G.f} \cdot \left(\sigma_{g.s.bot.2} + \gamma_{inf} \cdot \sigma_{g.pav.s.bot.2} + \sigma_{ep.s.bot.2}\right) \dots = \begin{bmatrix} 30.26 \\ -13.28 \end{bmatrix}$ ***MPa***

$+ \gamma_d \cdot \gamma_Q \cdot \left(\sigma_{Q.s.bot.2} + \sigma_{q.s.bot.2}\right)$

Total stress in top of timber

Min $\sigma_{min.t.top.ULS.6.10b.2} := \gamma_d \cdot \xi \cdot \left(\gamma_G \cdot \left(\sigma_{g.t.top.2} + \gamma_{sup} \cdot \sigma_{g.pav.t.top.2}\right) + \gamma_E \cdot \sigma_{ep.t.top.2}\right) \dots = \begin{bmatrix} -0.66 \\ 5.51 \end{bmatrix}$ ***MPa***

$\dots + \gamma_d \cdot \gamma_Q \cdot \left(\sigma_{Q.t.top.2} + \sigma_{q.t.top.2}\right) \dots$

$+ 0.6 \cdot \gamma_d \cdot \gamma_Q \cdot \left(\psi_{0.B} \cdot \sigma_{bk.t.top.2} + \psi_{0.Ö} \cdot \sigma_{sur.t.top.2}\right) + \gamma_d \cdot \psi_{0.th} \cdot \sigma_{th.t.top.2}$

Max $\sigma_{max.t.top.ULS.6.10b.2} := \gamma_d \cdot \gamma_{G.f} \cdot \left(\sigma_{g.t.top.2} + \gamma_{inf} \cdot \sigma_{g.pav.t.top.2} + \sigma_{ep.t.top.2}\right) \dots = \begin{bmatrix} -0.39 \\ 4.19 \end{bmatrix}$ ***MPa***

$+ \gamma_d \cdot \gamma_Q \cdot \left(\sigma_{Q.t.top.2} + \sigma_{q.t.top.2}\right)$

Total stress in bottom of timber

Min $\sigma_{min.t.bot.ULS.6.10b.2} := \gamma_d \cdot \gamma_{G.f} \cdot \left(\sigma_{g.t.bot.2} + \gamma_{inf} \cdot \sigma_{g.pav.t.bot.2} + \sigma_{ep.t.bot.2}\right) \dots = \begin{bmatrix} -0.39 \\ -4.19 \end{bmatrix}$ ***MPa***

$+ \gamma_d \cdot \gamma_Q \cdot \left(\sigma_{Q.t.bot.2} + \sigma_{q.t.bot.2}\right)$

Max $\sigma_{max.t.bot.ULS.6.10b.2} := \gamma_d \cdot \xi \cdot \left(\gamma_G \cdot \left(\sigma_{g.t.bot.2} + \gamma_{sup} \cdot \sigma_{g.pav.t.bot.2}\right) + \gamma_E \cdot \sigma_{ep.t.bot.2}\right) \dots = \begin{bmatrix} -0.66 \\ -5.51 \end{bmatrix}$ ***MPa***

$\dots + \gamma_d \cdot \gamma_Q \cdot \left(\sigma_{Q.t.bot.2} + \sigma_{q.t.bot.2}\right) \dots$

$+ 0.6 \cdot \gamma_d \cdot \gamma_Q \cdot \left(\psi_{0.B} \cdot \sigma_{bk.t.bot.2} + \psi_{0.Ö} \cdot \sigma_{sur.t.bot.2}\right) + \gamma_d \cdot \psi_{0.th} \cdot \sigma_{th.t.bot.2}$

Shear stress

$$\tau_{ULS.6.10b} := \gamma_d \cdot \xi \cdot \gamma_G \cdot \left(\tau_g + \gamma_{sup} \cdot \tau_{g.pav}\right) + \gamma_d \cdot \gamma_Q \cdot \left(\tau_Q + \tau_q\right) = 1.98 \ \textbf{MPa}$$

Fastener load

$$F_{conn.ULS.6.10b} := \gamma_d \cdot \xi \cdot \gamma_G \cdot \gamma_{sup} \cdot F_{conn.g.pav} + \gamma_d \cdot \gamma_Q \cdot \left(F_{conn.Q} + F_{conn.q}\right) = \left(2.07 \cdot 10^3\right) \ \textbf{kN}$$

Capacity check

Total stress in top of concrete - min

$$\eta_{min.s.top.ULS.6.10b.2} := \frac{\text{abs}\left(\sigma_{min.s.top.ULS.6.10b.2}(0,0) + \sigma_{min.s.top.ULS.6.10b.2}(1,0)\right)}{f_{yd}} = 14\%$$

Total stress in top of concrete - max

$$\eta_{max.s.top.ULS.6.10b.2} := \frac{\text{abs}\left(\sigma_{max.s.top.ULS.6.10b.2}(0,0) + \sigma_{max.s.top.ULS.6.10b.2}(1,0)\right)}{f_{yd}} = 10\%$$

Total stress in bottom of concrete - min

$$\eta_{min.s.bot.ULS.6.10b.2} := \frac{\text{abs}\left(\sigma_{min.s.bot.ULS.6.10b.2}(0,0) + \sigma_{min.s.bot.ULS.6.10b.2}(1,0)\right)}{f_{yd}} = 6\%$$

Total stress in bottom of concrete - max

$$\eta_{max.s.bot.ULS.6.10b.2} := \frac{\text{abs}\left(\sigma_{max.s.bot.ULS.6.10b.2}(0,0) + \sigma_{max.s.bot.ULS.6.10b.2}(1,0)\right)}{f_{yd}} = 4\%$$

Total stress in top of timber - min

$$\sigma_{Rd\_min.t.top.ULS.6.10b.2} := \sigma_{Rd}\left(\sigma_{min.t.top.ULS.6.10b.2}\right) = \begin{bmatrix} 17.64 \\ 21.6 \end{bmatrix} \textbf{\textit{MPa}}$$

$$\eta_{min.t.top.ULS.6.10b.2} := \text{abs}\left(\frac{\sigma_{min.t.top.ULS.6.10b.2}(0,0)}{\sigma_{Rd\_min.t.top.ULS.6.10b.2}(0,0)} + \frac{\sigma_{min.t.top.ULS.6.10b.2}(1,0)}{\sigma_{Rd\_min.t.top.ULS.6.10b.2}(1,0)}\right) = 22\%$$

Total stress in top of timber - max

$$\sigma_{Rd\_max.t.top.ULS.6.10b.2} := \sigma_{Rd}\left(\sigma_{max.t.top.ULS.6.10b.2}\right) = \begin{bmatrix} 17.64 \\ 21.6 \end{bmatrix} \textbf{\textit{MPa}}$$

$$\eta_{max.t.top.ULS.6.10b.2} := \text{abs}\left(\frac{\sigma_{max.t.top.ULS.6.10b.2}(0,0)}{\sigma_{Rd\_max.t.top.ULS.6.10b.2}(0,0)} + \frac{\sigma_{max.t.top.ULS.6.10b.2}(1,0)}{\sigma_{Rd\_max.t.top.ULS.6.10b.2}(1,0)}\right) = 17\%$$

Total stress in bottom of timber - min

$$\sigma_{Rd\_min.t.bot.ULS.6.10b.2} := \sigma_{Rd}\left(\sigma_{min.t.bot.ULS.6.10b.2}\right) = \begin{bmatrix} 17.64 \\ 21.6 \end{bmatrix} \textbf{\textit{MPa}}$$

$$\eta_{min.t.bot.ULS.6.10b.2} := \text{abs}\left(\frac{\sigma_{min.t.bot.ULS.6.10b.2}(0,0)}{\sigma_{Rd\_min.t.bot.ULS.6.10b.2}(0,0)} + \frac{\sigma_{min.t.bot.ULS.6.10b.2}(1,0)}{\sigma_{Rd\_min.t.bot.ULS.6.10b.2}(1,0)}\right) = 22\%$$

Total stress in bottom of timber - max

$$\sigma_{Rd\_max.t.bot.ULS.6.10b.2} := \sigma_{Rd}\left(\sigma_{max.t.bot.ULS.6.10b.2}\right) = \begin{bmatrix} 17.64 \\ 21.6 \end{bmatrix} \textbf{\textit{MPa}}$$

$$\eta_{max.t.bot.ULS.6.10b.2} := \text{abs}\left(\frac{\sigma_{max.t.bot.ULS.6.10b.2}(0,0)}{\sigma_{Rd\_max.t.bot.ULS.6.10b.2}(0,0)} + \frac{\sigma_{max.t.bot.ULS.6.10b.2}(1,0)}{\sigma_{Rd\_max.t.bot.ULS.6.10b.2}(1,0)}\right) = 29\%$$

Shear capacity check

$$\eta_{V.ULS.6.10b} := \frac{\tau_{ULS.6.10b}}{f_{v.d}} = 79\%$$

SLS - Characteristic combination

Total stress in top of concrete

Min $\sigma_{min.s.top.SLS.kar.2} := \sigma_{g.s.top.2} + \gamma_{sup} \cdot \sigma_{g.pav.s.top.sls.2} + \sigma_{ep.s.top.2.sls} + \left(\sigma_{Q.s.top.2.sls} + \sigma_{q.s.top.2.sls}\right) + 0.6 \cdot \left(\psi_{0.B} \cdot \sigma_{bk.s.top.2.sls} + \psi_{0.Ö} \cdot \sigma_{sur.s.top.2.sls}\right) + \gamma_d \cdot \psi_{0.th} \cdot \sigma_{th.s.top.2.sls} = \begin{bmatrix} 32.25 \\ 14.18 \end{bmatrix}$ ***MPa***

Max $\sigma_{max.s.top.SLS.kar.2} := \sigma_{g.s.top.2} + \gamma_{inf} \cdot \sigma_{g.pav.s.top.sls.2} + \sigma_{ep.s.top.2.sls} + \sigma_{Q.s.top.2.sls} + \sigma_{q.s.top.2.sls} = \begin{bmatrix} 23.89 \\ 10.66 \end{bmatrix}$ ***MPa***

Total stress in bottom of concrete

Min $\sigma_{min.s.bot.SLS.kar.2} := \sigma_{g.s.bot.2} + \gamma_{sup} \cdot \sigma_{g.pav.s.bot.sls.2} + \sigma_{ep.s.bot.2.sls} + \left(\sigma_{Q.s.bot.2.sls} + \sigma_{q.s.bot.2.sls}\right) + 0.6 \cdot \left(\psi_{0.B} \cdot \sigma_{bk.s.bot.2.sls} + \psi_{0.Ö} \cdot \sigma_{sur.s.bot.2.sls}\right) + \gamma_d \cdot \psi_{0.th} \cdot \sigma_{th.s.bot.2.sls} = \begin{bmatrix} 32.25 \\ -14.18 \end{bmatrix}$ ***MPa***

Max $\sigma_{max.s.bot.SLS.kar.2} := \sigma_{g.s.bot.2} + \gamma_{inf} \cdot \sigma_{g.pav.s.bot.sls.2} + \sigma_{ep.s.bot.2.sls} + \sigma_{Q.s.bot.2.sls} + \sigma_{q.s.bot.2.sls} = \begin{bmatrix} 23.89 \\ -10.66 \end{bmatrix}$ ***MPa***

Total stress in top of timber

$\sigma_{min.t.top.SLS.kar.2} := \sigma_{g.t.top.2} + \gamma_{sup} \cdot \sigma_{g.pav.t.top.sls.2} + \sigma_{ep.t.top.2.sls} + \left(\sigma_{Q.t.top.2.sls} + \sigma_{q.t.top.2.sls}\right) + 0.6 \cdot \left(\psi_{0.B} \cdot \sigma_{bk.t.top.2.sls} + \psi_{0.Ö} \cdot \sigma_{sur.t.top.2.sls}\right) + \gamma_d \cdot \psi_{0.th} \cdot \sigma_{th.t.top.2.sls} = \begin{bmatrix} -0.51 \\ 4.32 \end{bmatrix}$ ***MPa***

Max $\sigma_{max.t.top.SLS.kar.2} := \sigma_{g.t.top.2} + \gamma_{inf} \cdot \sigma_{g.pav.t.top.sls.2} + \sigma_{ep.t.top.2.sls} + \left(\sigma_{Q.t.top.2.sls} + \sigma_{q.t.top.2.sls}\right) = \begin{bmatrix} -0.32 \\ 3.75 \end{bmatrix}$ ***MPa***

Total stress in bottom of timber

Min $\sigma_{min.t.bot.SLS.kar.2} := \sigma_{g.t.bot.2} + \gamma_{inf} \cdot \sigma_{g.pav.t.bot.sls.2} + \sigma_{ep.t.bot.2.sls} + \left(\sigma_{Q.t.bot.2.sls} + \sigma_{q.t.bot.2.sls}\right) = \begin{bmatrix} -0.32 \\ -3.75 \end{bmatrix}$ ***MPa***

Max $\sigma_{max.t.bot.SLS.kar.2} := \sigma_{g.t.bot.2} + \gamma_{sup} \cdot \sigma_{g.pav.t.bot.sls.2} + \sigma_{ep.t.bot.2.sls} + \left(\sigma_{Q.t.bot.2.sls} + \sigma_{q.t.bot.2.sls}\right) + 0.6 \cdot \left(\psi_{0.B} \cdot \sigma_{bk.t.bot.2.sls} + \psi_{0.Ö} \cdot \sigma_{sur.t.bot.2.sls}\right) + \gamma_d \cdot \psi_{0.th} \cdot \sigma_{th.t.bot.2.sls} = \begin{bmatrix} -0.51 \\ -4.32 \end{bmatrix}$ ***MPa***

SLS - Frequent combination

Total stress in top of concrete

Min $\sigma_{min.s.top.SLS.freq.2} := \sigma_{g.s.top.2} + \gamma_{sup} \cdot \sigma_{g.pav.s.top.sls.2} + \sigma_{ep.s.top.2.sls} + \psi_{1.Q} \cdot \sigma_{Q.s.top.2.sls} + \psi_{1.q} \cdot \sigma_{q.s.top.2.sls} + \psi_{1.th} \cdot \sigma_{th.s.top.2.sls} = \begin{bmatrix} 23.23 \\ 10.42 \end{bmatrix}$ ***MPa***

Max $\sigma_{max.s.top.SLS.freq.2} := \sigma_{g.s.top.2} + \gamma_{inf} \cdot \sigma_{g.pav.s.top.sls.2} + \sigma_{ep.s.top.2.sls} + \psi_{1.Q} \cdot \sigma_{Q.s.top.2.sls} + \psi_{1.q} \cdot \sigma_{q.s.top.2.sls} = \begin{bmatrix} 20.23 \\ 9.14 \end{bmatrix}$ ***MPa***

Total stress in bottom of concrete

Min $\sigma_{min.s.bot.SLS.freq.2} := \sigma_{g.s.bot.2} + \gamma_{sup} \cdot \sigma_{g.pav.s.bot.sls.2} + \sigma_{ep.s.bot.2.sls} + \psi_{1.Q} \cdot \sigma_{Q.s.bot.2.sls} + \psi_{1.q} \cdot \sigma_{q.s.bot.2.sls} + \psi_{1.th} \cdot \sigma_{th.s.bot.2.sls} = \begin{bmatrix} 23.23 \\ -10.42 \end{bmatrix}$ ***MPa***

Max $\sigma_{max.s.bot.SLS.freq.2} := \sigma_{g.s.bot.2} + \gamma_{inf} \cdot \sigma_{g.pav.s.bot.sls.2} + \sigma_{ep.s.bot.2.sls} + \psi_{1.Q} \cdot \sigma_{Q.s.bot.2.sls} + \psi_{1.q} \cdot \sigma_{q.s.bot.2.sls} = \begin{bmatrix} 20.23 \\ -9.14 \end{bmatrix}$ ***MPa***

Total stress in top of timber

Min $\sigma_{min.t.top.SLS.freq.2} := \sigma_{g.t.top.2} + \gamma_{sup} \cdot \sigma_{g.pav.t.top.sls.2} + \sigma_{ep.t.top.2.sls} + \psi_{1.Q} \cdot \sigma_{Q.t.top.2.sls} + \psi_{1.q} \cdot \sigma_{q.t.top.2.sls} + \psi_{1.th} \cdot \sigma_{th.t.top.2.sls} = \begin{bmatrix} -0.36 \\ 3.7 \end{bmatrix}$ ***MPa***

Max $\sigma_{max.t.top.SLS.freq.2} := \sigma_{g.t.top.2} + \gamma_{inf} \cdot \sigma_{g.pav.t.top.sls.2} + \sigma_{ep.t.top.2.sls} + \psi_{1.Q} \cdot \sigma_{Q.t.top.2.sls} + \psi_{1.q} \cdot \sigma_{q.t.top.2.sls} = \begin{bmatrix} -0.28 \\ 3.5 \end{bmatrix}$ ***MPa***

Total stress in bottom of timber

Min $\sigma_{min.t.bot.SLS.freq.2} := \sigma_{g.t.bot.2} + \gamma_{inf} \cdot \sigma_{g.pav.t.bot.sls.2} + \sigma_{ep.t.bot.2.sls} + \psi_{1.Q} \cdot \sigma_{Q.t.bot.2.sls} + \psi_{1.q} \cdot \sigma_{q.t.bot.2.sls} = \begin{bmatrix} -0.28 \\ -3.5 \end{bmatrix}$ ***MPa***

Max $\sigma_{max.t.bot.SLS.freq.2} := \sigma_{g.t.bot.2} + \gamma_{sup} \cdot \sigma_{g.pav.t.bot.sls.2} + \sigma_{ep.t.bot.2.sls} + \psi_{1.Q} \cdot \sigma_{Q.t.bot.2.sls} + \psi_{1.q} \cdot \sigma_{q.t.bot.2.sls} + \psi_{1.th} \cdot \sigma_{th.t.bot.2.sls} = \begin{bmatrix} -0.36 \\ -3.7 \end{bmatrix}$ ***MPa***

Quasi permanent

Total stress in top of concrete $\sigma_{min.s.top.SLS.quasi.2} := \sigma_{g.s.top.2} + \psi_{1.th} \cdot \sigma_{th.s.top.2.sls} = \begin{bmatrix} 2.86 \\ 1.21 \end{bmatrix}$ ***MPa***

Total stress in bottom of concrete $\sigma_{min.s.bot.SLS.quasi.2} := \sigma_{g.s.bot.2} + \psi_{1.th} \cdot \sigma_{th.s.bot.2.sls} = \begin{bmatrix} 2.86 \\ -1.21 \end{bmatrix}$ ***MPa***

Total stress in top of timber $\sigma_{min.t.top.SLS.quasi.2} := \sigma_{g.t.top.1} + \psi_{1.th} \cdot \sigma_{th.t.top.sls.1} = \begin{bmatrix} 0 \\ -2.77 \end{bmatrix}$ ***MPa***

Total stress in bottom of timber $\sigma_{min.t.bot.SLS.quasi.2} := \sigma_{g.t.bot.1} + \psi_{1.th} \cdot \sigma_{th.t.bot.sls.1} = \begin{bmatrix} 0 \\ 2.77 \end{bmatrix}$ ***MPa***

Deformation

Deflection of free console - wing wall

Support moment from self weight $M_{s.g} := \frac{\left(-l_{wing.la} \cdot F_{wing} - l_{int.la} \cdot F_{int}\right)}{2} = -639\ \textbf{kNm}$

Maximum deflection for end console $w_{max.console} := min\left(\frac{a}{200}, 5\ \textbf{mm}\right) = 5\ \textbf{mm}$

Frequent combination LM1 - boggie load $Q_{1f} := Q_{1k} \cdot \psi_{1.Q} = 202.5\ \textbf{kN}$

Frequent combination LM1 - distributed load $q_{1f} := q_{1k} \cdot \psi_{1.q} \cdot w_1 = 8.64\ \frac{\textbf{kN}}{\textbf{m}}$

Point load at the end of the end console $a_{deflection} := a - 1.2\ \textbf{m} = 0.1\ \textbf{m}$

$$w_{LM1.console} := \left(\frac{Q_{1f} \cdot a^3}{3 \cdot EI_{eff.sls}}\right) + \left(\frac{Q_{1f} \cdot a^3}{3 \cdot EI_{eff.sls}} - \frac{Q_{1f} \cdot a^2}{6 \cdot EI_{eff.sls}} \cdot \left(3 \cdot a_{deflection} - \frac{a_{deflection}^3}{a^2}\right)\right) \cdot f_{Q.LM1} \dots = 0.3\ \textbf{mm}$$
$$+ \left(\frac{q_{1f} \cdot a^4}{8 \cdot EI_{eff.sls}}\right) \cdot f_{q.LM1} + \frac{\frac{-\left(M_{s.g} + M_{ep} + M_{s.g.pav}\right)}{2} \cdot a^2}{2 \cdot EI_{eff.sw.sls}} + \frac{\frac{-\left(M_{sur} + M_{bk}\right)}{2} \cdot a^2}{2 \cdot EI_{eff.sls}} + \frac{\frac{-\left(M_{thermal}\right)}{2} \cdot a^2}{2 \cdot EI_{eff.temp.sls}}$$

$\eta_{w.LM1.console} := \frac{w_{LM1.console}}{w_{max.console}} = 6.01\%$

Max deflection in midspan

Maximum deflection for midspan $w_{max.midspan} := \frac{l}{400} = 41\ \textbf{mm}$

Worst load placement of wheel 1 $a_1 := \frac{l}{2} - 0.6\ \textbf{m} = 7.6\ \textbf{m}$

Worst load placement of wheel 2 $b_1 := \frac{l}{2} + 0.6\ \textbf{m} = 8.8\ \textbf{m}$

$$w_{LM1.midspan} := \left(\frac{Q_{1f} \cdot l^2}{16 \cdot EI_{eff.sls}} \cdot \left(a_1 - \frac{4 \cdot a_1^3}{3 \cdot l^2}\right) + \frac{Q_{1f} \cdot l^2}{16 \cdot EI_{eff.sls}} \cdot \left(b_1 - \frac{4 \cdot b_1^3}{3 \cdot l^2}\right)\right) \cdot f_{Q.LM1} \dots = 34.1\ \textbf{mm}$$
$$+ \frac{5 \cdot q_{1f} \cdot l^4}{384 \cdot EI_{eff.sls}} \cdot f_{q.LM1} + \frac{5 \cdot \left(g_{tot} + g_{pav}\right) \cdot l^4}{384 \cdot EI_{eff.sw.sls}}$$

$\eta_{w.LM1.midspan} := \frac{w_{LM1.midspan}}{w_{max.midspan}} = 83.28\%$

Uplift of end console

$$\theta_{support} := \left(\frac{Q_{1f} \cdot a_1 \cdot l}{6 \cdot EI_{eff.sls}} \cdot \left(1 - \frac{a_1^2}{l^2}\right) + \frac{Q_{1f} \cdot b_1 \cdot l}{6 \cdot EI_{eff.sls}} \cdot \left(1 - \frac{b_1^2}{l^2}\right)\right) \cdot f_{Q.LM1} \dots = 3.4 \cdot 10^{-3}$$
$$+ \frac{q_{1f} \cdot l^3}{24 \cdot EI_{eff.sls}} \cdot f_{q.LM1} + \frac{g_{tot} \cdot l^3}{24 \cdot EI_{eff.sw.sls}} + \frac{\left(M_{s.g} + M_{ep} + M_{s.g.pav}\right) \cdot l \cdot 3}{6 \cdot EI_{eff.sw.sls}} + \frac{M_{f.g.pav} \cdot l}{24 \cdot EI_{eff.sw.sls}}$$

$w_{end.console.uplift} := \tan\left(\theta_{support}\right) \cdot a = 4.42\ \textbf{mm}$

$\eta_{w.end.console.uplift} := \frac{w_{end.console.uplift}}{5\ \textbf{mm}} = 88.4\%$

Verification of fasteners

$F_{Ed.conn} := \max\left(F_{conn.ULS.6.10a}, F_{conn.ULS.6.10b}\right)$

$F_{Ed.conn} = 2072.41\ \textbf{kN}$

Dowel-type fasteners

$n_c = 16$

Diameter $d := 20\ \textbf{mm}$

Ultimate tensile strength $f_u := 800\ \textbf{MPa}$

Length of dowel inside timber $t_1 := 200\ \textbf{mm}$

Length of dowel inside concrete $t_2 := 200\ \textbf{mm}$

Charachteristic strength of glulam $f_{h.1.k} := 0.082 \cdot \left(1 - 0.01 \cdot \left(\frac{d}{\textbf{mm}}\right)\right) \cdot \left(\frac{\rho_{t.k}}{\frac{\textbf{kg}}{\textbf{m}^3}}\right) \cdot \textbf{MPa} = 25.58\ \textbf{MPa}$

Charachteristic strength of concrete $f_{h.2.k} := 3\ f_{ck} = 105\ \textbf{MPa}$

Ratio between the strengths of materials $\beta := \frac{f_{h.2.k}}{f_{h.1.k}} = 4.1$

Yield moment of the dowel $M_{y.Rk} := 0.3 \cdot \frac{f_u}{\textbf{MPa}} \cdot \left(\frac{d}{\textbf{mm}}\right)^{2.6} \cdot \textbf{kNm} = \left(5.79 \cdot 10^5\right)\ \textbf{kNm}$

Pull-out strength $F_{ax.Rk} := 0\ \textbf{kN}$

Fasteners with single shear plane, failure modes:

$F_{v.Rk.dowel.a} := f_{h.1.k} \cdot t_1 \cdot d = 102.34\ \textbf{kN}$

$F_{v.Rk.dowel.b} := f_{h.2.k} \cdot t_2 \cdot d = 420\ \textbf{kN}$

$F_{v.Rk.dowel.c} := \frac{f_{h.1.k} \cdot t_1 \cdot d}{1+\beta} \cdot \left(\sqrt{\beta + 2 \cdot \beta^2 \cdot \left(1 + \frac{t_2}{t_1} + \left(\frac{t_2}{t_1}\right)^2\right) + \beta^3 \cdot \left(\frac{t_2}{t_1}\right)^2} - \beta \cdot \left(1 + \frac{t_2}{t_1}\right)\right) + \frac{F_{ax.Rk}}{4} = 100.13\ \textbf{kN}$

$F_{v.Rk.dowel.d} := 1.05 \cdot \frac{f_{h.1.k} \cdot t_1 \cdot d}{2+\beta} \cdot \left(\sqrt{2 \cdot \beta \cdot (1+\beta) + \frac{4 \cdot \beta \cdot (2+\beta) \cdot M_{y.Rk}}{f_{h.1.k} \cdot d \cdot {t_1}^2}} - \beta\right) + \frac{F_{ax.Rk}}{4} = \left(2.96 \cdot 10^4\right)\ \textbf{kN}$

$F_{v.Rk.dowel.e} := 1.05 \cdot \frac{f_{h.1.k} \cdot t_2 \cdot d}{2+\beta} \cdot \left(\sqrt{2 \cdot \beta \cdot (1+\beta) + \frac{4 \cdot \beta \cdot (2+\beta) \cdot M_{y.Rk}}{f_{h.1.k} \cdot d \cdot {t_2}^2}} - \beta\right) + \frac{F_{ax.Rk}}{4} = \left(2.96 \cdot 10^4\right)\ \textbf{kN}$

$F_{v.Rk.dowel.f} := 1.15 \cdot \sqrt{\frac{2 \cdot \beta}{1+\beta}} \cdot \sqrt{2 \cdot M_{y.Rk} \cdot f_{h.1.k} \cdot d} + \frac{F_{ax.Rk}}{4} = \left(3.55 \cdot 10^4\right)\ \textbf{kN}$

$F_{v.Rk.dowel} := min\left(F_{v.Rk.dowel.a}, F_{v.Rk.dowel.b}, F_{v.Rk.dowel.c}, F_{v.Rk.dowel.d}, F_{v.Rk.dowel.e}, F_{v.Rk.dowel.f}\right) = 100.13\ \textbf{kN}$

$F_{v.Rk.dowel.tot} := n_c \cdot F_{v.Rk.dowel} = \left(1.6 \cdot 10^3\right)\ \textbf{kN}$

$\eta_{conn.dowel} := \frac{F_{Ed.conn}}{F_{v.Rk.dowel.tot}} = 129\%$

Notched connections

Minimal shear length of the timber

$$l_{min} := 8 \cdot h_{notches} = 0.4\ \boldsymbol{m}$$

Strength reduction factor for concrete cracked in shear

$$v := 0.6 \cdot \left(1 - \frac{f_{ck}}{250\ \boldsymbol{MPa}}\right) = 0.52$$

Angle of the concrete strut

$$\theta := \max\left(\operatorname{atan}\left(\frac{0.5 \cdot \left(t_c + h_{notches}\right)}{\left(l_{notches} + l_{s.notches}\right)}\right), \operatorname{atan}\left(\frac{h_{notches}}{l_{notches}}\right)\right) = 18.43\ \boldsymbol{deg}$$

Effective design shear strength of concrete

$$f_{vcd} := \frac{v \cdot f_{cd}}{\left(\cot\left(\theta\right) + \tan\left(\theta\right)\right)} = 3.61\ \boldsymbol{MPa}$$

Notched connections, failure modes:

Shear of concrete

$$F_{Rd.notches.a} := f_{vcd} \cdot b_{notches} \cdot l_{notches} = 514.71\ \boldsymbol{kN}$$

Crushing of concrete

$$F_{Rd.notches.b} := f_{cd} \cdot b_{notches} \cdot l_{notches} = 3325\ \boldsymbol{kN}$$

Shear of timber

$$F_{Rd.notches.c} := k_{cr} \cdot f_{v.d} \cdot b_{notches} \cdot l_{min} = 820.66\ \boldsymbol{kN}$$

Crushing of timber

$$F_{Rd.notches.d} := f_{c.0.d} \cdot b_{notches} \cdot h_{notches} = 837.9\ \boldsymbol{kN}$$

Governing failure mode:

$$F_{Rd.notches} := min\left(F_{Rd.notches.a}, F_{Rd.notches.b}, F_{Rd.notches.c}, F_{Rd.notches.d}\right) = 514.71\ \boldsymbol{kN}$$

Utilization ratio

$$\eta_{conn.notchesl} := \frac{F_{Ed.conn}}{F_{Rd.notches} + F_{v.Rk.dowel.tot}} = 98\%$$

Check for lateral torsional buckling in production

Ekvationer hämtade frånm Bärande konstruktioner del 1

Moment caused by selfweight of timber and concrete during casting

$$M_{deck} := \gamma_d \cdot \gamma_G \cdot \frac{\left(g_c + g_{eb} + g_t\right) \cdot l^2}{8} = \left(1.74 \cdot 10^3\right)\ \boldsymbol{kNm}$$

Moment of intertia along the weak axis

$$I_{t.z} := \frac{h_t \cdot b_t^{\,3}}{12} = 0.09\ \boldsymbol{m}^4$$

Torsional moment of intertia

$$K_v := \frac{h_t \cdot b_t^{\,3}}{3} \cdot \left(1 - 0.63 \cdot \frac{b_t}{h_t}\right)$$

Critical moment

$$M_{cr} := \frac{\pi}{l} \cdot \sqrt[2]{E_{t.0.05} \cdot I_{t.z} \cdot G_{05} \cdot K_v} = \left(6.35 \cdot 10^4\right)\ \boldsymbol{kNm}$$

Capacity check

$$\eta_{LT} := \frac{M_{deck}}{M_{cr}} = 2.7\%$$

Bearing stress perpendicular to grain capacity

$$R_A := \gamma_d \cdot \xi \cdot \gamma_G \cdot \left(\frac{2 \cdot \left(g_{tot} + g_{pav} \right) \cdot \left(L - 2 \cdot t_i \right)}{2} + F_{int} + F_{wing} \right) + \gamma_d \cdot \gamma_Q \cdot \begin{pmatrix} f_{q.LM1} \cdot \left(w_1 \cdot L \cdot \left(q_{1k} + q_{2k} \right) + w_{rk} \cdot L \cdot q_{rk} \right) \\ + f_{Q.LM1} \cdot \left(2 \cdot Q_{1k} + Q_{2k} \right) \end{pmatrix} = \left(4.22 \cdot 10^3 \right) \ \textbf{kN}$$

Maximum upplagslängd	$l_t := 600 \ \textbf{mm}$
Effective upplagslängd	$l_{ef} := l_t = 0.6 \ \textbf{m}$
Factor according to Eurocode 5	$k_1 := 1$
Factor according to Eurocode 5	$k_{c.90} := 1$
Stresses acting perpendicular to the grain	$\sigma_{c.90.d} := \frac{R_A \div 2}{b_t \cdot l_{ef}} = 3.7 \ \textbf{MPa}$
Stress capacity from the glulam	$\sigma_{Rk.90} := f_{c.90d} \cdot k_1 \cdot k_{c.90} = 1.8 \ \textbf{MPa}$
Utlization ratio	$\eta_{c.90} := \frac{\sigma_{c.90.d}}{\sigma_{Rk.90}} = 206\%$

Risk of cracking over support

Normal stress from composite action	$\sigma_{g.pav.c.2} := \frac{\gamma_{c.uls} \cdot E_{cm} \cdot a_{c.uls}}{EI_{eff.uls}} \cdot M_{s.g.pav} = -30.215 \ \textbf{kPa}$
Stress from bending	$\sigma_{g.pav.m.c.2} := \frac{E_{cm} \cdot t_c \cdot 0.5}{EI_{eff.uls}} \cdot M_{s.g.pav} = -21.94 \ \textbf{kPa}$
Total stress in top of concrete	$\sigma_{g.pav.c.top.2} := \begin{bmatrix} -\sigma_{g.pav.c.2} \\ -\sigma_{g.pav.m.c.2} \end{bmatrix} = \begin{bmatrix} 30.21 \\ 21.94 \end{bmatrix} \ \textbf{kPa}$
Normal stress from composite action	$\sigma_{Q.c.2} := \frac{\gamma_{c.uls} \cdot E_{cm} \cdot a_{c.uls}}{EI_{eff.uls}} \cdot M_{Q.s.min} = -0.722 \ \textbf{MPa}$
Stress from bending	$\sigma_{Q.m.c.2} := \frac{E_{cm} \cdot t_c \cdot 0.5}{EI_{eff.uls}} \cdot M_{Q.s.min} = -0.524 \ \textbf{MPa}$
Total stress in top of concrete	$\sigma_{Q.c.top.2} := \begin{bmatrix} -\sigma_{Q.c.2} \\ -\sigma_{Q.m.c.2} \end{bmatrix} = \begin{bmatrix} 0.722 \\ 0.524 \end{bmatrix} \ \textbf{MPa}$
Normal stress from composite action	$\sigma_{q.c.2} := \frac{\gamma_{c.uls} \cdot E_{cm} \cdot a_{c.uls}}{EI_{eff.uls}} \cdot M_{q.s.min} = -40.732 \ \textbf{kPa}$
Stress from bending	$\sigma_{q.m.c.2} := \frac{E_{cm} \cdot t_c \cdot 0.5}{EI_{eff.uls}} \cdot M_{q.s.min} = -29.577 \ \textbf{kPa}$
Total stress in top of concrete	$\sigma_{q.c.top.2} := \begin{bmatrix} -\sigma_{q.c.2} \\ -\sigma_{q.m.c.2} \end{bmatrix} = \begin{bmatrix} 40.732 \\ 29.577 \end{bmatrix} \ \textbf{kPa}$
Normal stress from composite action	$\sigma_{ep.c.2} := \frac{\gamma_{c.uls} \cdot E_{cm} \cdot a_{c.uls}}{EI_{eff.uls}} \cdot M_{ep} = -0.422 \ \textbf{MPa}$
Stress from bending	$\sigma_{ep.m.c.2} := \frac{E_{cm} \cdot t_c \cdot 0.5}{EI_{eff.uls}} \cdot M_{ep} = -0.307 \ \textbf{MPa}$
Total stress in top of concrete	$\sigma_{ep.c.top.2} := \sigma_{0.k} + \begin{bmatrix} -\sigma_{ep.c.2} \\ -\sigma_{ep.m.c.2} \end{bmatrix} = \begin{bmatrix} 0.37 \\ 0.307 \end{bmatrix} \ \textbf{MPa}$

Normal stress from composite action $\sigma_{sur.c.2} := \frac{\gamma_{c.uls} \cdot E_{cm} \cdot a_{c.uls}}{EI_{eff.uls}} \cdot M_{sur} = -0.155$ **MPa**

Stress from bending $\sigma_{sur.m.c.2} := \frac{E_{cm} \cdot t_c \cdot 0.5}{EI_{eff.uls}} \cdot M_{sur} = -0.113$ **MPa**

Total stress in top of concrete $\sigma_{sur.c.top.2} := \sigma_{ö} + \begin{bmatrix} -\sigma_{sur.c.2} \\ -\sigma_{sur.m.c.2} \end{bmatrix} = \begin{bmatrix} 0.127 \\ 0.113 \end{bmatrix}$ **MPa**

Normal stress from composite action $\sigma_{bk.c.2} := \frac{\gamma_{c.uls} \cdot E_{cm} \cdot a_{c.uls}}{EI_{eff.uls}} \cdot M_{bk} = -0.556$ **MPa**

Stress from bending $\sigma_{bk.m.c.2} := \frac{E_{cm} \cdot t_c \cdot 0.5}{EI_{eff.uls}} \cdot M_{bk} = -0.404$ **MPa**

Total stress in top of concrete $\sigma_{bk.c.top.2} := \sigma_{Break} + \begin{bmatrix} -\sigma_{bk.c.2} \\ -\sigma_{bk.m.c.2} \end{bmatrix} = \begin{bmatrix} 0.487 \\ 0.404 \end{bmatrix}$ **MPa**

Normal stress from composite action $\sigma_{th.c.2} := \frac{\gamma_{c.uls} \cdot E_{cm} \cdot a_{c.uls}}{EI_{eff.uls}} \cdot M_{thermal} = -0.275$ **MPa**

Stress from bending $\sigma_{th.m.c.2} := \frac{E_{cm} \cdot t_c \cdot 0.5}{EI_{eff.uls}} \cdot M_{thermal} = -0.2$ **MPa**

Total stress in top of concrete $\sigma_{th.c.top.2} := \sigma_{th} + \begin{bmatrix} -\sigma_{th.c.2} \\ -\sigma_{th.m.c.2} \end{bmatrix} = \begin{bmatrix} 0.195 \\ 0.2 \end{bmatrix}$ **MPa**

Total stress in top of concrete

$$\sigma_{min.c.top.ULS.6.10b.2} := \gamma_d \cdot \xi \cdot \left(\gamma_G \cdot \left(\gamma_{sup} \cdot \sigma_{g.pav.c.top.2}\right) + \gamma_E \cdot \sigma_{ep.c.top.2}\right) \hookleftarrow + \gamma_d \cdot \gamma_Q \cdot \left(\sigma_{Q.c.top.2} + \sigma_{q.c.top.2}\right) \hookleftarrow + 0.6 \cdot \gamma_d \cdot \gamma_Q \cdot \left(\psi_{0.B} \cdot \sigma_{bk.c.top.2} + \psi_{0.Ö} \cdot \sigma_{sur.c.top.2}\right) + \gamma_d \cdot \psi_{0.th} \cdot \sigma_{th.c.top.2} = \begin{bmatrix} 2.14 \\ 1.68 \end{bmatrix}$$ **MPa**

$\sigma_{Rd\_min.c.top.ULS.6.10b.2} := \sigma_{c.Rd}\left(\sigma_{min.c.top.ULS.6.10b.2}\right) = [1.47]$ **MPa**

$\eta_{min.c.top.ULS.6.10b.2} := \frac{\text{abs}\left(\sigma_{min.c.top.ULS.6.10b.2}(0,0) + \sigma_{min.c.top.ULS.6.10b.2}(1,0)\right)}{\sigma_{Rd\_min.c.top.ULS.6.10b.2}(0,0)} = 260\%$

Crack width

According to SS-EN 1994-2, 7.4.2

Factor	$k_s := 0.9$
Factor	$k := 0.8$
Effective tensile strength concrete	$f_{ct.eff} := f_{ctm} = 3.2\ \textbf{MPa}$
Effective width of concrete slab	$b_{eff.1} = 3.75\ \textbf{m}$
Area of concrete	$A_{ct} := A_c = 1.1\ \textbf{m}^2$
Concrete flange thickness	$h_{c.m} := \frac{A_c}{b_{eff.1}} = 0.29\ \textbf{m}$
Distance between center of gravity for the uncracked concrete and the glulam beam	$z_0 := z = 0.76\ \textbf{m}$
Factor which takes stress distribution into account	$k_c := min\left(\frac{1}{1+\frac{h_{c.m}}{2 \cdot z_0}}, 1\right) = 0.84$
Maximum allowed tensile stress in reinforcement, interpolated between fi16 and fi25	$\sigma_{s.till.20} := \frac{(200+160)}{2}\ \textbf{MPa} = 180\ \textbf{MPa}$
Minimum reinforcement area required for not exceeding crack width 0.20mm	$A_{s.min} := \frac{k_s \cdot k \cdot k_c \cdot f_{ct.eff} \cdot A_{ct}}{\sigma_{s.till.20}} = 0.01\ \textbf{m}^2$
Reinforcement area over support	$A_a := \frac{(20\ \textbf{mm})^2 \cdot \pi}{4} \cdot \frac{b}{0.100\ \textbf{m}} = 0.02\ \textbf{m}^2$
Utlilzation degree	$\eta := \frac{A_{s.min}}{A_a} = 50\%$ Crack width not exceeded 0.20mm

Mängdstatistik

Concrete volume	
Slab	$V_c := L \cdot t_c \cdot b = 42.75\ \textbf{m}^3$
End console	$V_{c.i} := 2 \cdot h_i \cdot b_i \cdot t_i = 30.15\ \textbf{m}^3$
Edge beam	$V_{c.eb} := 2 \cdot A_{eb} \cdot L$
Wing wall	$V_{wing} := 4 \cdot 3.70\ \textbf{m}^3 = 14.8\ \textbf{m}^3$
Glulam beam volume	$V_t := 2 \cdot A_t \cdot (L - 2 \cdot t_i) = 44.14\ \textbf{m}^3$
Pavement volume	$V_{pavement} := t_{pavement} \cdot b \cdot L = 9.98\ \textbf{m}^3$
Weigh per glulam beam	$M_t := \frac{V_t}{2} \cdot \rho_{t.mean} = 9.49\ \textbf{tonne}$

Density reinforcement $\rho_{rebar} := 7800 \ \frac{kg}{m^3}$

Area fi20 rebar $A_{20} := \frac{(20 \ mm)^2 \cdot \pi}{4}$

Area fi16 rebar $A_{16} := \frac{(16 \ mm)^2 \cdot \pi}{4}$

Area fi12 rebar $A_{12} := \frac{(12 \ mm)^2 \cdot \pi}{4}$

Area fi10 rebar $A_{10} := \frac{(10 \ mm)^2 \cdot \pi}{4}$

Ammount of rebar s100 $n_{s.100} := \frac{b}{0.100 \ m} = 75$

Ammount of rebar s200 $n_{s.200} := \frac{b}{0.200 \ m} = 37.5$

Ammount of rebar, cross s100 $n_{s.100.cross} := \frac{L}{0.100 \ m} = 190$

Ammount of rebar, cross s200 $n_{s.200.cross} := \frac{L}{0.200 \ m} = 95$

Ammount of rebar, edge beam $n_{edgebeam} := 10$

Length support rebar $l_{support} := a + 1.1 \ m = 2.4 \ m$

Length span rebar $l_{span} := l + 2 \cdot 1.1 \ m = 18.6 \ m$

Length edgebeam LX $l_{LX} := 2.020 \ m$

Length C-rebar edge $l_{edge} := (0.250 + 2 \cdot 0.800) \ m = 1.85 \ m$

Reinforcement volume, support $M_{rebar.support} := 2 \cdot \rho_{rebar} \cdot A_{20} \cdot n_{s.100} \cdot l_{support} = 882 \ kg$

Reinforcement volume,span $M_{rebar.span} := \rho_{rebar} \cdot A_{16} \cdot n_{s.200} \cdot l_{span} \hookleftarrow = 1709 \ kg$
$+ \rho_{rebar} \cdot A_{12} \cdot n_{s.200} \cdot l_{span}$

Reinforcement volume, cross ÖK $M_{rebar.cross.ÖK} := \rho_{rebar} \cdot A_{16} \cdot n_{s.100.cross} \cdot (b + 0 \ .9 \cdot m) = 2235 \ kg$

Reinforcement volume, cross UK $M_{rebar.cross.UK} := \rho_{rebar} \cdot A_{16} \cdot n_{s.100.cross} \cdot (b + 0 \ .9 \cdot m) = 2235 \ kg$

Reinforcement edge beam $M_{rebar.edgebeam} := 2 \cdot \rho_{rebar} \cdot A_{10} \cdot n_{s.200.cross} \cdot L \hookleftarrow = 2444 \ kg$
$+ 2 \cdot \rho_{rebar} \cdot A_{10} \cdot n_{edgebeam} \cdot L$

Reinforcement edges $M_{rebar.edges} := 2 \cdot \rho_{rebar} \cdot A_{12} \cdot 3 \cdot L \hookleftarrow = 720.72 \ kg$
$+ 2 \cdot \rho_{rebar} \cdot A_{12} \cdot n_{s.100.cross} \cdot l_{edge}$

$M_{tot} := M_{rebar.support} + M_{rebar.span} + M_{rebar.cross.ÖK} \hookleftarrow = 10226 \ kg$
$+ M_{rebar.cross.UK} + M_{rebar.edgebeam} \hookleftarrow$
$+ M_{rebar.edges}$

B

LCA calculation

B.1 LCA for Concrete bridge

Kalkylmapp		Klimatkalkyl	
Kontakperson:	Internet user	**Kalkylnamn:**	Concrete bridge
Namn:	TCC Exjobb	**Kalkyl-ID**	IC1456
Objektnummer:	1	**Skede:**	Klimatdeklaration
Objektnamn:		**Org. GKI/underlagskalkyl**	1
Åtgärdsnummer:	1	**Revideringsdatum GKI/u**	2025-04-29
Åtgardsnamn:		**Status:**	Arbetsversion
Ärendenummer:	1	**Investeringskostnad:**	
Beskrivning:		**Prisnivå:**	2025
Skapad av:	Internet user 2025-04-29 13:55:30	**Region:**	Norra
Senast ändrad av:	Internet user 2025-04-29 13:55:30	**Modellversion:**	Version 8.0
		Beskrivning:	
		Kalkylnivå:	Ingång C: Investeringsobjekt, flexibel ingång (kombination av kalkynivåer 1, 2 och 3)
		Skapad av:	Internet user 2025-04-29 13:59:29
		Senast ändrad av:	Internet user 2025-04-29 13:59:29

Resultatsammanställning

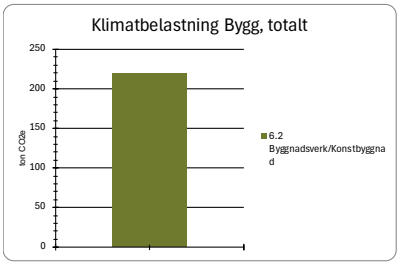

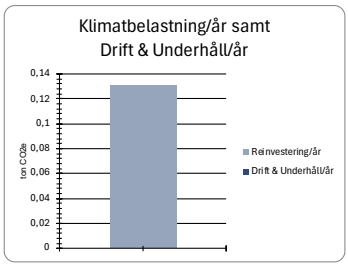

BYGG	ton CO2e	GJ
6.2 Byggnadsverk/Konstbyggnad	219,5944837	2000,148844
TOTALT	**219,5944837**	**2000,148844**

ÅRLIGT	ton CO2e	GJ
Bygg & Reinvestering, per år	2,842816063	31,07334198
Drift & Underhåll.per år	0	0
TOTALT	**2,842816063**	**31,07334198**

Fördelning av material/arbetsmoment, årligt

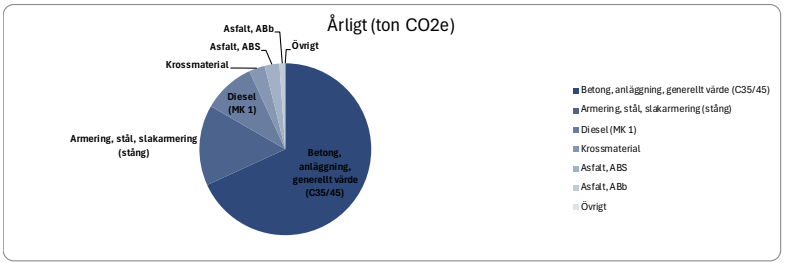

Indatasammanställning

Ingående objekt:	Mängd	Enhet	Klimat (ton CO2e) Byggskede totalt	Reinvestering/år * * byggdelar med livslängd ≤ 60 år	Bygg & reinvest/år * * samtliga byggdelar	Drift & Underhåll/år	Energi (GJ) Byggskede totalt	Reinvestering/år * * byggdelar med livslängd ≤ 60 år	Bygg & reinvest/år * * samtliga byggdelar	Drift & Underhåll/år
Totalt			219,5944837	0,130474348	2,842816063	0	2000,148844	7,953815152	31,07334198	0
Totalt exklusive produktion och transport av TGM			219,5944837	0,130474348	2,842816063	0	2000,148844		31,07334198	0
Typåtgärder										
Vägbro, betongplatta (6.2)	215,25	m2	139,1199609	0,130474348	1,836884528		1374,422246	7,953815152	23,25175952	

Kommentar typåtgärd

Byggdelar i typåtgärd	Standardv	Egen mängd	Enhet
Jord Fall A, Fyll, Väg (6.2)		0	m3/m2
Jord Fall B, Fyll, Väg (6.2)		0	m3/m2
Bergschakt Fall A, Väg (6.2)		0	m3/m2
Jordschakt Fall A, Väg (6.2)		0	m3/m2
Bergschakt Fall B, Väg (6.2)		0	m3/m2
Asfalt, ABb 50 mm (6.2)		1,2	m2/m2
Stål, konstruktion, Väg (6.2)		0	ton/m2
Betong, anläggning, generellt värde, Väg (6.2)		1,1	m3/m2
Jordschakt Fall B, Väg (6.2)		4,4	m3/m2
Armering, armeringsstål, Väg (6.2)		0,14	ton/m2
Asfalt, ABS 40 mm (6.2)		1	m2/m2
Berg Fall B, Fyll, Väg (6.2)		4,4	m3/m2
Berg Fall A, Fyll, Väg (6.2)		0	m3/m2

Byggdelar			Byggskede totalt	Reinvestering/år	Bygg & reinvest/år	Byggskede totalt	Reinvestering/år	Bygg & reinvest/år
Armering, armeringsstål, Väg (6.2)	19,1	ton	13,98590624	0	0,174823828	223,7902828	0	2,797378535

Kommentar byggdel

Material och arbetsmoment	Standardmäng	Egen män	Enhet
Stål, armering	1		ton/ton

Emissionsfaktor: Armering, stål, slakarmering (stång)

	Klimat (kg C	Energi (MJ/kg)
Standardvärde	0,7	11,1
Eget värde		

Kommentar material och arbetsmoment

Transport material

			Avstånd (km)	Transportparameter
D1	Järnväg	Standard	500	Armeringsstål
		Eget värde		
D2	Lastbil lands	Standard	300	Armeringsstål
		Eget värde		
D3	Lastbil närdis	Standard	40	Armeringsstål
		Eget värde		

Emissionsfaktor:

D1	El, ursprungs	Standard	0,012	kg CO2e/kWh	3,02	MJ/kWh
		Eget värde				
D2	Diesel (MK 1)	Standard	2,8	kg CO2e/l	43,3	MJ/l
		Eget värde				
D3	Diesel (MK 1)	Standard	2,8	kg CO2e/l	43,3	MJ/l
		Eget värde				

Kommentar transporter

Betong, anläggning, generellt värde, Väg (6.2)	165,51	m3	66,48861658	0	0,831107707	401,9363145	0	5,024203931	
Drift & Underhåll						Drift & Underhåll/år			Drift & Underhåll/år
Vägbro, betongplatta (6.2)						Schablon saknas			Schablon saknas

Ingående emissionsfaktorer

Namn	Klimat Standardvärde	Eget värd	Enhet	Energi Standardvärde	Eget värde	Enhet	Kommentar
Armering, stål, slakarmering (stång)	0,7		kg CO2e/kg	11,1		MJ/kg	
Asfalt, ABb	0,043		kg CO2e/kg	2,59		MJ/kg	
Asfalt, ABS	0,049		kg CO2e/kg	3,58		MJ/kg	
Betong, anläggning, generellt värde (C35/45)	0,164		kg CO2e/kg	0,926		MJ/kg	
Diesel (MK 1)	2,8		kg CO2e/l	43,3		MJ/l	
El, ursprungsmärkt förnybar (inköpt av Trafikverket)	0,012		kg CO2e/kWh	3,02		MJ/kWh	
Jord	0,0003		kg CO2e/kg	0,005		MJ/kg	
Krossmaterial	0,004		kg CO2e/kg	0,06		MJ/kg	
Massor	0		kg CO2e/kg	0		MJ/kg	
Sprängämne	2,65		kg CO2e/kg	23,5		MJ/kg	
Stål, konstruktionsstål, generellt värde, ej varmförzinkat	2,27		kg CO2e/kg	28,2		MJ/kg	

Ingående transportparametrar

Namn	Standardavstå	Eget värde	Enhet	Kommentar
Armeringsstål				
Järnväg	500		km	
Lastbil landsvägtransport	300		km	
Lastbil närdistribution, från byggvaruhandel	40		km	
Fall A-upplag				
Dumper	2		km	
Lastbil regiontransport	0		km	
Fall B-upplag/täkt				
Dumper	0		km	
Lastbil regiontransport	30		km	
Konstruktionsstål				
Järnväg	1000		km	
Lastbil landsvägtransport	200		km	
Lastbil regiontransport	100		km	
Lastbil närdistribution, från byggvaruhandel	40		km	
Platsgjuten betong				
Lastbil närdistribution	35		km	

Egna noteringar

Rubrik	Notering	Skapad	Skapad av

Sammanställning av justeringar

Typåtgärder	Byggdel	Standardv	Egen mängd	Enhet					
								Verifikat	
Byggdelar	Material och a	Emission	Standardmängd	Egen mängd	Enhet	Förfrågnings-ID	Utgångsdatum	Status	
Transporter bygg delar/material	Material	Transport	Avstånd (km)	Eget avstånd (km)	Emissionsfaktor	Standard	Eget värde		Enhet
Drift och underhåll	Standardmäng	Egen män	Enhet						
Ingående emissionsfaktorer	Klimat	Eget klim	Enhet	Energi	Egen energi	Enhet			
Ingående transportparametrar	Standardavstå	Eget värd	Enhet						

B.2 LCA for TCC bridge

Kalkylmapp		Klimatkalkyl	
Kontakperson:	Internet user	**Kalkylnamn:**	TCC
Namn:	TCC Exjobb	**Kalkyl-ID**	IC1455
Objektnummer:	1	**Skede:**	Klimatdeklaration
Objektnamn:		**Org. GKI/underlagskalky**	1
Åtgärdsnummer:	1	**Revideringsdatum GKI/u**	2025-04-29
Åtgardsnamn:		**Status:**	Arbetsversion
Ärendenummer:	1	**Investeringskostnad:**	0
Beskrivning:		**Prisnivå:**	2025
Skapad av:	Internet user 2025-04-29 13:55:30	**Region:**	Norra
Senast ändrad av:	Internet user 2025-04-29 13:55:30	**Modellversion:**	Version 8.0
		Beskrivning:	
		Kalkylnivå:	Ingång C: Investeringsobjekt, flexibel ingång (kombination av kalkylnivåer 1, 2 och 3)
		Skapad av:	Internet user 2025-04-29 13:57:45
		Senast ändrad av:	Internet user 2025-04-29 13:57:45

Resultatsammanställning

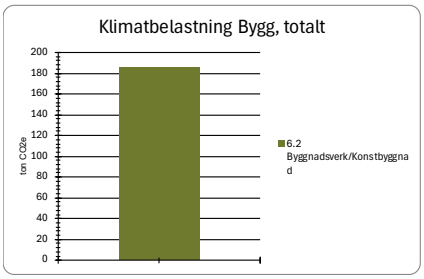

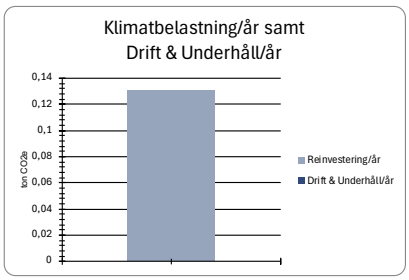

BYGG	ton CO2e	GJ
6.2 Byggnadsverk/Konstbyggnad	186,0471364	2218,079498
TOTALT	**186,0471364**	**2218,079498**

ÅRLIGT	ton CO2e	GJ
Bygg & Reinvestering, per år	2,423474222	33,79747516
Drift & Underhåll.per år	0	0
TOTALT	**2,423474222**	**33,79747516**

Fördelning av material/arbetsmoment, årligt

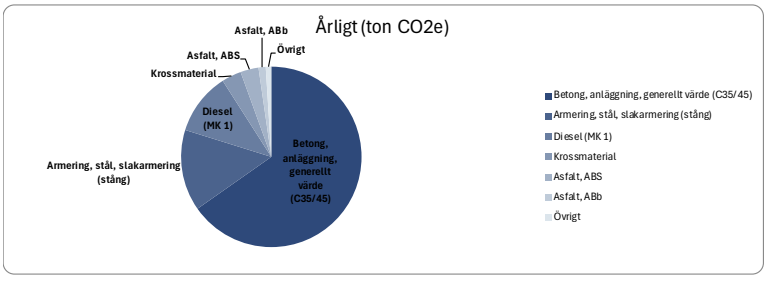

Indatasammanställning

Ingående objekt:	Mängd	Enhet	Klimat (ton CO2e) Byggskede totalt	Reinvestering/år * * byggdelar med livslängd ≤ 60 år	Bygg & reinvest/år * * samtliga byggdelar	Drift & Underhåll/år	Energi (GJ) Byggskede totalt	Reinvestering/år * * byggdelar med livslängd ≤ 60 år	Bygg & reinvest/år * * samtliga byggdelar	Drift & Underhåll/år
Totalt			186,0471364	0,130474348	2,423474222	0	2218,079498	7,953815152	33,79747516	0
Totalt exklusive produktion och transport av TGM			186,0471364	0,130474348	2,423474222	0	2218,079498		33,79747516	0
Typåtgärder										
Vägbro, betongplatta (6.2)	215,25	m2	139,1199609	0,130474348	1,836884528		1374,422246	7,953815152	23,25175952	

Kommentar typåtgärd

Byggdelar i typåtgärd	Standardmän	Egen mängd	Enhet
Jord Fall A, Fyll, Väg (6.2)	0		m3/m2
Jord Fall B, Fyll, Väg (6.2)	0		m3/m2
Bergschakt Fall A, Väg (6.2)	0		m3/m2
Jordschakt Fall A, Väg (6.2)	0		m3/m2
Bergschakt Fall B, Väg (6.2)	0		m3/m2
Asfalt, ABb 50 mm (6.2)	1,2		m2/m2
Stål, konstruktion, Väg (6.2)	0		ton/m2
Betong, anläggning, generellt värde, Väg (6.2)	1,1		m3/m2
Jordschakt Fall B, Väg (6.2)	4,4		m3/m2
Armering, armeringsstål, Väg (6.2)	0,14		ton/m2
Asfalt, ABS 40 mm (6.2)	1		m2/m2
Berg Fall B, Fyll, Väg (6.2)	4,4		m3/m2
Berg Fall A, Fyll, Väg (6.2)	0		m3/m2

Byggdelar			Byggskede totalt	Reinvestering/år	Bygg & reinvest/år	Byggskede totalt	Reinvestering/år	Bygg & reinvest/år
Armering, armeringsstål, Väg (6.2)	10,2	ton	7,46891328	0	0,093361416	119,5110411	0	1,493888014

Kommentar byggdel

Material och arbetsmoment	Standardmä	Egen mängd	Enhet
Stål, armering	1		ton/ton

Emissionsfaktor: Armering, stål, slakarmering (stång)

	Klimat (kg	Energi (MJ/kg)	Kommentar material och arbetsmoment
Standardvärde	0,7	11,1	
Eget värde			

Transport material

			Avstånd (km)	Transportparameter
D1	Järnväg	Standard	500	Armeringsstål
		Eget värde		
D2	Lastbil lanc	Standard	300	Armeringsstål
		Eget värde		
D3	Lastbil närc	Standard	40	Armeringsstål
		Eget värde		

Emissionsfaktor:

D1	El, ursprun	Standard	0,012	kg CO2e/kWh	3,02	MJ/kWh
		Eget värde				
D2	Diesel (MK	Standard	2,8	kg CO2e/l	43,3	MJ/l
		Eget värde				
D3	Diesel (MK	Standard	2,8	kg CO2e/l	43,3	MJ/l
		Eget värde				

Kommentar transporter

Betong, anläggning, generellt värde, Väg (6.2)	91,49	m3	36,75332929	0	0,459416616	222,1808556	0	2,777260695

Kommentar byggdel

Material och arbetsmoment	Standardmä	Egen mängd	Enhet
Betong	1		m3/m3
Densitet, betong	2350		kg/m3

Emissionsfaktor: Betong, anläggning, generellt värde (C35/45)

	Klimat (kg	Energi (MJ/kg)	Kommentar material och arbetsmoment
Standardvärde	0,164	0,926	
Eget värde			

Transport material

			Avstånd (km)	Transportparameter
D1	Lastbil närc	Standard	35	Platsgjuten betong
		Eget värde		

Emissionsfaktor:

D1	Diesel (MK	Standard	2,8	kg CO2e/l	43,3	MJ/l
		Eget värde				

Kommentar transporter

Trä, limträ (6.2)	44,14	m3	2,704932967	0	0,033811662	501,9653551	0	6,274566939

Kommentar byggdel

Material och arbetsmoment	Standardmä	Egen mängd	Enhet
Trä, limträ	1		m3/m3

Emissionsfaktor: Trä, limträ

	Klimat (kg	Energi (MJ/kg)	Kommentar material och arbetsmoment
Standardvärde	0,095	24,38	
Eget värde			

Transport material

			Avstånd (km)	Transportparameter
D1	Lastbil lanc	Standard	400	
		Eget värde		
D2	Lastbil närc	Standard	40	
		Eget värde		

Emissionsfaktor:

D1	Diesel (MK	Standard	2,8	kg CO2e/l	43,3	MJ/l
		Eget värde				
D2	Diesel (MK	Standard	2,8	kg CO2e/l	43,3	MJ/l
		Eget värde				

Kommentar transporter

Drift & Underhåll	Drift & Underhåll/år	Drift & Underhåll/år
Vägbro, betongplatta (6.2)	Schablon saknas	Schablon saknas

Ingående emissionsfaktorer

	Klimat			Energi			Kommentar
Namn	Standardvär	Eget värde	Enhet	Standardvärde	Eget värde	Enhet	
Armering, stål, slakarmering (stång)	0,7		kg CO2e/kg	11,1		MJ/kg	
Asfalt, ABb	0,043		kg CO2e/kg	2,59		MJ/kg	
Asfalt, ABS	0,049		kg CO2e/kg	3,58		MJ/kg	
Betong, anläggning, generellt värde (C35/45)	0,164		kg CO2e/kg	0,926		MJ/kg	
Diesel (MK 1)	2,8		kg CO2e/l	43,3		MJ/l	
El, ursprungsmärkt förnybar (inköpt av Trafikverket)	0,012		kg CO2e/kWh	3,02		MJ/kWh	
Jord	0,0003		kg CO2e/kg	0,005		MJ/kg	
Krossmaterial	0,004		kg CO2e/kg	0,06		MJ/kg	
Massor	0		kg CO2e/kg	0		MJ/kg	
Sprängämne	2,65		kg CO2e/kg	23,5		MJ/kg	
Stål, konstruktionsstål, generellt värde, ej varmförzir	2,27		kg CO2e/kg	28,2		MJ/kg	
Trä, limträ	0,095		kg CO2e/kg	24,38		MJ/kg	

Ingående transportparametrar

Namn	Standardavs	Eget värde	Enhet	Kommentar
Armeringsstål				
Järnväg	500		km	
Lastbil landsvägtransport	300		km	
Lastbil närdistribution, från byggvaruhandel	40		km	
Fall A-upplag				
Dumper	2		km	
Lastbil regiontransport	0		km	
Fall B-upplag/täkt				
Dumper	0		km	
Lastbil regiontransport	30		km	
Konstruktionsstål				
Järnväg	1000		km	
Lastbil landsvägtransport	200		km	
Lastbil regiontransport	100		km	
Lastbil närdistribution, från byggvaruhandel	40		km	
Platsgjuten betong				
Lastbil närdistribution	35		km	

Egna noteringar

Rubrik	Notering	Skapad	Skapad av

Sammanställning av justeringar

Typåtgärder	Byggdel	Standardmän	Egen mängd	Enhet					Verifikat	
Byggdelar	Material och	Emissionsfal	Standardmängd	Egen mängd	Enhet	Förfrågnings-ID	Utgångsdatum	Status		
Transporter byggdelar/material	Material	Transporttyp	Avstånd (km)	Eget avstånd (km)	Emissionsfaktor	Standard	Eget värde			Enhet
Drift och underhåll	Standardmä	Egen mängd	Enhet							
Ingående emissionsfaktorer	Klimat	Eget klimat	Enhet	Energi	Egen energi	Enhet				
Ingående transportparametrar	Standardavs	Eget värde	Enhet							

C

LCC calculation

LCC - Low					
TCC bridge					
Design	Quantity	Unit	Price	Unit	Total cost
Bridge superstructure	1	st	350 000 kr	SEK	350 000 kr
Production	Quantity	Unit	Price	Unit	Total cost
Concrete C35/45	91,5	m^3	3 500 kr	SEK/m^3	320 250 kr
Reinforcement steel K500C	10,2	ton	20 000 kr	SEK/ton	204 000 kr
Glulam GL30c (1305mm x 950mm)	21,1	m^3	1 500 kr	SEK/m^3	31 614 kr
Processing/Transport glulam	1	st	150 000 kr	SEK	150 000 kr
Reinforced rubber bearing	4	st	15 000 kr	SEK/st	60 000 kr
Pavement	145	m2	1 200 kr	SEK/m^2	174 000 kr
Railing	38	m	2 500 kr	SEK/m	95 000 kr
Form underside	120	m^2	1 500 kr	SEK/m^2	180 000 kr
Form sides/ edge beam	26	m^2	2 000 kr	SEK/m^2	52 000 kr
Falsework	1	st	50 000 kr	SEK	50 000 kr
Site establishment /mangement etc.	1	st	325 000 kr	SEK	325 000 kr
Crane (Lift of main beams)	1	st	100 000 kr	SEK	100 000 kr
Crane	1	st	50 000 kr	SEK	50 000 kr
Maintenance	Quantity	Unit	Price	Unit	Total cost
Replacement of edge beam, (3 st)	38	m	9 000 kr	SEK/m	342 000 kr
Replacement of railing (3st)	38	m	3 000 kr	SEK/m	114 000 kr
Replacement of pavement (3st)	145	m^2	1 500 kr	SEK/m^2	217 500 kr
Repainting (2st)	1	st	20 000 kr	SEK	20 000 kr
Inspection (Yearly)	1	st	50 000 kr	SEK	50 000 kr
End of life (Net present value)	Quantity	Unit	Price	Unit	Total cost
Demolition of bridge superstructure	1	st	4 028 kr	SEK	4 028 kr
					2 889 392 kr

LCC - High					
TCC bridge					
Design	Quantity	Unit	Price	Unit	Total cost
Bridge superstructure	1	st	450 000 kr	SEK	450 000 kr
Production	Quantity	Unit	Price	Unit	Total cost
Concrete C35/45	91,5	m^3	4 000 kr	SEK/m^3	366 000 kr
Reinforcement steel K500C	10,2	ton	25 000 kr	SEK/ton	255 000 kr
Glulam GL30c (1305mm x 950mm)	21,1	m^3	2 500 kr	SEK/m^3	52 689 kr
Processing/Transport glulam	1	st	250 000 kr	SEK	250 000 kr
Reinforced rubber bearing	4	st	25 000 kr	SEK/st	100 000 kr
Pavement	145	m2	1 500 kr	SEK/m^2	217 500 kr
Railing	38	m	3 500 kr	SEK/m	133 000 kr
Form underside	120	m^2	2 000 kr	SEK/m^2	240 000 kr
Form sides/ edge beam	26	m^2	3 000 kr	SEK/m^2	78 000 kr
Falsework	1	st	75 000 kr	SEK	75 000 kr
Site establishment /mangement etc.	1	st	400 000 kr	SEK	400 000 kr
Crane (Lift of main beams)	1	st	200 000 kr	SEK	200 000 kr
Crane	1	st	60 000 kr	SEK	60 000 kr
Maintenance	Quantity	Unit	Price	Unit	Total cost
Replacement of edge beam, (3 st)	38	m	10 000 kr	SEK/m	380 000 kr
Replacement of railing (3st)	38	m	3 500 kr	SEK/m	133 000 kr
Replacement of pavement (3st)	145	m^2	2 000 kr	SEK/m^2	290 000 kr
Repainting (2st)	1	st	25 000 kr	SEK	25 000 kr
Inspection (Yearly)	1	st	65 000 kr	SEK	65 000 kr
End of life (Net present value)	Quantity	Unit	Price	Unit	Total cost
Demolition of bridge superstructure	1	st	4 834 kr	SEK	4 834 kr
					3 775 023 kr

LCC - Low					
Concrete bridge					
Design	Quantity	Unit	Price	Unit	Total cost
Bridge superstructure	1	st	200 000 kr	SEK	200 000 kr
Production	Quantity	Unit	Price	Unit	Total cost
Concrete C35/45	165,6	m^3	3 500 kr	SEK/m^3	579 600 kr
Reinforcement steel K500C	19,1	ton	20 000 kr	SEK/ton	382 000 kr
Pavement	145	m^2	1 200 kr	SEK/m^2	174 000 kr
Railing	38	m	2 500 kr	SEK/m	95 000 kr
Form underside	163	m^2	1 000 kr	SEK/m^2	163 000 kr
Form sides/ edge beam	26	m^2	1 500 kr	SEK/m^2	39 000 kr
Falsework	1	st	200 000 kr	SEK	200 000 kr
Crane	1	st	50 000 kr	SEK	50 000 kr
Site establishment /mangement etc.	1	st	350 000 kr	SEK	350 000 kr
Maintenance	Quantity	Unit	Price	Unit	Total cost
Replacement of edge beam, (3 st)	38	m	9 000 kr	SEK/m	342 000 kr
Replacement of railing (3st)	38	m	3 000 kr	SEK/m	114 000 kr
Replacement of pavement (3st)	145	m^2	1 500 kr	SEK/m^2	217 500 kr
Inspection (Yearly)	1	st	50 000 kr	SEK	50 000 kr
End of life (Net present value)	Quantity	Unit	Price	Unit	Total cost
Demolition of bridge superstructure	1	st	3 222 kr	SEK	3 222 kr
					2 959 322 kr

LCC - High					
Concrete bridge					
Design	Quantity	Unit	Price	Unit	Total cost
Bridge superstructure	1	st	250 000 kr	SEK	250 000 kr
Production	Quantity	Unit	Price	Unit	Total cost
Concrete C35/45	165,6	m^3	4 000 kr	SEK/m^3	662 400 kr
Reinforcement steel K500C	19,1	ton	25 000 kr	SEK/ton	477 500 kr
Pavement	145	m^2	1 500 kr	SEK/m^2	217 500 kr
Railing	38	m	3 500 kr	SEK/m	133 000 kr
Form underside	163	m^2	1 500 kr	SEK/m^2	244 500 kr
Form sides/ edge beam	26	m^2	2 000 kr	SEK/m^2	52 000 kr
Falsework	1	st	250 000 kr	SEK	250 000 kr
Crane	1	st	60 000 kr	SEK	60 000 kr
Site establishment /mangement etc.	1	st	400 000 kr	SEK	400 000 kr
Maintenance	Quantity	Unit	Price	Unit	Total cost
Replacement of edge beam, (3 st)	38	m	10 000 kr	SEK/m	380 000 kr
Replacement of railing (3st)	38	m	3 500 kr	SEK/m	133 000 kr
Replacement of pavement (3st)	145	m^2	2 000 kr	SEK/m^2	290 000 kr
Inspection (Yearly)	1	st	65 000 kr	SEK	65 000 kr
End of life (Net present value)	Quantity	Unit	Price	Unit	Total cost
Demolition of bridge superstructure	1	st	4 028 kr	SEK	4 028 kr
					3 618 928 kr

	Conc - Low	Conc - High	TCC - Low	TCC - High
Design	200 000 kr	250 000 kr	350 000 kr	450 000 kr
Production	2 032 600 kr	2 496 900 kr	1 791 864 kr	2 427 189 kr
Maintenance	723 500 kr	868 000 kr	743 500 kr	893 000 kr
End of life	3 222 kr	4 028 kr	4 028 kr	4 834 kr

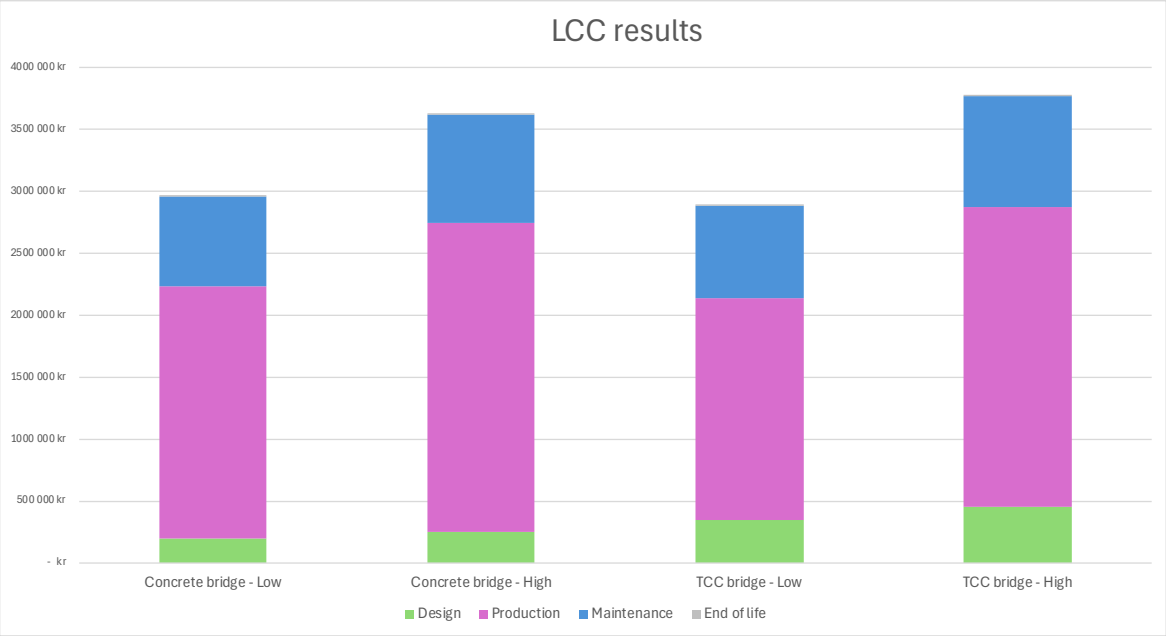
LCC results
4000 000 kr
3500 000 kr
3000 000 kr
2500 000 kr
2000 000 kr
1500 000 kr
1000 000 kr
500 000 kr
- kr
Concrete bridge - Low
Concrete bridge - High
TCC bridge - Low
TCC bridge - High
Design
Production
Maintenance
End of life

C.1 Elevation view and plan view of concrete bridge

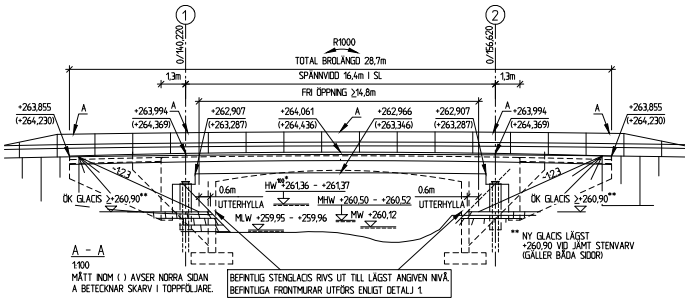

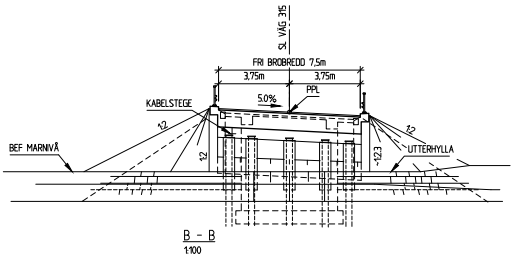

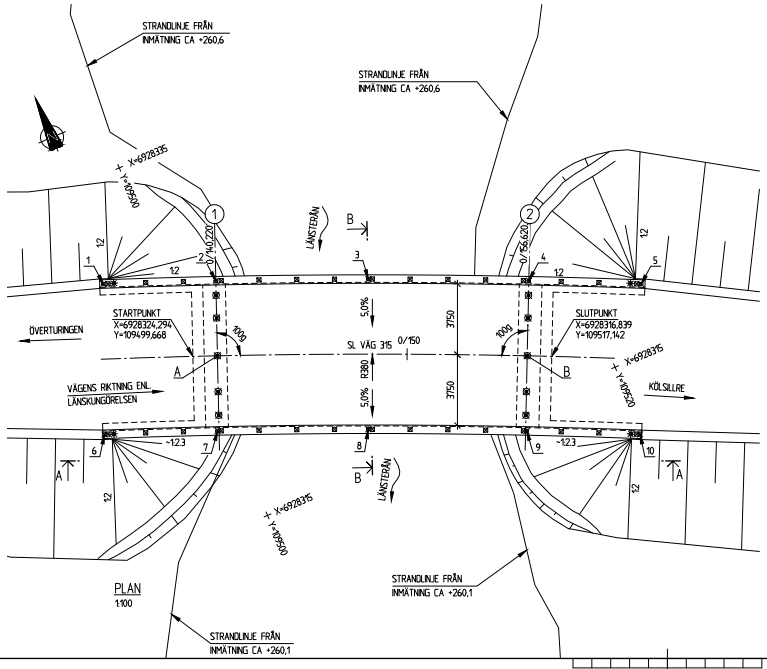

1:100 1 0 1 2 3 4 5 6 7 8 9 10 m

GRUNDHANDLINGSSKEDE / SKEDE:	
HANDLINGSSLAG:	
DATUM:	LEVERANS- / ANDRINGS-PM:
OBJEKT:	
DELOMRÅDE / BANDEL:	
ANLÄGGNINGSDEL:	
OBJEKTNUMMER / KSK:	KONSTRUKTIONSNUMMER:
BESTÄLLARE: TRAFIKVERKET	LEVERANTÖR:
GRANSKAD AV:	UPPDRAGSNUMMER:
GODKÄND AV:	ANDRING:
RITNINGSTYP:	
TJÄNSTOMRÅDE / TJÄNSTGRUPP:	
BESKRIVNING:	
SKALA:	FORMAT: FORVALTNINGSNUMMER:
RITNINGSNUMMER:	BLAD: BLADEN BLAD: SIST:

DEPARTMENT ARCHITECTURE AND CIVIL ENGINEERING
CHALMERS UNIVERSITY OF TECHNOLOGY
Gothenburg, Sweden
www.chalmers.se

CHALMERS
UNIVERSITY OF TECHNOLOGY